Institut für Pathologie

Universitätsmedizin Rostock

Head: Prof. Dr. Andreas Erbersdobler

Supervisor: PD Dr. med. habil. Annette Zimpfer

Establishment of Preclinical Tumor Models for Colorectal Cancer Precision Medicine

Inaugural dissertation to apply for the academic degree

Doctor of medicine (Dr. med.)

of University Medical Center Rostock

Submitted by

Meng Dai

Born on 10/01/1989, Anhui, China

Rostock, March 2026

https://doi.org/10.18453/rosdok_id00005813

Reviewers:

Reviewer 1:

PD Dr. med. habil. Annette Helene Zimpfer,
Institute of Pathology
Rostock University Medical Center
Strempelstr. 14, D-18057 Rostock, Germany

Reviewer 2:

PD Dr. rer. nat. habil. Claudia Maletzki,
Department of Medicine, Clinic III-Hematology/Oncology/Palliative Care
Rostock University Medical Center
Schillingallee 70, D-18057 Rostock, Germany

Reviewer 3:

Prof. Dr. med. Daniela Aust
Institute of Pathology
University Hospital Carl Gustav Carus
Schubertstraße 15, 01307 Dresden, Germany

Date of submission: October, 2025
Date of oral defence: March, 2026

Table of contents

I. Abbrevations 7

II. Figures 10

III. Tables 11

1. Introduction 12

1.1 Epidemiology of colorectal cancer 12

1.2 Risk and protective factors of CRC 13

1.3 Genetic factors of CRC 15

1.4 Diagnosis of CRC 18

1.5 Staging and treatment of CRC 20

1.5.1 Chemotherapy 21

1.5.2 Targeted therapy 22

1.5.3 Immunotherapy 23

1.6 Precision medicine for CRC 24

1.6.1 Molecular characterization of CRC 24

1.6.2 Organoid models for CRC precision medicine 24

2. Aims of the study and study design 27

3. Materials and methods 28

3.1 Materials 28

3.1.1 Resource of tumor samples from patients with CRC 28
3.1.2 Experimental instruments.....29
3.1.3 Reagents.....30
3.1.4 Disposable lab consumables 31
3.2 Methods 31
3.2.1 Establishment of CRC organoids and TILs.....31
3.2.1.1 Components and Concentration of the washing solution 31
3.2.1.2 Components of organoid culture medium.....32
3.2.1.3 Preparation and aliquot of biological factors and chemicals.....32
3.2.1.4 Establishment procedures of organoid culture systems 33
3.2.2 Histological and immunohistochemical validation of organoids 37
3.2.2.1 Fixation of organoids 37
3.2.2.2 Agarose-Paraffin embedding of organoids 39
3.2.2.3 Sectioning and HE staining of agarose-paraffin-embedded organoids.....40
3.2.2.4 Immunohistochemistry of agarose-paraffin-embedded organoids.....41

3.2.3 Immunofluorescence of agarose-paraffin-embedded organoids 44
3.2.4 Genomic analysis and validation of organoid 45
3.2.4.1 DNA extraction of CRC tissues.....45
3.2.4.2 DNA sequencing and analysis.....46
3.2.5 Establishment of tumor infiltrating lymphocytes (TILs) of CRC 49
3.2.5.1 Components of TILs culture medium.....49
3.2.5.2 Establishment procedures of TILs 50
3.2.5.3 Co-culture of organoids and paired TILs 50
3.2.6 Procedures of droplet digital PCR.....51
3.2.7 Flow cytometry analysis.....54
3.2.8 Drug sensitivity assay of CRC organoids 56
3.3 Software and websites of statistical analysis.....57
4. Results.....58
4.1. Prospective construction of a CRC cohort.....58
4.2 Molecular characterization of the CRC cohort 59
4.3 MSI status of the cohort.....60
4.4. Results of established CRC organoids 61
4.4.1 Histological characterization of CRC Organoids 63
4.4.1.1 Morphology.....63

4.4.1.2 Immunohistochemistry 64
4.4.1.2 Immunofluorescence 65
4.5 Targeted gene sequencing between primary CRC tumors and paired organoids and their molecular characterization 66
4.6 CRC organoid models in drug sensitivity assay and targeted therapy 68
4.7. Establishment and Analysis of TILs 69
5. Discussion 74
5.1. Discussion of results 74
5.1.1 Molecular characterization of the CRC cohort 74
5.1.2 Establishment of CRC organoids 77
5.1.3 Comparison of histomorphology, immunohistochemistry and targeted gene sequencing between primary CRC and paired organoids 78
5.1.4 Establishment of TILs and coculture 79
5.1.5 CRC organoid models in drug sensitivity assay and targeted therapy 80
5.2. Discussion of methods 81
5.2.1 Prospective cohort study 81
5.2.2 Target sequencing of the 818-gene mutation panel 81
5.2.3 The method of establishing CRC organoids 82

5.2.4 The methods of establishing TILs from CRC tissues 84

5.3. Conclusion 85

6. Summary.....87

Bibliography 89

IV. Appendix.....113

V. Dissertation statements 119

VI. Acknowledgement 121

VII. Personal Curriculum Vitae.....122

VIII. Eidestattliche Erlärungen/Declarations.....124

I. Abbrevations

ACC	Adoptive cell therapy
ADC	Antibody-Drug Conjugate
AJCC	American Joint Committee on Cancer
BER	Base Excision Repair
BSA	Bovine Serum Albumin
CDX-2	Caudal-Related homeobox Transcription Factor 2
CAR	C-reactive protein-to-albumin ratio
CEA	Carcinoembryonic antigen
CI	Confidence Interval
CIN	Chromosomal Instability
CIMP	CpG island methylator phenotype
CK-20	Cytokeratin 20
CMMRD	Constitutional Mismatch Repair Deficiency
CRC	Colorectal Cancer
CT	Computed tomography
CTECs	Circulating tumor endothelial cells
CTCs	Circulating tumor cells
DAPI	4',6-diamidino-2-phenylindole
ddPCR	Droplet digital PCR
dMMR	Deficiency of Mismatch Repair Genes
DMSO	Dimethyl Sulfoxide

ECOG	Eastern Cooperation Oncology Group
EGF	Epidermal Growth Factor
EGFR	Epidermal Growth Factor Receptor
EpCAM	Epithelial Cell Adhesion Molecule
FAP	Familial Adenomatous Polyposis
FAR	Fibrinogen-to-Albumin Ratio
FBS	Fetal Bovine Serum
FGF-10	Fibroblast Growth Factor 10
FOLFOX	Folinic Acid, 5-fluorouracil, and Oxaliplatin
HE or H&E	Hematoxylin-Eosin Staining
HEPES	4-(2-hydroxyethyl)-1-piperazineethanesulfonic acid
HMPS	Hereditary Mixed Polyposis Syndrome
IBD	Inflammatory Bowel Disease
ICIs	Immune checkpoint inhibitors
IF	Immunofluorescence
IFN-γ	Interferon-gamma
IHC	Immunohistochemistry
IC50	Half Maximal Inhibitory Concentration
IL-2	Interleukin-2
Ki-67	Antigen Kiel 67
LOH	Loss of heterozygosity
MMR	Mismatch repair

MSI	Microsatellite instability
NCCN	National comprehensive cancer network
MRI	Magnetic resonance imaging
MHC	Major histocompatibility complex
MSS	Microsatellite Stability
NGS	Next-Generation Sequencing
PBS	Phosphate Buffered Saline
PCR	Polymerase chain reaction
PD-1	Programmed cell death protein-1
PD-L1	Programmed cell death ligand-1
PJ	Peutz-Jeghers
PPAP	Polymerase proofreading-associated polyposis
PDOs	Patient-Derived Organoids
SPS	Serrated Polyposis Syndrome
TILs	Tumor Infiltrating Lymphocytes
TMB	Tumor Mutation Burden
TME	Tumor Microenvironment
Tregs	Regulatory T Cells
VEGFR	Vascular Epidermal Growth Factor Receptor
WHO	World Health Organization
WT	Wild Type

II. Figures

Figure 1: Global cancer statistics in 2022 12
Figure 2: Risk factors classification for CRC. 13
Figure 3: Genetic factors of CRC 15
Figure 4: Model of CRC initiation and progression 18
Figure 5. Flowchart of study design for CRC patient cohort 27
Figure 6: Detection of MSI with droplet digital PCR 51
Figure 7. Mutational landscape of the CRC cohort 59
Figure 8: Mutation sites and types of *TP53, APC, RAS,* and *ARHGEF12* 60
Figure 9: Examples of two CRC cases harboring MSI (A) or MSS status (B) detected by droplet digital PCR 61
Figure 10: Morphological characterization of CRC organoids and primary tumor tissues 63
Figure 11: IHC of CRC organoids and primary tumor tissues 65
Figure 12: The localization of EpCAM, DAPI and CD-133 in CRC organoids by IF staining 66
Figure 13: The genetic characteristics were maintained between the primary cancer samples and the established CRC organoids 67
Figure 14: Drug sensitivity assay 69
Figure 15: CD-45 immunohistochemistry of CRC tumor tissues 71
Figure 16: The analysis diagram of flow cytometry describes the results of multiparametric immunophenotyping of TILs from three CRC tumors ... 72
Figure 17: Co-culture system of CRC organoids and paired TILs 73

III. Tables

Table 1. The definitions for tumor satging based on Tumor (T), Node (N), Metastasis (M) criteria 21
Table 2. Experimental instruments used and supplier 29
Table 3. Reagents used and supplier 30
Table 4. Disposable lab consumables used and supplier 31
Table 5. Preparation of complete culture medium of TILs 31
Table 6. Preparation of organoid culture medium 32
Table 7. Preparation of the stock sulution for organoids culture medium 33
Table 8. Primary antibodies, clone, supplier, concentration for IHC 43
Table 9. Primary antibodies, clone, supplier, concentration for IF 45
Table 10. Applied ClinVar-based filtering criteria 49
Table 11. Components of the TILs culture medium 49
Table 12. Preparation of primers and probes for ddPCR 53
Table 13. Reaction system preparation for ddPCR 53
Table 14. Procedures preparation of ddPCR amplication 53
Table 15. Informations of antibodies for Flow Cytometry 55
Table 16. Clinical and pathological information of 102 CRC patients 58
Table 17. Clinicopathological information of established organoids 62

1. Introduction

1.1 Epidemiology of colorectal cancer

Colorectal cancer (CRC) ranks as the third most prevalent and the second deadliest cancer in the world, constituting about 10 % of all cancer diagnoses[1-4]. According to the latest global cancer statistics from world health organization, in 2022 among 19,976,499 newly diagnosed cancer cases worldwide, 1,926,425 cases were diagnosed with CRC, and among 9,743,832 cancer deaths, 904,019 were from this disease, ranked as the second leading cause of cancer-related death worldwide[5,6] (Figure 1).

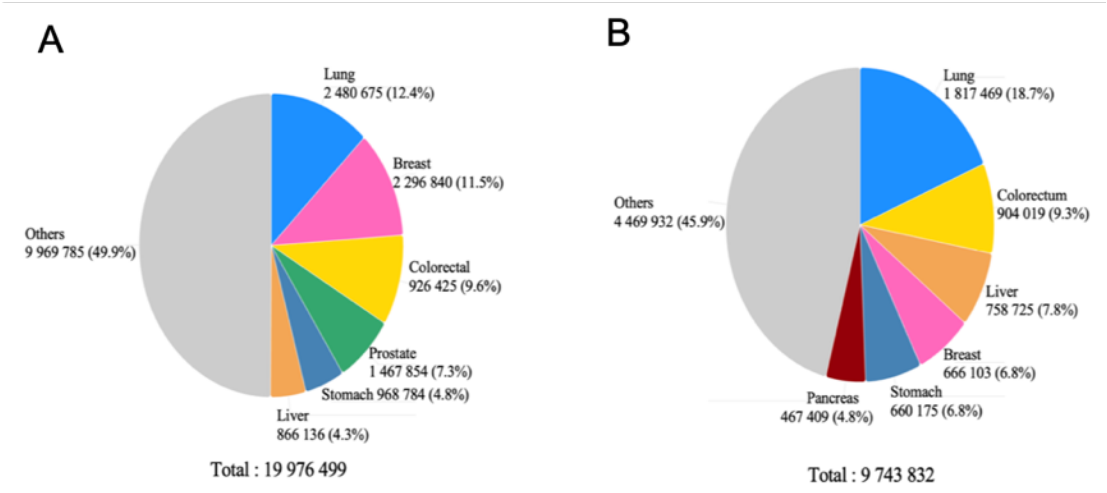

Figure 1: Global cancer statistics in 2022

(**A**) The global incidence of newly diagnosed cancers of both genders in 2022. (**B**) The global mortality of all cancers of both genders in 2022. The data of figure A[7] and B[8] are from the website of Cancer Today.

According to a 2024 study from Robert Koch Institute, approximately 135,598 CRC cases are diagnosed among adults aged 35–84 years in Germany[9] and one out of 15 men and one out of 19 women in Germany will develop CRC during their lifetime[10]. Projection for future CRC diagnosis is also concerning for global public health[11]. By 2040 CRC is projected to increase dramatically to 3.2 million new cases per year, representing a 63% jump from 2020[12]. CRC

mortality is expected to rise even more substantially, with estimated 1.6 million deaths per year by 2040, constituting a 73% increase. More than 80% of new CRC cases projected for 2040 are expected to occur in developed countries, such as Iceland, Norway and Switzerland.

1.2 Risk and protective factors of CRC

Factors that are related to CRC incidence can be attributed to several key categories (Figure 2).

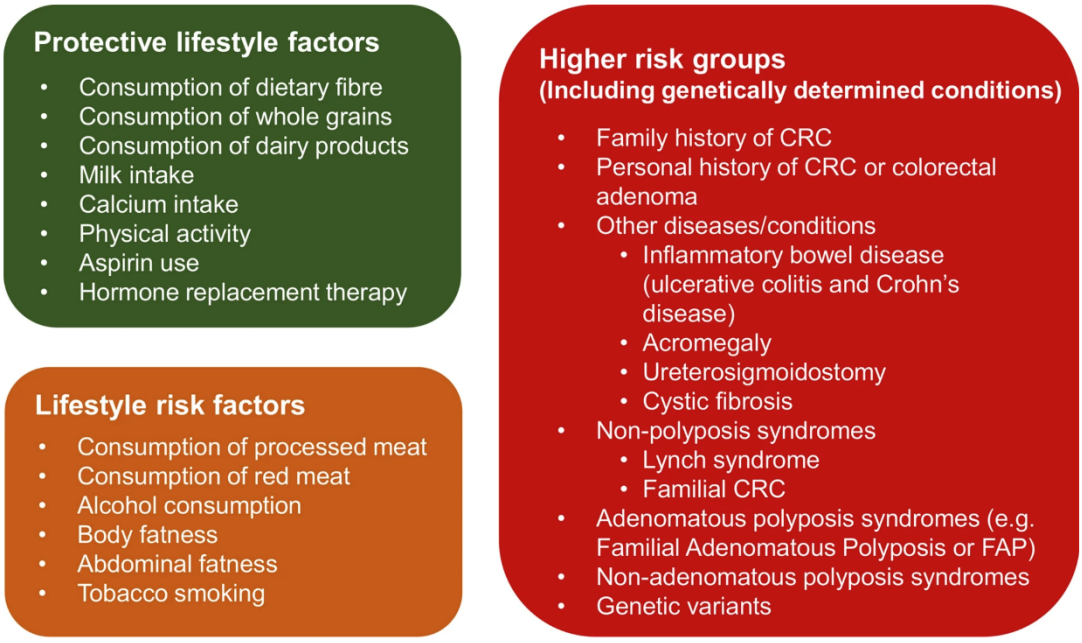

Figure 2: Risk factors classification for CRC[13-15].

This figure clarifies three categories of risk factors that affect CRC. Protective lifestyle factors, including dietary fiber, whole grains, dairy product consumption, calcium and milk intake, physical activity, aspirin use, and hormone replacement therapy, which are factors that can reduce CRC risk. The lifestyle risk factors, such as processed meat and red meat consumption, alcohol consumption, body obesity, abdominal obesity, and tobacco smoking, which can increase CRC risk. The higher risk groups, including family history of CRC, medical history, inflammatory bowel disease (IBD) history, and various hereditary syndromes, such as Lynch syndrome, familial adenomatous polyposis.

Generally, CRC risk factors are classified into two components: lifestyle risk factors, which could be meliorated by changes in people's lifestyle, and higher risk group factors. CRC is largely preventable, as several actionable risk factors have been clearly identified, including smoking, unhealthy diet, excessive alcohol consumption, physical inactivity, and overweight[16-20]. In contrast, dietary fibres, whole grains, natural nuts, dairy products, milk and moderate calcium intake, vitamin supplements, especially vitamin A, as well as aspirin use and hormone replacement therapy for a specific group of people, have been shown to offer protective effects against CRC[21-27].

Family history represents a significant risk factor, with meta-analyses demonstrating that individuals with affected first-degree relatives have a relative risk of 1.80 (95% CI 1.61-2.02), increasing to 2.75 among those with two or more affected relatives[28,29]. This risk is particularly pronounced in younger individuals, with those under 45 having a relative risk of 5.37 if they have affected first-degree relatives[29]. IBD substantially increases CRC risk (RR = 2.93, 95% CI 1.79-4.81) due to pro-neoplastic effects of chronic intestinal inflammation, with risk factors including disease duration, extent, severity, inflammatory pseudopolyps, and coexistent primary sclerosing cholangitis[28-30]. Hereditary syndromes like Lynch syndrome significantly elevate risk, with patients developing CRC at younger ages (median age 36.0 years), and those with ulcerative colitis facing even higher risk[31]. Familial Adenomatous Polyposis (FAP), responsible for <1% of all CRC cases, is characterized by hundreds to thousands of colorectal adenomas, with nearly 100% of untreated patients developing CRC[32]. Acromegaly, ureterosigmoidostomy, and cystic fibrosis are additional conditions associated with elevated CRC risk. The decline in IBD-related CRC incidence over the past 30 years can be attributed to improved surveillance programs and better control of mucosal inflammation, highlighting the importance of targeted screening and preventive interventions for these high-risk populations[33,34].

1.3 Genetic factors of CRC

CRC is one of the most common malignancies with significant genetic susceptibility. CRC patients can be divided into two categories: non-polyposis and polyposis (Figure 3).

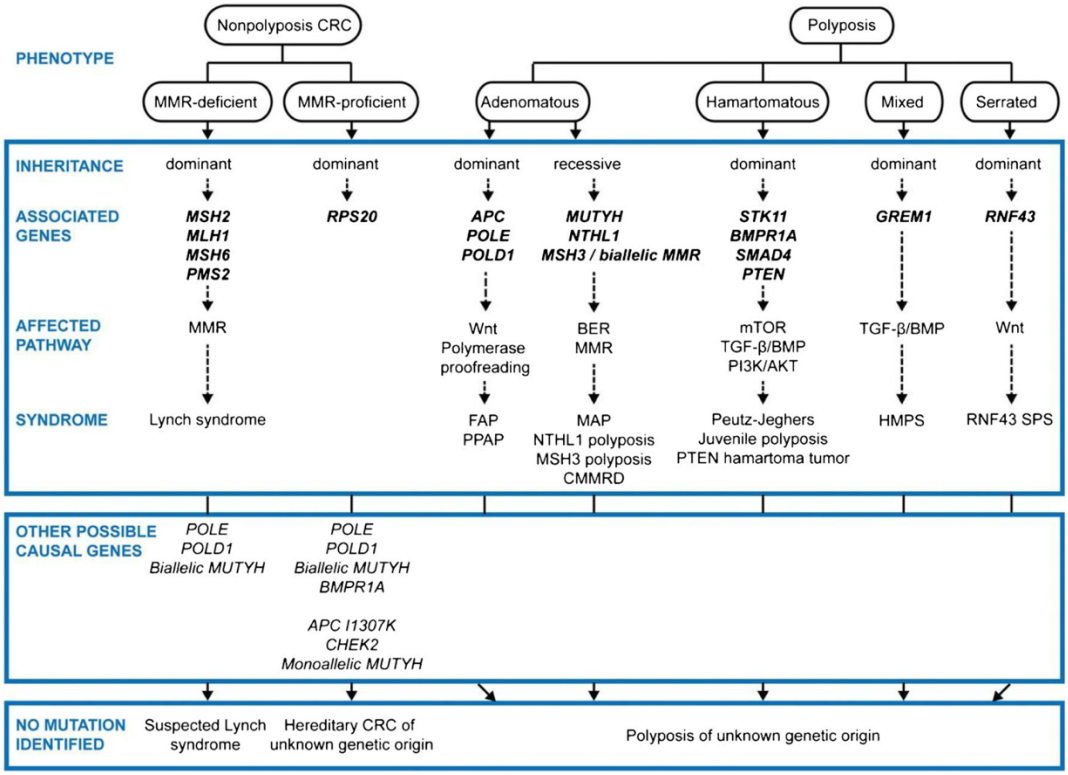

Figure 3: Genetic factors of CRC

Based on phenotype, CRC syndromes are classified into two subtypes: polyposis and nonpolyposis, distinguished by the properties of inheritance, causative genes, and molecular pathway dysregulation.

Abbreviations: FAP, familial adenomatous polyposis; PPAP, polymerase proofreading-associated polyposis; CMMRD, constitutional mismatch repair deficiency; BER, base excision repair; HMPS, hereditary mixed polyposis syndrome; SPS, serrated polyposis syndrome.

Non-polyposis can be further divided into MMR gene defective and non-defective types, while polyposis can be divided into four phenotypes: adenomatous, hamartomatous, mixed, and serrated[35]. Adenomatous polyposis mainly includes dominantly inherited familial adenomatous polyposis (FAP) and recessively inherited *MUTYH*-associated polyposis (MAP)[36,37]. Among them,

FAP is caused by germline pathogenic variants of the *APC* gene, while MAP is caused by biallelic pathogenic variants of the *MUTYH* gene[38]. Hamartomatous polyposis compromises distinct syndromes, such as Peutz-Jeghers (PJ) syndrome, juvenile polyposis syndrome, and *PTEN* hamartoma syndrome, each characterized by the development of hamartomatous polyps with distinctive smooth muscle proliferation and arborizing architecture[39,40]. These syndromes are caused by mutations in various genes including *STK11/LKB1* (PJ syndrome), *SMAD4* and *BMPR1A* (juvenile polyposis), and *PTEN* (Cowden syndrome)[41-45]. Mixed polyposis is characterized by the presence of multiple histologically polyp types such as hyperplastic, adenomatous, and atypical juvenile polyps[46]. The autosomal dominance is caused by duplications in the *GREM1* gene region[47]. Serrated polyposis syndrome is defined by the presence of multiple serrated polyps throughout the colon with characteristic saw-toothed epithelial architecture[48]. The diagnosis requires meeting specific WHO criteria including either five or more serrated lesions proximal to the rectum (with two ≥1cm) or more than 20 serrated lesions distributed throughout the colon[49]. The syndrome carries a lifetime risk of CRC and is characterized by *BRAF* mutations and CpG island methylator phenotype (CIMP)[50-52].

Lynch syndrome is the most common hereditary colorectal cancer syndrome, accounting for approximately 2-4% of CRC patients[53-55], caused by the deficiency of mismatch repair genes (dMMR), including *MLH1, MSH2, MSH6* and *PMS2*, critical proteins in DNA mismatch repair pathway. The mechanisms inactivating MMR genes are diverse, including mutations, promoter methylation, and loss of heterozygosity (LOH), leading to microsatellite instability (MSI), and is dominantly inherited[55-58]. Thus, MSI serves as a crucial molecular hallmark of Lynch syndrome[59-61].

In recent decades, with the development of next-generation sequencing (NGS) technology, researchers have identified several new genes associated with CRC susceptibility, such as *RPS20, POLE, POLD1, AXIN2, NTHL1, MSH3,*

RNF43, FMN1, and *GREM1*[36,62-69]. These findings have expanded our understanding of hereditary CRC and provided new mechanisms for clinical diagnosis and personalized treatment.

CRCs are broadly categorized by two major forms of genetic instability. Approximately 85% of sporadic CRC exhibit chromosomal instability (CIN), while the other 15% are hypermutated and characterized by MSI[70,71]. The accumulation of genetic and epigenetic changes inactivates tumor suppressor genes and activates oncogenes, ultimately leading to the generation of cancer stem cells and the formation of CRC. Most CRC develop from polyps that typically starts with the formation of an abnormal crypt, which gradually transforms into a neoplastic precursor lesion (polyp). Generally, over an estimated time of 10 to 15 years, these polyps may further progress and eventually develop into CRC[1,72,73] (Figure 4).

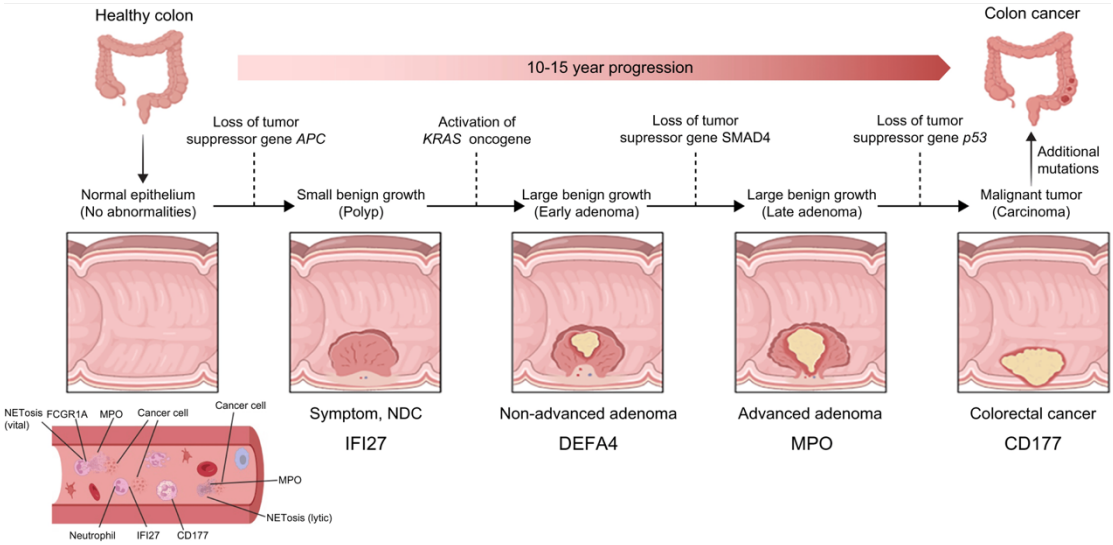

Figure 4: Model of CRC initiation and progression

It is estimated that it typically takes 10 to 15 years from a healthy colon to progress to CRC. First, normal colon epithelial cells develop into small benign growths (polyps) after losing the *APC*. Subsequently, activation of the *KRAS* oncogene drives the polyps to grow further into early adenomas. With the loss of the *SMAD4* tumor suppressor gene, the adenomas continue to grow and enter the advanced adenoma stage. Finally, the loss of the *TP53* tumor suppressor gene and the accumulation of other mutations lead to the transformation of adenomas into CRC (carcinomas). Representative molecular markers that can be detected at different stages are also marked below the picture. In addition, the illustration at the lower left corner shows the interaction between neutrophils and cancer cells during tumor progression, suggesting the role of the immune microenvironment in tumor development. Overall, this picture intuitively reveals the multi-stage, molecularly driven evolution of colon cancer and its potential biomarkers[74].

1.4 Diagnosis of CRC

CRC is diagnosed by pathological examination of tissue samples from regular colonoscopy with biopsy or surgery resection. Experienced pathologist is critical to improve the diagnosing and screening accuracy of the colorectal polyps with high-grade dysplasia[75-79]. In addition, histopathological and molecular examination combined with clinical characteristics are critical to formulate neo-adjuvant and adjuvant treatment strategies[80-82].

Based on WHO classification of digestive system tumors (5th edition), adenocarcinoma is the predominant histological subtype, constituting 90% of all CRCs. Its defining characteristic is the invasion from the muscularis mucosa

to the submucosa. Although the majority of CRC patients are diagnosed as adenocarcinoma Not Otherwise Specified (NOS), some histopathological subtypes is can be distinguished with the distinct clinical presentations and molecular profiles[83].

Colonoscopy is the gold standard for CRC detection. In head-to-head comparison studies, colonoscopy demonstrates exceptional diagnostic performance with an overall weighted sensitivity of 98.5% (95% confidence interval: 96.3-100%) and specificity of 100% (99.9-100%) for detecting advanced neoplasia[84]. However, colonoscopy is not without its limitations. The miss rate of colonoscopy in adenoma diagnosis ranges from 15% to 24%, while that of advanced adenoma ranges from 5.4% to 11%[85,86]. The miss rate for colorectal adenomas is influenced by several factors, including polyp size, number of detected polyps, and procedural quality measures such as withdrawal time and bowel preparation adequacy[86].

In recent years, imaging and molecular testing have emerged to complement the traditional colonoscopy approach in CRC diagnosis. For average-risk screening populations, Computed tomography (CT) colonography has demonstrated a sensitivity and specificity of 82.9% (95% CI: 74-89%) and 91.4% (95% CI: 84-96%), respectively, for adenomas ≥6 mm[87]. For larger adenomas (≥1cm), the sensitivity increases to 87.9% (95% CI: 82-92%) with specificity of 97.6% (95% CI: 95-99%)[87]. In patients with positive fecal occult blood tests, CT colonography shows approximately 89% sensitivity for adenomas ≥6 mm and cancer with 75% specificity[88]. Carcinoembryonic antigen (CEA) remains the most widely utilized tumor biomarker in CRC management and has demonstrated clinical utility primarily in monitoring for recurrent disease. Serial measurements of CEA can achieve approximately 80% sensitivity and 70% specificity for detecting CRC recurrence, providing a lead time of approximately 5 months[89]. Recent research has explored biomarker combinations to enhance diagnostic accuracy, such as combined assessment of fibrinogen-to-albumin

ratio (FAR), fibrinogen-to-prealbumin ratio (FPR), C-reactive protein-to-albumin ratio (CAR), and C-reactive protein-to-prealbumin ratio (CPR), as complementary diagnostic tools[90].

The development of liquid biopsy technologies has introduced promising new approaches to CRC diagnosis and monitoring. Circulating tumor cells (CTCs) combined with circulating tumor endothelial cells (CTECs), CEA, and CA19-9 achieve the highest diagnostic accuracy with an AUC of 0.935[91,92].

1.5 Staging and treatment of CRC

In order to formulate treatment plans before and after surgery for cancer patients, the TNM (tumor, node, metastasis) staging criteria is established by the American Joint Committee on Cancer (AJCC) (Table 1)[93].

The prognosis of patients with CRC varies significantly based on the stages at diagnosis, with survival rates ranging from over 90% for localized disease to approximately 16% for metastatic cases[94,95].

Table 1. The definitions for tumor satging based on Tumor (T), Node (N), Metastasis (M) criteria

TNM / *Stage*	*T*	*N*	*M*
Stage 0	Tis	N0	M0
Stage I	T1, T2	N0	M0
Stage II A	T3	N0	M0
Stage II B	T4a	N0	M0
Stage II C	T4b	N0	M0
Stage III A	T1-T2	N1/N1c	M0
	T1	N2a	M0
Stage III B	T3-T4a	N1/N1c	M0
	T2-T3	N2a	M0
	T1-T2	N2b	M0
Stage III C	T4a	N2a	M0
	T3-T4a	N2b	M0
	T4b	N1-N2	M0
Stage IV A	Any T	Any N	M1a
Stage IV B	Any T	Any N	M1b
Stage IV C	Any T	Any N	M1c

1.5.1 Chemotherapy

Chemotherapy serves as the cornerstone of CRC management, with applications spanning neoadjuvant, adjuvant, and palliative settings[96,97]. The

evolution of chemotherapeutic regimens has significantly improved patient outcomes, with modern combination protocols demonstrating superior efficacy compared to historical single-agent approaches[98]. The most widely utilized regimens include FOLFOX (folinic acid, 5-fluorouracil, and oxaliplatin) and FOLFIRI (folinic acid, 5-fluorouracil, and irinotecan), which have shown comparable response rates of 54-56% in metastatic disease[98,99].

1.5.2 Targeted therapy

Targeted therapy represents a paradigm shift toward precision oncology, with treatment selection based on specific molecular characteristics of individual tumors[100,101]. The most clinically relevant targets in CRC include the epidermal growth factor receptor (EGFR) and vascular endothelial growth factor (VEGF) pathways[102]. Monoclonal antibodies can bind to the extracellular domain of EGFR to prevent downstream signaling, promoting cell proliferation and cell survival[103]. However, tumors with mutations in the genes of *KRAS, NRAS,* or *BRAF* are resistant to EGFR inhibition[104,105]. For example, *KRAS* is mutated in 30-40% of CRC[106], which contributes to poor prognosis and resistance to anti-EGFR therapy and makes their detection crucial for treatment plan[106,107], especially in light of recent advances in the development of inhibitors targeting *KRAS* mutations[108-111]. Bevacizumab, targeting VEGF, represents another cornerstone of targeted therapy for CRC. Recent advances have expanded CRC targeted therapy landscape to include novel agents for specific molecular subsets, particularly for tumors harboring *BRAF* V600E mutations[112-114].

1.5.3 Immunotherapy

Represented by antibodies targeting the programmed cell death protein-1/ programmed cell death ligand-1 (PD-1/PD-L1) axis, immune checkpoint inhibitors (ICIs) has emerged as a transformative approach in cancer treatment. However, immunotherapy is primarily restricted to specific molecular subsets in CRC[115]. The most significant success has been achieved in tumors with high level of MSI (MSI-H) or dMMR, which comprise approximately 10-15% of CRCs[116,117]. Thus, MSI testing has become an essential component of CRC diagnosis and management. Initial screening typically involves immuno-histochemistry for MMR proteins (MLH1, PMS2, MSH2, MSH6), followed by *MLH1* hypermethylation or *BRAF* mutation test.

Other than ICIs, adoptive cell therapy (ACT) has made tremendous progress in recent years. Tumor-infiltrating lymphocytes (TILs) are immune cells that migrate into tumors and play a crucial role in anti-tumor immunity[118]. TILs can recognize and attack cancer cells and their presence within the tumor microenvironment (TME) is associated with improved prognosis in various cancers, including CRC[119]. FDA approved Lifileucel, the world's first TIL therapy treating metastatic melanomas in February 2024. Many clinical studies have demonstrated the potential of TIL therapy in solid tumors, even in patients developing resistance to ICIs[120-125]. Thus, TIL therapy is an exciting new direction in CRC treatment that warrants further exploration.

The integration of multiple treatment modalities requires careful consideration of the order of treatments, combination strategies, and patient selection criteria[126]. Treatment-related toxicities remain a significant concern, particularly with combination regimens[127].

1.6 Precision medicine for CRC

1.6.1 Molecular characterization of CRC

NGS profiling of tumors provides crucial evidence for personalized treatment strategy and prognosis evaluation by accurately identifying tumor-specific molecular variations. Recently, NGS becomes indispensable for optimal treatment, with guidelines for testing *RAS* mutations, *BRAF* status, MSI/dMMR status, and other biomarkers such as *NTRK* fusions *and HER2* amplification[128-132]. Studies have revealed that Chinese CRC patients exhibit distinct mutational profiles, such as high-frequency mutations in *TP53* (72%), *APC* (63%), and *KRAS* (42%)[133], demonstrating significant differences from patients in western countries. By capturing driver gene variations in key signaling pathways such as MAPK, WNT, TGF-pathways, potential therapeutic targets can be identified. For instance, patients with *KRAS G12C* mutations demonstrate significantly improved objective response rates when treated with targeted inhibitors combined with anti-EGFR therapy[134,135]. Molecular subtyping based on targeted sequencing can guide precision treatment. For instance, colon cancer patients with *RAS/BRAF* (wild-type, left-sided) show extended median survival with cetuximab-chemotherapy combinations[136], while *MET* amplification or *MAP2K1 K57T* mutations in metastases induce EGFR antibody resistance which is reversible with MEK inhibitor combinations[137]. It has been demonstrated that CRC patients with *HER2*-amplification can achieve objective response rates of 52% and disease control rates >90% with trastuzumab[136,138].

1.6.2 Organoid models for CRC precision medicine

Despite advances in treatment modalities, the complexity and heterogeneity of CRC complicate effective management and therapeutic outcomes. Recent

developments in cancer research have highlighted the potential of tumor organoids—three-dimensional (3D) cell culture systems derived from patient tissues—as innovative models for studying CRC biology and testing sensitivity to cancer therapeutics[139]. Organoids can preserve the genetic and phenotypic characteristics of the original tumors, providing a platform for investigating tumor biology and treatment responses in ways that traditional two-dimensional (2D) cell cultures cannot achieve.

Organoids are miniature, simplified versions of organs produced *in vitro* from tissues and/or biopsies. They replicate the architecture and functionality of their corresponding tissues, making them invaluable for studying disease mechanisms, drug responses, and therapeutic strategies. In the context of CRC, patient-derived organoids (PDOs) have emerged as powerful tools for modeling tumor biology and assessing treatment efficacy, allowing researchers to investigate the molecular underpinnings of CRC initiation and progression[140-142]. One of the most promising applications of PDOs is their ability to predict individual patient responses to therapies[143,144]. Studies have demonstrated that organoids can accurately reflect the treatment responses observed in patients, with predictive values significantly higher than those achieved through conventional approaches[145-149]. This capability enables clinicians to tailor treatment plans based on drug sensitivity data obtained from organoids, potentially improving patients' outcomes[150].

Traditional models, such as cell lines and animal models, have limitations that often hinder their applicability to human cancers[151]. For instance, 2D cultures fail to mimic the complex TME, which plays a critical role in cancer progression and response to therapy. Animal models, while useful, do not always accurately reflect human disease due to species-specific differences in biology[152-155]. In contrast, organoids derived from human tissues maintain key aspects of the TME, including cellular interactions and extracellular matrix components[156,157]. This fidelity allows for more relevant studies on tumor behavior and drug testing.

Such is also the case for cancer immunotherapy, especially in ACT therapy. Tumors often develop mechanisms to evade immune detection such as upregulating PD-L1 expression of tumor cells or recruiting regulatory T (Tregs) cells [158-160]. The interaction between TILs and tumor cells is complex and can influence treatment outcomes significantly, particularly in response to immunotherapy and chemotherapy[161].

Integrating studies of TILs with organoid technology present a novel approach to understanding immune-tumor interactions in CRC. By co-culturing organoids with TILs derived from patient samples, researchers can observe how these immune cells interact with tumor cells in a controlled environment that closely resembles the original tumor context[140,146]. This approach not only enhances our understanding of immune evasion mechanisms but also aids in identifying potential therapeutic targets for immunotherapy.

2. Aims of the study and study design

The study aimed to 1) analyzing the genetic features of CRC tissues with the 818 gene penal for individual precision medicine; 2) establishing preclinical models of CRC organoids and paired TILs; 3) identifying established CRC organoids to test sensitive drugs for precision medicine; 4) co-culture of CRC organoids to explore TME.

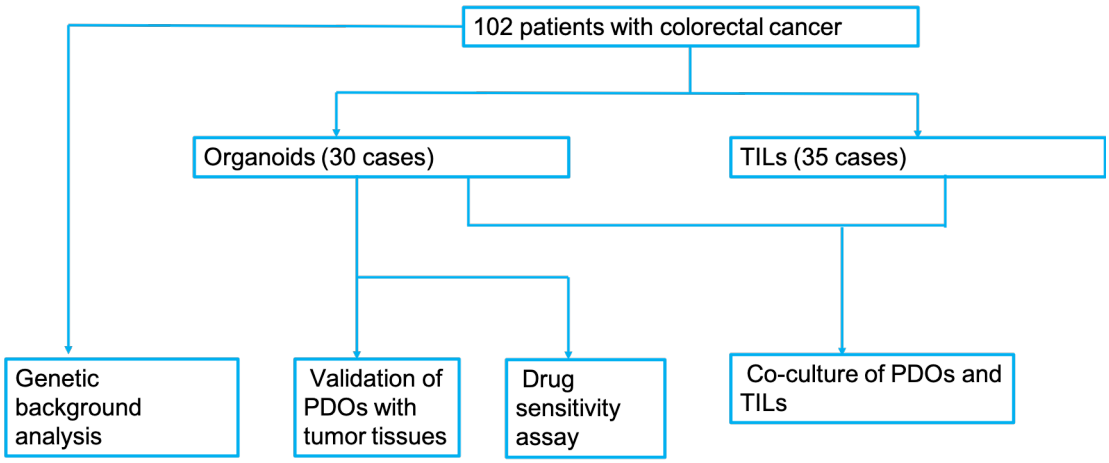

Figure 5. Flowchart of study design for CRC patient cohort

102 tumor tissues from patients with CRC were collected. With the 818-mutation-gene panel, all the tumor tissues were performed with targeted gene sequencing and genetic background analysis. And 30 organoids and paired 35 TILs were established from the fresh tumor samples. The established organoids were validated with HE staining, IHC and targeted gene sequencing to verify whether they were originated from the primary tumor tissues. The established organoids were utilized to perform drug sensitivity and co-culture with the paired TILs.

3. Materials and methods

3.1 Materials

3.1.1 Resource of tumor samples from patients with CRC

This research project was completed under the joint corporation from the Department of General Surgery of Shanghai Jiaotong University affiliated Ruijin Hospital, Mission Medical Biotechnology (Ningbo, China), and the Department of Pathology, University Medical Center Rostock (Rostock, Germany).

In this study, surgically resected tumor tissues from 102 patients with colorectal carcinoma were collected from the Department of General Surgery of Shanghai Jiaotong University affiliated Ruijin Hospital.

Inclusion criteria: 1) Diagnosed with colorectal cancer by coloscopy and pathological biopsy; 2) tumor can be resected; 3) preoperative clinical staging completed, including enhanced abdominal CT, Magnetic resonance imaging (MRI), or endoscopic ultra-sonography; 4) age between 25 and 85 years; 5) Eastern Cooperation Oncology Group (ECOG) performance status score of two, with the ability to tolerate radical colorectal cancer surgery; 6) no significant chronic diseases affecting the heart, liver, or kidneys, and no history of other malignancies; 7) capable of complying with the study protocol and has signed the informed consent form. Exclusion criteria: 1) patients refuse to sign the informed consent form before surgery.

The baseline information of all patients is shown in Table 16, and the detailed information of patients with successful organoid cultures is listed in Table 17.

This study has been approved by the Ethics Committee of Ruijin Hospital (Ethics No.: 2024-570). All patients involved have signed the informed consent.

3.1.2 Experimental instruments

Table 2. Experimental instruments used and supplier

Instruments	Manufactures	Country
Bio-Safety Cabinet	Eppendorf	Germany
Centrifuge 5810R	Eppendorf	Germany
Centrifuge 5425R	Eppendorf	Germany
Water Bath	Thermo Fisher Scientific	USA
Mini-Centrifuge	Thermo Fisher Scientific	USA
Nanodrop One	Thermo Fisher Scientific	USA
Pipette Controller	Eppendorf	Germany
Qubit 4	Invitrogen	USA
Cell Counter	DeNovix	USA
CO_2 Incubator	Thermo Fisher Scientific	USA
Light Microscope	Leica	Germany
Fluorescent Inverted Microscope	Leica	Germany
4℃ Fridge	Haier	China
-20℃ Fridge	Haier	China
-80℃ Fridge	Thermo Fisher Scientific	USA
Liquid Nitrogen Storage System	Thermo Fisher Scientific	USA
Ultrapure Water System	Merck Millipore	USA
Vortex Mixer	Kylin-Bell	China

3.1.3 Reagents

Table 3. Reagents used and supplier

Components	Company	Country
Penicillin-Streptomycin-Amphotericin B (100x)	Abcam	USA
Primocin (50mg/ml)	InviviGen	USA
Collagenase Type II	Sigma-Aldrich	USA
Hyaluronidase Type IV	Sigma-Aldrich	USA
Vancomycin	Sigma-Aldrich	USA
RPMI 1640	Gibco	USA
HEPES	Merck Millipore	USA
Interleukin-2	MedChemExpress	USA
Human AB Serum	GeminiBio	USA
Gentamycin	PanReac AppliChem	Spain
Matrigel	Corning	USA
Advanced DMEM F12	Gibco	USA
GlutaMax	Gibco	USA
Human Recombinant R-Spondin-1	Pepro Tech	USA
Human Recombinant Noggin	Pepro Tech	USA
Nicotinamide	MedChemExpress	USA
N-Acetylcysteine		
Y-27632 Dihydrochloride	MedChemExpress	USA
A83-01	MedChemExpress	USA
SB202190	MedChemExpress	USA
Human Recombinant EGF	Noveprotein	China
B-27 Plus Supplement (50x)	Thermo Fisher Scientific	USA
FGF-7	Novoprotein	China
TryPle Express	Thermo Fisher Scientific	USA

3.1.4 Disposable lab consumables

Table 4. Disposable lab consumables used and supplier

Consumables Name	Company	Country
Pipette Tips	Axygen Scientific	USA
15ml Centrifuge Tube	Axygen Scientific	USA
50ml Centrifuge Tube	Axygen Scientific	USA
1.5ml Eppendorf Tube	Axygen Scientific	USA
Cell Culture Plate	Grenier Bio-One	Germany
100μm Cell Strainer	Corning	USA
Petri Dish	SARSTEDT	Germany
Serological Pipette	SARSTEDT	Germany

3.2 Methods

3.2.1 Establishment of CRC organoids and TILs

3.2.1.1 Components and Concentration of the culture medium of CRC oganoids and TILs

Table 5. Preparation of complete culture medium of TILs

Components	Final Concentration
RPMI 1640 Medium	Basal Medium
Interleukin-2	6000IU/ml
Penicillin-Streptomycin-Amphotericin B (100x)	1x
Primocin	100μg/ml
Vancomycin	10μg/ml
Gentamycin	10μg/ml

3.2.1.2 Components of organoid culture medium

Table 6. Preparation of organoid culture medium

Components	Final Concentration	Function
Advanced DMEM/F12	Basal Medium	Basal Medium
HEPES (100x)	1x	Buffer Agent
GlutaMAX (100x)	1x	Amino Acid Additive
Penicillin-Streptomycin-Amphotericin B	1x	Antibiotics
Human Recombinant R-Spondin-1	100ng/ml	Activate the canonical WNT signaling pathway
Human Recombinant Noggin	100ng/ml	TGF-β signaling
B-27 Plus Supplement (50x)	1x	Insulin signaling
Nicotinamide	10mM	Co-enzyme precursor
N-acetylcysteine	1.25mM	Antioxidant
Human Recombinant EGF	5ng/ml	FGFR2b signaling
Y-27632 dihydrochloride	10μM	ROCK signaling
SB202190	3μM	P38 MAPK signaling
A-83-01	500nM	TGF-β signaling
Recombinant Human Fibroblast Growth Factor 7	25ng/ml	Epithelial cell-specific growth factor

3.2.1.3 Preparation and aliquot of biological factors and chemicals

Stock solutions were prepared and stored at -20°C. Table 7 lists the chemicals used and the concentrations of the stock solutions.

Table 7. Preparation of the stock sulution for organoids culture medium

Chemical	Medium	Concentration stock solution
N-Acetylcysteine (NAC)	PBS	500mM
Human recombinant epithelial growth factor (EGF)	BSA/PBS	500 µg/ml
Y-27632 dihydrochloride	DMSO	10mM
SB202190	DMSO	10mM
A83-01	DMSO	500µM
Nicotinamide	PBS	1M
Noggin	ddH_2O	100µg/ml
Wnt-3a	ddH_2O	100µg/ml
Hyaluronidase type IV-S	ddH_2O	10mg/ml
Collagenase type II	BSA/PBS	15mg/ml
Recombinant Human R-spondin-1	ddH_2O	100µg/ml

3.2.1.4 Establishment procedures of organoid culture systems

Tumor Processing

After CRC tissue samples were resected, tumor tissues were cut with sterile scissors and forceps, placed in tissue preservation solution for organoid culture and DNA extraction, and the remaining samples were immediately stored in sterile cryovials, placed on ice, transferred to a laboratory within an hour and stored in -80°C freezer or liquid nitrogen for long-term storage.

1) Tumor tissues were rinsed with about 1-2ml of PBS with penicillin-streptomycin, the PBS discarded, and the procedure repeated 3-5 times to wash away as much blood and mucus as possible.
2) A surgical scalpel was used to remove necrotic and fatty tissue in a sterile petri dish.
3) A small amount of PBS with penicillin-streptomycin was added and a surgical scalpel was used to cut tumor tissues into pieces of around

1.5x1.5x1.5 mm.

4) Tumor pieces were pipetted and resuspended 5 to 10 times with a 1ml pipette tip every 5 minutes until formation of cell clusters of three to five cells and single cells.

5) Culture medium of 10ml was added to avoid over-digestion.

6) Digestion solution was centrifuged at 300g for 5 minutes at 4°C.

7) The supernatant was discarded and resuspend the sediment was responded in culture medium of 10ml.

8) The sediment was filtered with a 100μm cell strainer and centrifuged at 300g for 5 min at 4°C.

9) The supernatant was discarded, the cells were resuspended in 1 ml of culture medium, the number of viable cells was counted, and centrifuged at 300 g for 5 minutes at 4 °C.

10) The cells were aliquoted in centrifuge tubes.

Procedures of organoid establishment

1) The 24-well plate was placed in an incubator to be preheated.

2) The aliquoted cells were centrifuged at 300g for 5 minutes at 4°C.

3) The pellet with Matrigel was resuspended (usually 10,000 cells were suspended with 10μl Matrigel, the volume of Matrigel must be more than 70%).

4) 3-4 drops of 10μl Matrigel mixed with cells were added per well.

5) The plate was placed in the incubator for 20-30 minutes and the Matrigel should be solidified.

6) 450-500μl complete culture medium was pipetted to each well of a 24-well plate.

Cryopreservation of organoids

1) Preparation of cryopreservation solution.
2) 10% FBS/DMSO solution: 5ml FBS (Fetal Bovine Serum) + 45ml DMSO (Dimethyl Sulfoxide).
3) Preparation of organoids: After the organoids had been cultured for 3-5 weeks, the number of cultured organoids reached the harvested volume amount and then were prepared for cryopreservation.
4) To improve the success rate of organoid resuscitation, the medium was changed every 3 days before freezing and one day before subculture.
5) The pipette tip was placed at the bottom edge of the well to aspirate the original culture medium, 500μl pre-cooled Advanced D-MEM/F12 was used to puff away the matrix gel droplets in each well, the gel was transferred to a 15ml centrifuge tube and then the tube was added to 5ml and centrifuged at 300g, 4°C for 5 minutes. The sediment was resuspended with pre-cooled cryopreservation solution and the concentration of organoids was adjusted to 3-5*10^4 cells/ml.
6) The cell suspension was added to the cryopreservation tube, and then the tube was placed in a cryopreservation box at -80°C overnight. The next day, the tube was placed in liquid nitrogen for long-term storage.

Resuscitation of organoids

1) The cryopreservation tube containing the organoids was taken out from the liquid nitrogen tank and it was quickly placed in the water bath of 37°C for rewarming.
2) After the cryopreservation solution melted, the organoids were transferred to a 15ml centrifuge tube, and then 4ml of preheated advanced DMEM/F12 medium should be added to the tube.

3) The tube was centrifuged for 5 minutes: 300g, 4°C.

4) The supernatant was aspirated and discarded, and 100μl Matrigel was added to resuspend (as the amount of organoids in each tube was about $5*10^4$). The Matrigel suspension containing organoids was trans-passaged to 3 wells of a 24-well plate.

5) The organoid establishment steps were restarted as described above and the organoid suspension was spread in a 24-well plate.

6) After the dome was completely solidified, 400-500μl of organoid culture medium was added for culture, and the remaining steps were the same as described before.

Passaging of organoids

1) Preparation: the Matrigel was thawed on ice; the organoid culture medium was taken out and restored at room temperature (15-25°C). Several reagents were prepared: digestion buffer: Tryple Express containing 10μM Y-27632 dihydrochloride; digestion termination solution (Advanced DMEM/F12, 1xGlutaMAX (100x), 10mM HEPES, 100ug/ml Penicillin-Streptomycin, 5μM Y-27632, 5% FBS) to room temperature. A 24-well plate was preheated in the incubator and 200μl pipette tips were precooled with ice.

2) The original culture medium was aspirated at the bottom edge of each well of the organoid to be passaged, in order not to damage the dome of the Matrigel.

3) 400μl digestion buffer was added to each well, the dome was blown away with a rinsed pipette tip and incubated at room temperature (15-25°C) for 5-15 minutes.

4) 800μl of stop solution was added to stop digestion, transferred to a 15ml centrifuge tube, washed again with 400ul of stop buffer and then transferred

to a centrifuge tube.

5) The tube was centrifuged for 5 minutes, 300g, 4°C and the supernatant was aspirated carefully in order not to touch the cell pellet.

6) The cell pellet was resuspended with 1ml Advanced DMEM/F12+++ and the suspension was transferred to a 1.5ml centrifuge tube; the tube was centrifuged for 5 minutes, 300g, 4°C; the supernatant was aspirated.

7) The organoids were passaged at the ratio of 1:3; the Matrigel was added, blown up and down for at least 10 times; the cell pellet was resuspended.

8) A pre-cold pipette tip was used to aspirate 40μl the culture medium with Matrigel mixture, and the mixture was added to the center of the 24-well culture plate to form a dome.

9) The lid of the plate was covered and let it stand in the incubator for 3-5 minutes; then it was turned over and let it stand for another 25 minutes until the Matrigel was solidified.

10) 500μl of organoid culture medium was added to each well along the side wall of the well to avoid destroying the Matrigel dome.

11) The lid of the culture plate was covered and the plate was cultured in a 37°C and 5% CO_2 incubator. The medium was changed twice a week.

3.2.2 Histological and immunohistochemical validation of organoids

3.2.2.1 Fixation of organoids

1) Preparation: the lower half of the 200μl PCR tube was cut off to obtain a ring as a mold for subsequent agarose embedding; 4 grams of agarose powder was melted in 100ml PBS, microwave on medium-low heat for 1

minute, 3 times, and then transferred into a 15ml centrifuge tube. The agarose was melted with boiling water before use. It was placed in a water bath of 60°C to prevent solidification. 4% paraformaldehyde was precooled to 4°C and used as cell fixation solution.

2) The culture medium was aspirated from the inner edge of the 24-well plate and 1ml of 4% paraformaldehyde was added.

3) A 1ml pipette tip was used to resuspend the organoids and the organoid suspension from the required wells was added to the same 15ml centrifuge tube.

4) The suspension was mixed and incubated at 4°C for 1 hour and centrifuged at 300g, 4°C for 5 minutes and the 4% paraformaldehyde was carefully discarded.

5) The sediment of organoids was washed with pre-cooled PBS, transferred to an EP tube, and centrifuged for 5 minutes at 4°C, 300g. And then the PBS was discarded.

6) The organoids were resuspended with pre-cooled 4% paraformaldehyde and incubated at 4°C overnight.The prepared mold was placed in the culture dish so that it was flushed with the bottom, and then it was placed on ice.

7) The organoids were mixed, centrifuged for 5 minutes at 300g, 4°C. The supernatant was aspirated avoiding the contact with the precipitated organoids.

8) To fix the organoids, 4% agarose was melted in boiling water and placed in 60-70°C water bath.

9) To avoid damage to the organoids, a 200μl pipette tip with the tail cut off was used, and 75ml of agarose solution was added to resuspend the organoids.

10) The resuspended organoids and agarose mixture were transferred into the prepared mold on ice. This process was completed as quickly as possible to avoid solidification of agarose in the pipette tip and avoid bubbles.

11) The number, quality and position of agarose-embedded organoids was checked under an inverted microscope and placed on ice for more than one hour to ensure that the agarose solution was solidified.

12) By a toothpick, the agarose block with organoids in the mold was picked out, wrapped with moist filter paper and transferred to a tissue box, stored in 70% ethanol, and proceeded to the next step of wax embedding in due course.

3.2.2.2 Agarose-Paraffin embedding of organoids

1) The organoids were rinsed with running water for 2-10 hours.

2) The organoids were dehydrated by shifting from low to high ethanol concentration in order: 70% ethanol for 60 minutes, 80% ethanol for 1 hour, 90% ethanol for 1 hour, 95% ethanol (I) for 1 hour, 95% ethanol (II) for 1 hour, 100% ethanol (I) for 1 hour, and 100% ethanol (II) for 1 hour.

3) Transparency: the organoids were immersed in xylene for 30 minutes.

4) Wax dipping: the process of immersing organoids in melted paraffin after transparency was called wax dipping. It took 2-3 immersions to complete. The melting point of paraffin was 52-56°C, and the total time was 3 hours.

5) Embedding: First, added the melted paraffin to the embedding frame, then hot tweezers were used to place the organoids into it, making sure the embedding surface was neat. After the paraffin was slightly solidified, it could be placed in a refrigerator to accelerate the solidification.

6) Slicing: The wax block also needed to go through the steps of trimming,

slicing, spreading, scooping, baking, etc., and then stored at 4°C.

3.2.2.3 Sectioning and HE staining of agarose-paraffin-embedded organoids

1) After slicing the wax block (6-8μm), it was baked at 55-60°C for 4-6 hours to prevent the subsequent steps from peeling off.
2) The slices were dewaxed in xylene (I) for 5 minutes, in xylene (II) for 5 minutes, anhydrous ethanol for 5 minutes, 90% ethanol for 2 minutes, 80% ethanol for 2 minutes, 70% ethanol for 2 minutes, and finally, in PBS for 5 minutes.
3) Staining with hematoxylin stain: filter paper was used to break the oxide film on the surface of the liquid, then stained for 5 minutes, and rinsed with tap water for 5 minutes.
4) Differentiation solution for 20 seconds (prepared with concentrated hydrochloric acid and 75% alcohol in a ratio of 1:99. This solution needed to be replaced after a period of use. The differentiation time of the new liquid should be shorter. Generally, it was pulled 2-3 times, and a light purple-red color could be seen on the glass slide).
5) Soaked in tap water for 15 minutes.
6) Eosin staining for 2 minutes (the specific time was adjusted according to the staining results).
7) Dehydration, transparency: 90% ethanol (I) 2-3 seconds; soaked in tap water for 5 minutes. 90% ethanol (II) 2-3 seconds; 100% ethanol (I) 2-3 seconds.
8) Sealing: 100% ethanol (II) 30 seconds; xylene (I) 3 minutes; xylene (II) 5 minutes. Neutral gum sealing; observation under microscope.

3.2.2.4 Immunohistochemistry of agarose-paraffin-embedded organoids

Immunohistochemistry is a histopathological procedure in which specific proteins such as CDX-2, CK-20, Ki-67, CD-45 in this study are visualized under a light microscope with a corresponding primary antibody in combination with a detection system consisting of a secondary antibody with a chromogen. In the first step, a primary antibody is used that selectively binds to epitopes of the targeted antigen and label them. The antibody can be either monoclonal or polyclonal. To detect the formed antigen-antibody complex, a secondary antibody is used in a further step. Nowadays, an enzyme-coupled secondary antibody is often used, which binds to the previously formed antigen-antibody complex. Finally, a chromogenic substrate is used which is converted by an enzyme into a colored precipitate. The antigen bound by the antibody can thus be visualized under the light microscope.

1) The paraffin slices were put into the microwave oven for baking. The temperature of the microwave oven was set to 55-60°C. The slices were baked for 5 hours, and adjusted depending on the amount of paraffin.
2) The slices were dewaxed in xylene for 20 minutes until the wax disappeared. The xylene solution was divided into two cylinders, 15 minutes in the first cylinder and 5 minutes in the second cylinder, and the slices needed to be pulled up and down during the process.
3) The dewaxed slices were hydrated with 100%, 90%, 80%, 70%, 50% gradient concentration (volume/volume) of ethanol, 5 minutes for every concentration.
4) The slices ware soaked in deionized water for 10 minutes, and the slices were lift up and down during the period, or the slices were soaked in PBS

for two times, 5 minutes for every time.

5) The slices were soaked in 3% H_2O_2 for 10 minutes (prepared immediately before use) to eliminate endogenous peroxidase activity in cells; wrapped in tin foil to avoid light exposure.

6) The slices were soaked in PBS for two times, 3 to 5 minutes for every time.

7) The slices were soaked in a container containing the corresponding antigen repair solution (prepared the corresponding repair solution according to the antibody instructions). The slices were put in a microwave oven and heated it at the medium and low gear for 10 minutes for antigen repairing. The container was taken out of the microwave oven, and cooled at room temperature for 20-30 minutes.

8) The slices were soaked in PBS for 3 times, 2 minutes for every time, and in order to mark the required areas, the areas were drawn with an oily pen.

9) Non-specific binding sites were blocked with serum of the same source as the secondary antibody. The diluted serum was applied to the required area. And then the slices were incubated at 37°C for 30 minutes, and blot off the redundant serum was removed with the absorbent tissue.

10) The slices were incubated with primary antibody (Table 8): Primary antibodies diluent was used to dilute the antibody to an appropriate concentration, an appropriate volume of diluted primary antibodies was added to each slice, and the primary antibodies were added to the target areas, incubated in a humidified box at room temperature for 1.5 hours and then placed at 4°C overnight.

11) The slices were washed with PBS for 3 times, 5 minutes for each time.

12) Then the slices were incubated with the secondary antibodies. 50μl of secondary antibodies were added to each slice. The slices were placed in a humidified box and incubated at room temperature for 20 minutes and

finally washed with PBS for 3 times, 5 minutes for each time.

13) DAB coloring: DAB reagent was evenly distributed and completely covered the target areas for 10 minutes, and then rinsed with tap water after staining.

14) Counterstaining: To outline cell contours and better localize target proteins, perform the following steps were performed: Hematoxylin staining for 30 seconds, differentiation with 0.5% hydrochloric-acid ethanol for 2 seconds, followed by immersion in running water for 15 minutes. During dehydration, slices were immersed with gradient concentrations of ethanol: 50%, 70%, 95%, 100%, each for 2 minutes. Xylene solution was used for transparency for 10 minutes. The sections were dried at room temperature.

15) Sealing: an amount of neutral resin was added on the slices, and the slides were covered with a coverslip to avoid bubbles.

16) The staining results were observed under a microscope and the results were photographed for documentation.

Table 8. Primary antibodies, clone, supplier, concentration for IHC

Antibody	Clone	Source	Concentration	Supplier
CDX-2	Monoclonal	Rabbit	1μg/ml	Cell Singnaling Technology, USA
CK-20	Monoclonal	Rabbit	0.25μg/ml	Cell Singnaling Technology, USA
Ki-67	Monoclonal	Rabbit	0.75μg/ml	Cell Singnaling Technology, USA
CD-45	Monoclonal	Rabbit	1μg/ml	Cell Singnaling Technology, USA

Abbreviations: CDX-2, Caudal-Related homeobox Transcription Factor 2; CK-20, Cytokeratin 20; Ki-67, Antigen Kiel 67; CD-45, Protein Tyrosine Phosphatase, Receptor Type C.

3.2.3 Immunofluorescence of agarose-paraffin-embedded organoids

The principle of indirect immunofluorescence staining is to utilize two antibody systems to detect the targeted antigen and amplify the signal. It applies a two-step antibody binding process: firstly, an unlabeled primary antibody binds to the targeted antigen; secondly, a secondary antibody labeled with fluorescence to bind to the primary antibody. This two-step method enhanced detection sensitivity and achieves significant signal amplification.

Prior to secondary antibody incubation, the immunofluorescence staining procedures for agarose-paraffin-embedded slices were identical to immune-histochemical staining, which had been described above. The remaining steps are as follows:

1) After incubation of primary antibodies, the slices were washed for three times with PBS solution, 5 minutes for each time.
2) The solution of secondary antibodies was prepared at room temperature, the solution was dispensed onto the slices to ensure even distribution and the target areas were completely covered, and then the slices were incubated in the dark for 1 hour.
3) The residual secondary antibody solution was discarded. The sections were washed with PBS solution under dark conditions for three times, 5 minutes for each time.
4) The slices were incubated with 0.5μg/mL DAPI solution for 5 minutes.
5) The slices were washed with PBS solution for three times, 5 minutes for each time.
6) The slides were dried with absorbent paper and blocked with a coverslip reagent containing anti-fluorescence quencher.

7) The staining results were observed under a confocal microscope. And the staining results were photographed for documentation.

Table 9. Primary antibodies, clone, supplier, concentration for IF

Antibody	Clone	Source	Concentration	Supplier
EpCAM	Polyclonal	Rabbit	5μg/ml	Abcam, USA
DAPI	Fluorescent dye	Chemosynthesis	0.5μg/ml	Abcam, USA
CD-133	Polyclonal	Rabbit	5μg/ml	Abcam, USA

Abbreviations: CD-133, Prominin-1; DAPI, 4',6-diamidino-2-phenylin-dole; EpCAM, Epithelial Cell Adhesion Molecule; IF, Immunofluencin.

3.2.3 Genomic analysis and validation of organoid

3.2.3.1 DNA extraction of CRC tissues

1) Tumor tissue was mixed with 800μl lysing solution and 5ul proteinase K in an EP tube.
2) The tube was shaken 20 minutes at 50°C for 2 hours.
3) 750μL anhydrous ethanol was added and shaken. The DNA clumps were pocked out, put in a new EP tube with 70% ethanol, inverted gently and centrifuged at full speed for 5 minutes.
4) As much as possible the supernatant was aspirated and let the remaining DNA sediment at the bottom of the EP tube.
5) An appropriate amount of Tris-EDTA was added, the DNA concentration was measured with NanoDrop One, and the EP tube was stored at -20°C.

3.2.3.2 DNA sequencing and analysis

Targeted sequencing is a method for sequencing specific genomic regions. In this study hybridization capture were performed for the enrichment of targeted genes, which can achieve selective enrichment of target regions based on the principle of DNA-DNA hybridization. This technology employs biotin-labeled oligonucleotide probes (baits) that possess complementary sequences to the target genomic regions. The fundamental workflow of hybridization capture involves: firstly, randomly fragment genomic DNA and ligate sequencing adapters to prepare a library; secondly, in the hybridization conditions, biotin labeled probes was used to hybridize and bind to targeted DNA fragments; thirdly, the hybridized complexes were captured with streptavidin magnetic beads to remove unbound DNA fragments; lastly, the captured targeted DNA was eluted from the magnetic beads for PCR amplification and sequencing.

1) Quality Test of Sample DNA

Agarose gel electrophoresis was performed to analyze the degree of DNA degradation and whether there was RNA or protein contamination; meanwhile, Qubit 4.0 was used to accurately measure the DNA concentration to ensure that the DNA concentration was ≥ 20ng/μl, and the total amount of DNA was ≥ 0.3μg. Then, DNA samples were able to be put on the sequencing machine. In this study, a total of 102 patients' targeted genes were sequenced, including tumor tissue and 4 organoids samples.

2) Establishment and Quality Test of DNA Library

Covaris fragmentation instrument was used to randomly fragment 0.3μg DNA into DNA fragments with a length of 180-280bp. Agilent SureSelect Human All Exon V5/V6 kit was used to perform corresponding library construction and

capture experiments. After end repair, phosphorylation and addition of A after tailing, connected adapters to both ends of the fragments, and then prepared the corresponding DNA library. A library with a specific index was used to perform liquid phase hybridization with a sufficient number of biotin-labeled probes, and then used magnetic beads with streptomycin to capture the exons, and then performed polymerase chain reaction (PCR) amplification to check the quality of the library. Then, in this study Qubit 4.0 was used for initial quantification, and Agilent 2100 was utilized to conduct strict quality testing on the fragment size of the library. After meeting the requirements, the qPCR method was used to accurately quantify the effective concentration of the DNA library. After passing the test, sequencing was performed.

3) Sequencing

The captured DNA library was added to the channels of the Flow Cell chip. Through complementary hybridization and a series of polymerase chain reactions, DNA chains complementary to the original sequences were obtained. NaOH solution was added to denature the DNA, retaining the newly synthesized DNA chains. After adding neutralization solution, the DNA chains underwent complementary hybridization and polymerase reactions again to synthesize new DNA chains. After a certain number of cycles, the DNA reached sufficient copy numbers. Upon completion of the bridge PCR process, sequencing was performed with the Illumina platform PE150.

4) Bioinformatic analysis of sequencing data

Raw Sequence Data Preprocessing

During preprocessing of raw NGS data (FASTQ format), low-quality reads and adapter sequences were removed with fastp (v0.23.4)[162]. Processed reads were aligned to the hg38 reference genome (GRCh38.p14.genome.fa.gz) with

BWA-MEM (v0.7.18-r1243) with flags, generating sequence alignment files in SAM format[163]. Resulting alignments were sorted and converted to BAM format using SAMtools (v1.20)[164].

Following alignment, Picard MarkDuplicates was employed to identify and remove PCR and optical duplicates originating from identical DNA fragments.

Variant Calling

Somatic variant calling followed the GATK (v4.2.0) Best Practices workflow. BAM files underwent Base Quality Score Recalibration (BQSR) to adjust base quality scores using empirical error models. The Mutect2 workflow comprised four steps:

1. Initial variant calling: Mutect2 performed local *de novo* assembly of haplotypes to call candidate SNVs/indels[165].
2. Contamination estimation: Cross-sample contamination was quantified using Get Pileup Summaries and Calculate Contamination.
3. Orientation bias modeling: Learn Read Orientation Model corrected sequencing-strand artifacts using F1R2 counts.
4. Variant filtering: Filter Mutect Calls applied context-aware filters using prior-step outputs.

Variant Annotation and Filtering

To obtain high-confidence somatic variants, the following filters were applied:

1. Depth filter: Tumor sequencing depth < 10×

2. Allele fraction filter: Tumor VAF < 0.05 or > 0.9 (suggesting potential artifacts or homozygosity)

Retained variants were annotated using VEP (cache v112) via the Personal Cancer Genome Reporter (PCGR v2.0.3)[166]. Due to the absence of paired

normal samples, additional ClinVar-based filtering criteria were applied as specified in the following Table 10.

Table 10. Applied ClinVar-based filtering criteria

Condition	Action	Clinical Rationale
Germline + Benign/Likely Benign	Drop	Exclude non-pathogenic inherited variants
Germline + Pathogenic/Likely Pathogenic	Keep	Retain disease-associated inherited variants
Germline + VUS +VAF 45-65%	Drop	Exclude possible germline contamination
Somatic or Mixed origin	Keep	Prioritize tumor-specific variants
Unknown origin + Benign/VUS	Drop	Conservative exclusion of non-pathogenic variants
Unknown origin + Pathogenic	Keep	Prioritize potential disease drivers

3.2.4 Establishment of tumor infiltrating lymphocytes (TILs) of CRC

3.2.4.1 Components of TILs culture medium

In the following Table 11, the components of CRC TILs culture medium are listed.

Table 11. Components of the TILs culture medium

Components	Stock Solution	Final Concentration	Function
RPMI 1640	Basal medium	Basal medium	Basal medium
Human AB Serum	1x	10%	Nutrient
HEPES	1M	25mM	Buffer Solution
Interleukin-2	$1.7*10^6$ IU/ml	6000IU/ml	Promote the proliferation and activation of TILs and the anti-tumor effects
Penicillin-Streptomycin	100X	1X	Antibiotics

3.2.4.2 Establishment procedures of TILs

1) The tumor tissue samples were placed in 6cm sterile petri dishes and the samples were washed with washing solution containing antibiotics with pipette up and down for at least 3 times.
2) The tumor tissues were cut into tubes of 1-3mm^3, pipetted and washed with PBS containing antibiotics.
3) 3-5ml digestion solution was added to the tissue tubes and the tumor tubes were digested for at least 30 minutes to ensure that the tumor tubes became a single-cell suspension.
4) The cells were mixed with Trypan Blue solution and the cells were counted.
5) The cells were centrifuged and pelleted; the pellets were resuspended in TIL culture medium.
6) One million cells/well of 24-well-plates of cell culture were pipetted to the plates.
7) The plates were placed at 37°C, 6% CO_2 and 60% humidity incubator.
8) The TIL culture medium was changed every 3 days until there was obvious. growth of TILs.

3.2.4.3 Co-culture of organoids and paired TILs

200ng/ml IFN-γ was added to culture organoids for the enhancement of antigen presentation. The culturing organoids were cultured overnight.

Tissue culture-treated 96-well plate was coated with 5μg/mL anti-CD-28 antibody in PBS (50μL per well). The plate was wrapped with Parafilm and incubated for 24 hours, 4°C. In the meantime, it was proceeded with the

following steps. The anti-CD28 antibody provided co-stimulatory signals during coculture.

Plated each of the group in triplicate:

CRC organoids + TILs: 100µL (1×10^4) CRC organoids + 100 µL (5×10^4) TILs per well.

3.2.5 Procedures of droplet digital PCR

The principle of the technique is illustrated in Figure 6.

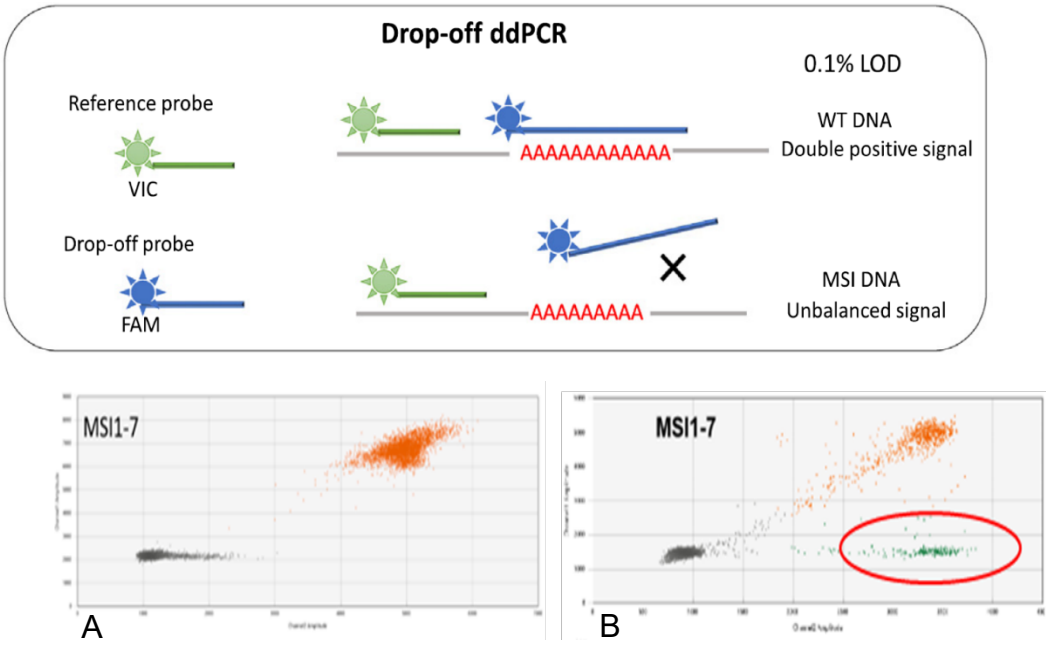

Figure 6: Detection of MSI with drop-off digital PCR

Illustration of the drop-off PCR methodology (Top figure). A target probe with a red fluorescence is designed against the wild-type polyA locus, which is highly unstable in the MSI tumors, and a reference probe a green fluorescence is designed against a stable DNA sequence in the same PCR amplicon. In the normal tissues, the target and reference probes generate equal amount of red and green fluorescence, resulting in net orange fluorescence signal output (left panel in B). When mismatch occurs in tumor tissues (MSI), the altered polyA sequences disrupt the binding of the reference probe to the locus, resulting in loss of the red fluorescence signal, and the net fluorescence signal output becomes green as highlighted in the red circle (right panel in B).

1) Primer and probe preparation:

Before performing ddPCR, forward and reverse primers, forward and reverse probes were prepared. And the stimulated signaling of probes labelled with different fluorescein can be read with different channels, which are listed in Table 12.

Table 12. Preparation of primers and probes for ddPCR

Primer and probe No.	Primers and probes	Signal channel
1-7	Forward primer	
	Reverse primer	
	Forward probe	CY5
	Forward probe	ROX
2-14	Forward primer	
	Reverse primer	
	Forward probe	FAM
	Reverse probe	HEX

2) Preparation of reaction system:

In order to produce the amplification of targeted genes, the reaction reagents should be prepared for ddPCR.

Table 13. Reaction system preparation for ddPCR

Components	Volume (μL)
ddPCR Multiplex Supermix for Probes (BioRad)	7.5
Template DNA (10ng/uL)	3
Primer mix (10μM)	3
ddH2O	16.5
Total Volume	30

3) PCR amplification:

After preparation of reaction reagents for ddPCR to amplify targeted genes, procedures for ddPCR amplification are listed in table 14.

Table 14. Procedures preparation of ddPCR amplication

Procedures	Temperature	Time	Cycling
Chip sealing	50°C	10mins	1
Pre-denaturation	95°C	5mins	1
Denaturation	94°C	30s	40
Annealing	58°C	15s	
Extension	72°C	20s	

4) Result reading and data analysis

The chip preparation, PCR amplification, chip scanning and analysis were performed with BioDigital SCI PCR systems (Shanghai Turtle Tech Co, Ltd, China).

3.2.6 Flow cytometry analysis

1) Preparation of established TILs

An appropriate amount of established tumor-infiltrating lymphocytes (TILs) was collected and stained with trypan blue. Cells were counted using a cell counter to ensure a viability of ≥80%. After counting, the cell concentration was adjusted to 1×10^6 cells/tube for subsequent analysis.

2) Multi-parameter Flow Cytometry

Cells were first incubated with the live/dead cell dye LIVE/DEAD Fixable Blue (1:1000 dilution) at 4°C in the dark for 20 minutes to exclude dead cells. Fc receptors were then blocked by incubation with 5% human AB serum for 15 minutes at room temperature. The following antibody combination was used for surface markers: CD3-APC, CD4-FITC, CD8-BV510, PD-1-BV421, and CD25-PE (see Table 15 for antibody details). The antibody mixture was incubated at 4°C in the dark for 30 minutes, washed twice with PBS, and resuspended in 300μL of FACS buffer for analysis.

Table 15. Informations of antibodies for Flow Cytometry

Antibodies	Fluorescein	Clone No.	Working concentration	Supplier
PD-1	BV421	NAT105	4.0 μg/mL	BioLegend
CD-25	PE	BC96	2.0 μg/mL	BioLegend
CD-8	BV510	SK1	2.0 μg/mL	BioLegend
CD-4	FITC	OKT4	0.5 μg/mL	BioLegend
CD-3	APC	OKT3	2.0 μg/mL	BioLegend

Abbreviations: PD-1, programmed cell death protein-1; CD-25, the α chain of the interleukin-2 receptor (IL-2R), which together with the β chain (CD122) and γ chain (CD132) forms a high-affinity heterotrimeric receptor complex; CD-8, Cluster of differentiation 3 of T cell receptor complex; CD-4, Cluster of differentiation 4 of T-helper cell glycoprotein; CD-3, Cluster of differentiation 3 of T-lymphocyte cytotoxic glycoprotein; BV421, Brilliant Violet 421; PE, Phycoerythrin; BV510, Brilliant Violent 510; FITC, Fluorescein isothiocyanate; APC, Allophycocyanin.

3) Data Acquisition and Gating Analysis

Data acquisition was performed using DxFLEX flow cytometery (Beckman Coulter, USA), with at least 100,000 events acquired per sample to ensure sufficient lymphocyte populations for analysis. Flow rate was maintained in low-speed mode to guarantee data quality. Fluorescence minus one (FMO) controls were established to determine positive thresholds for each marker, while single-stained controls were used for fluorescence compensation settings.

Data analysis was performed with FlowJo software (version 10.8.1) with standardized gating strategies: (1) Selection of lymphocyte populations via forward scatter/side scatter (FSC/SSC) gates; (2) Removal of doublets using FSC-H/FSC-A biparametric gating; (3) Dead cell exclusion via live/dead cell dye staining; (4) Selection of T cells within live cells based on CD3 expression; (5) Differentiating helper T cells ($CD4^+$) and cytotoxic T cells ($CD8^+$) within T cells using CD4/CD8 double staining; (6) Analyzing PD-1 and CD25 expression levels in $CD4^+$ and $CD8^+$ T cell subsets, respectively, and calculating each subset's percentage of total T cells.

4) Quality Control

Quality control standards included: (1) Cell viability ≥80%; (2) Double-stained cell proportion <10%; (3) Minimum event count of ≥150 per analyzed cell subset to minimize statistical bias; (4) Inclusion of unstained controls, single-stained controls, and FMO controls for background fluorescence and threshold calibration.

5) Statistical Analysis

Results are expressed as the percentage of each T cell subset relative to total viable cells or total T cells.

3.2.7 Drug sensitivity assay of CRC organoids

1) The complete culture medium was aspirated from the 48-well plate.
2) 200μl Tryple Express enzyme solution (Gibco) with 10μL Y-27632 was added to each well. Incubated and digested at 37°C for 2–5 minutes. The organoids were pipetted up and down every 2-5 minutes and the wells were observed under an optical microscope. When the organoids were digested into 3–5 cells clusters, 800μl Advanced DMEM/F12 medium was added to terminate the organoid digestion.
3) The organoids digestion was pipetted into a 15ml centrifuge tube. The tube was centrifuged at 300g, 4°C for 5 minutes, the supernatant was discarded and the pellet was resuspended in 2ml CRC complete culture medium. The mixture was centrifuged at 300g, 4°C for 5 minutes. The supernatant was discarded.
4) Clusters were seeded into a 96-well plate with the density of 5,000 clusters per well in 20μL Matrigel, followed by supplementation with 200μL complete

culture medium of CRC organoid per well. After 24 hours, the medium was replaced with fresh complete culture medium of CRC organoids containing different concentration gradients of chemo-drugs.

5) After the plate was incubated for 72 hours, 100μl of CellTiter-Blue reagent was added to each well and the plate was incubated for 1 to 2 hours to measure the viability of organoids under standard culture conditions. Fluorescence intensity was quantified with a microplate reader configured for 560nm excitation and 590nm emission wavelengths.

3.3 Software and websites of statistical analysis

The following statistical programs were used:

For bioinformatic analysis R Language (http://www.R-project.org), RStudio (http://www.R-project.org) and Bioconductor (https://www.bioconductor.org) were used.

The curves and IC50 of drug sensitivity testing were obtained with nonlinear regression method of GraphPad Prism 10 (https://www.graphpad.com).

The data of flow cytometry were analyzed and visualized with FlowJo 10.

4. Results

4.1. Prospective construction of a CRC cohort

A total of 102 CRC tissue specimens and corresponding clinical information were collected in this prospective cohort study with patients enrolled from June 22nd, 2024 to December 10th, 2024 at Ruijin Hospital. Clinical and pathological information of 102 CRC patients is listed in Table 16. All the tumor samples were sequenced with the targeted gene panel including essentially all the actionable gene targets.

Table 16. Clinical and pathological informaton of 102 CRC patients

Patients' characteristics	***N***
Age (years)	
Mean age (range)	61(36-83)
≤60	40
>60	62
Male	65
Female	37
Stage	
I	7
II	27
III	27
IV	8
Unknown	18
WHO-Grading	
Low	6
Medium	71
High	1
Unknown	9
MSI Status	
MSS	75
MSI	14
Unknown	13

4.2 Molecular characterization of the CRC cohort

Targeted sequencing was performed for all the tumor samples with the 818-gene panel. The 818 genes included in this panel are listed in the appendix Table 1.

The most frequent genetic mutations detected are *TP53* (63.7%, 65/102), *APC* (55%, 56/102), *KRAS* (36.3%, 37/102). The heat map visualizes all mutations found in all 102 CRC cases (Figure 6).

One characteristic stands out is the extremely high mutation burden in MSI-H tumors (Z1253612, Z1263465, Z1263478, Z1295793, Z1297030, Z1313804, Z1280347, Z1247153, Z1284276, Z1269569, Z1312363). *POLE* mutations (Z1312363, Z1269569, Z1285789, Z1215903, Z1259419, Z1279391, Z1292212) and *POLD1* mutations (Z1295793, Z1297030, Z1260613) were also tested, which set these tumors apart from the rest (Figure 7).

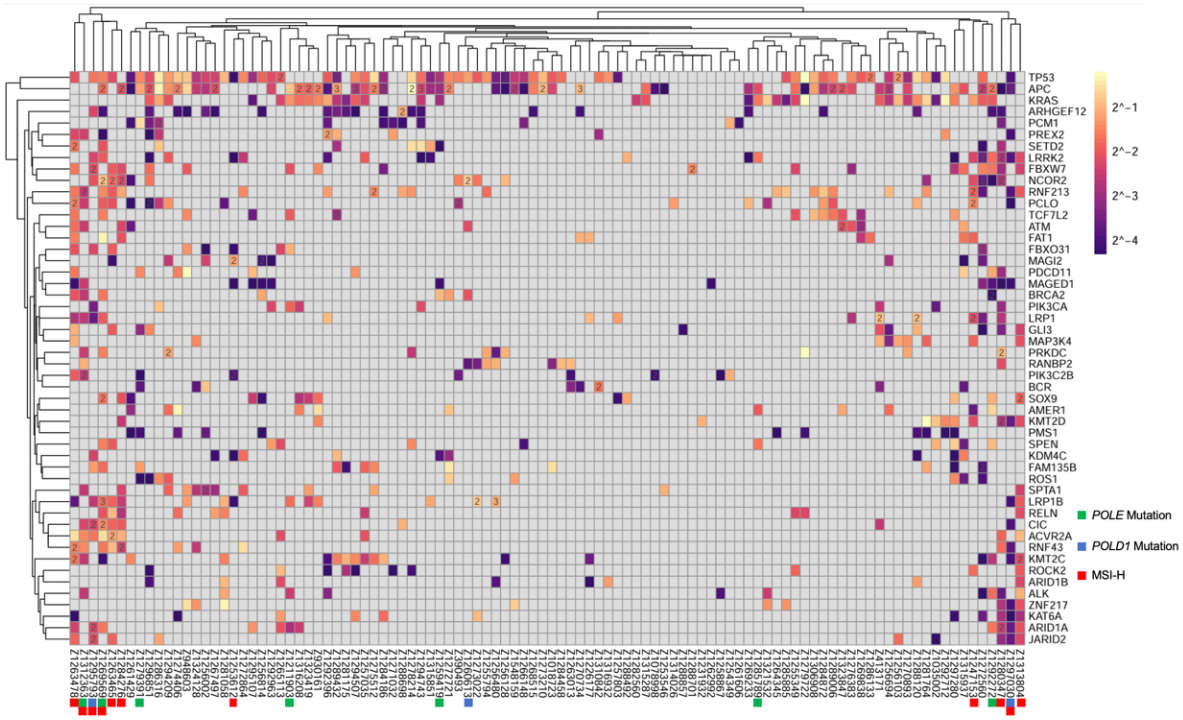

Figure 7. Mutational landscape of the CRC cohort

The heatmap displays a comprehensive mutation matrix. The hierarchical clustering dendrogram at the top of the heatmap groups patients based on their similar mutation patterns,

revealing distinct molecular subtypes within the cohort. The color scheme indicates the frequency of the mutation in tumors as shown in the bar on the right.

In addition, the specific mutation sites of the most frequently mutated genes *TP53*, *APC*, *RAS*, and *ARHGEF12* were illustrated using Lollipops. These visualizations allowed the mutation sites and their frequency to be represented in different colors and heights (Figure 8).

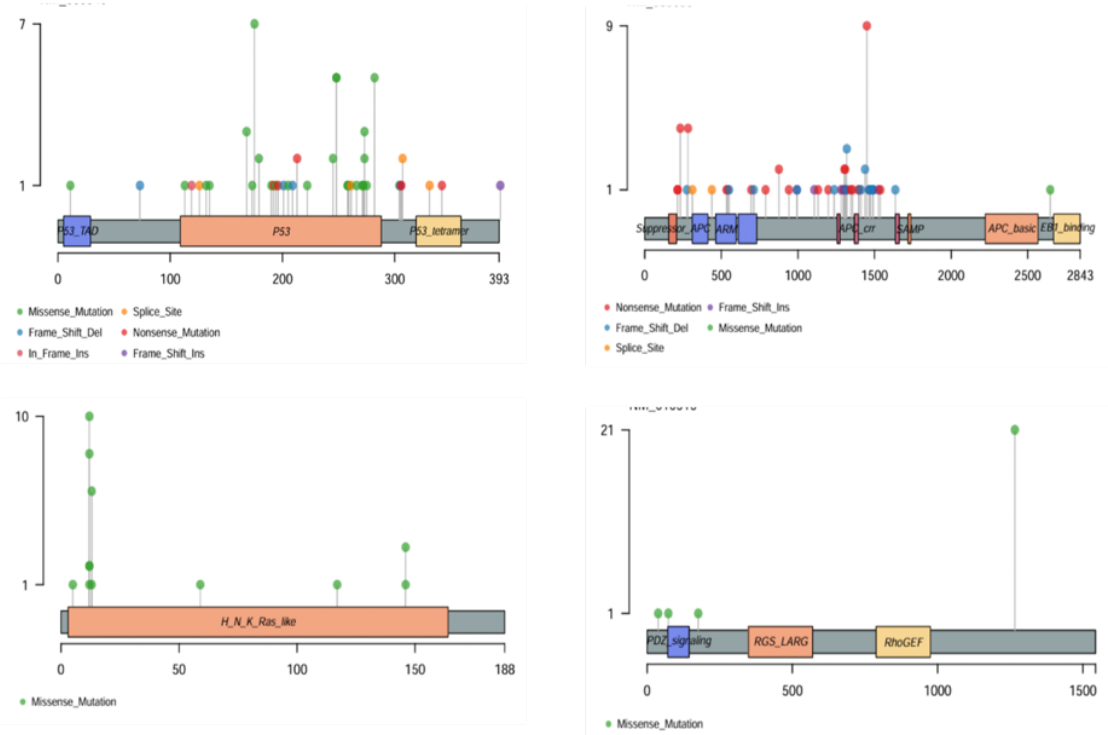

Figure 8: Mutation sites and types of TP53, APC, RAS, and ARHGEF12

If a mutation occurs in the region of promotor, factors fail to bind to the gene promoter region, preventing expression of genes regulated by p53. This leads genetic inactivation, loss of tumor suppressor function, and promotion of tumorigenesis. The genetic sites visualized with lollipops represent point mutations. A higher number of mutation sites indicates a hotspot mutation. Height represents the frequency of mutations; colors of lollipops denoted mutation sites and types of mutations.

4.3 MSI status of the cohort

With a droplet digital PCR (ddPCR) method developed by Mission Medical Biotechnology, China (Figure 6), all tumor samples were analyzed using the

five-loci panel, which includes single nucleotide repeats at gene loci *ACVR2A*, *GUCY1A2*, *SMG1*, *RNF112*, and *DIDO1*.

Among the 102 samples, 14 (13.7%) were identified as MSI (Figure 9). Interestingly, in the MSI-positive tumor tissues, the MSI signal fraction was lower than 20%, indicating that proportions of tumor cells in these tumor tissues were lower than 20%, which is the standard requirement of other methods for MSI detection. This suggested that ddPCR is more sensitive than the standard PCR detection method for MSI.

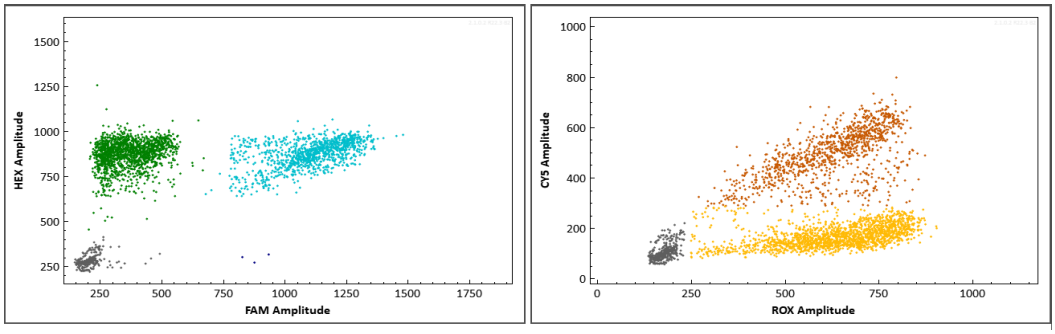

A

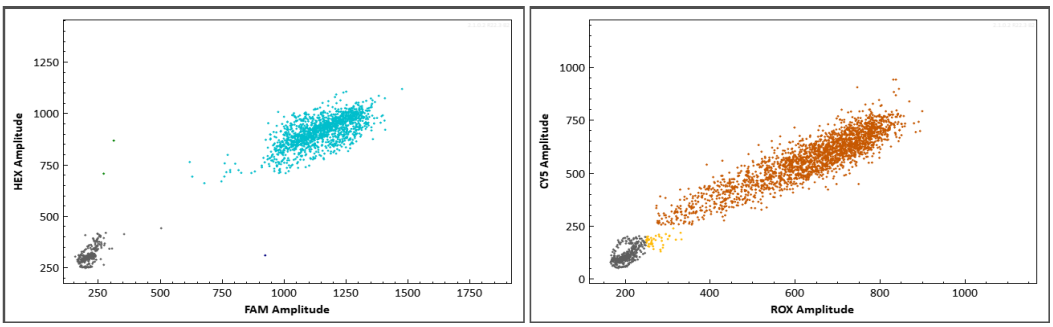

B

Figure 9: Examples of two CRC cases with MSI (A) or MSS status (B) detected by drop-off PCR

The figures were the examples of ddPRC detection for MSI tumor (A) and MSS tumor (B).

4.4. Results of established CRC organoids

Among the resected tumors, 40 CRC samples from different patients were randomly selected including 30 MSS tumor samples and 10 MSI tumor samples.

And a total of 30 CRC organoids and 35 paired TILs were established (Appendix Table 1). The successful establishment rate of CRC PODs and TILs was 75%, 87.5% respectively.

All the CRC organoids were established with the standard procedures described above. However, only 3 MSI CRC organoids could be established. The clinical and pathological information of all organoids established are listed in table 17.

Table 17. Clinicopathological information of established organoids

PDO ID	Age (Year)	Gender	Stage	MS Status
CRC-OR-01(Z1256480)	64	Male	T4N1M0, II	MSS
CRC-OR-02 (Z1255794)	78	Male	T4N2M0, III	MSS
CRC-OR-03 (Z1273210)	39	Male	T3N1M0, III	MSS
CRC-OR-04 (Z1280347)	65	Male	T3N1M0, III	MSS
CRC-OR-05 (Z1272721)	67	Male	T3N0M0, II	MSS
CRC-OR-06 (Z1274406)	72	Male	T3N0M0, II	MSS
CRC-OR-07 (Z1263465)	71	Female	T4N1M0, III	MSI-H
CRC-OR-08 (Z1263478)	73	Female	T3N0M0, II	MSI-H
CRC-OR-09 (Z1346556)	53	Male	T3N0M0, II	MSS
CRC-OR-10 (Z930161)	70	Male	T2N1M0, III	MSS
CRC-OR-11 (Z1306908)	73	Male	T2N2M0, III	MSS
CRC-OR-12 (Z1270893)	65	Male	T3N0M0, II	MSS
CRC-OR-13 (Z1323419)	63	Male	T3N0M0, II	MSS
CRC-OR-14 (Z1351303)	64	Male	T3N2M1, IV	MSS
CRC-OR-15 (Z1336414)	67	Male	T3N0M0, II	MSI-H
CRC-OR-16 (Z1254349)	60	Male	T3N2M1, IV	MSS
CRC-OR-17 (Z1256694)	75	Male	T3N0M1, IV	MSS
CRC-OR-18 (Z1256814)	77	Male	T4N1M1, IV	MSS
CRC-OR-19 (Z1259419)	43	Female	T2N0M0, I	MSS
CRC-OR-20 (Z1255349)	77	Female	T3N10, III	MSS
CRC-OR-21 (Z1256103)	59	Female	T2N0M0, I	MSS
CRC-OR-22 (Z1257035)	72	Female	T2N0M0, I	MSS
CRC-OR-23 (Z1275572)	71	Male	T3N2M0, III	MSS

CRC-OR-24 (Z1255793)	43	Male	T1N0M0, I	MSS
CRC-OR-25 (Z1333557)	62	Male	T2N0M0, I	MSS
CRC-OR-26 (Z1323847)	63	Male	T3N0M0, II	MSS
CRC-OR-27 (Z1328543)	60	Male	T3N0M0, II	MSS
CRC-OR-28 (Z1324128)	52	Female	T2N0M0, I	MSS
CRC-OR-29 (Z1354890)	48	Female	T3N0M0, II	MSS
CRC-OR-30 (Z1354184)	52	Female	T3N0M0, II	MSS

4.4.1 Histological characterization of CRC Organoids

4.4.1.1 Morphology

To characterize the organoid cultures established, hematoxylin and eosin (H&E) staining was performed on paired tumor tissue samples and established organoids, demonstrating that the established organoids faithfully recapitulated the histological characteristics of the primary cancer samples (Figure 10). Both the primary tumors and the organoids exhibited significant nuclear atypia and irregular structures. Three to four micrometers thick H&E-stained tissue sections of all 102 CRCs are available for comparison.

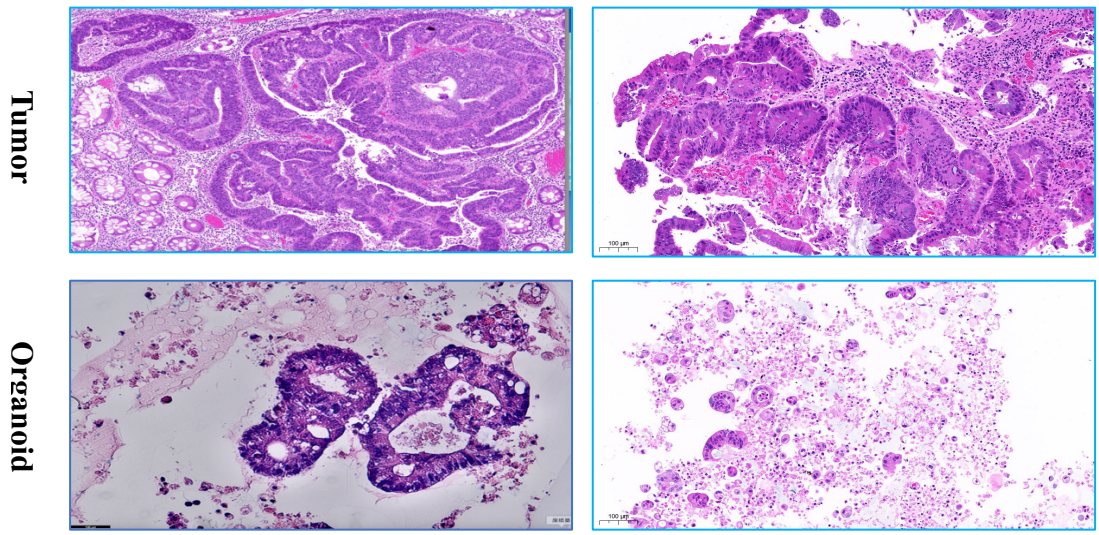

Figure 10: Morphological characterization of CRC organoids and primary tumor tissues

H&E staining indicates the morphological similarity between the original tumor tissues and established CRC organoids. (Scale bar, 100μm).

4.4.1.2 Immunohistology

To further characterize histological characteristics of organoids, immuno-histochemistry (IHC) was performed to examine the expression patterns of common CRC biomarkers such as Caudal Type Homeobox Transcription Factor 2 (CDX-2), Cytokeratin 20 (CK-20), and Ki-67 in tumor tissues and corresponding organoids. The gastrointestinal differentiation marker CDX-2 for gastric, small intestinal and colonic epithelial cells, along with the epithelial marker CK-20 and proliferative marker Ki-67, demonstrated extensive expression and elevated proliferation activity in both primary tumors and organoids (Figure 11).

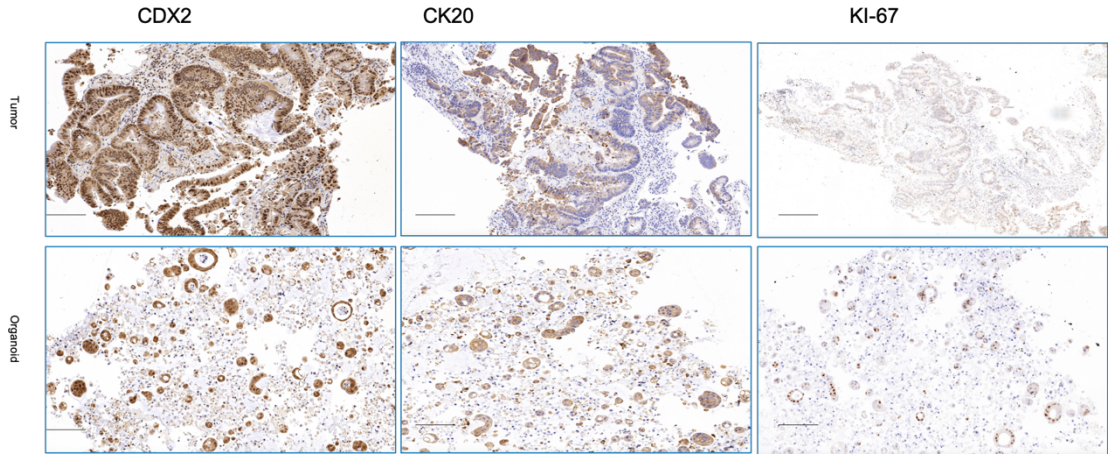

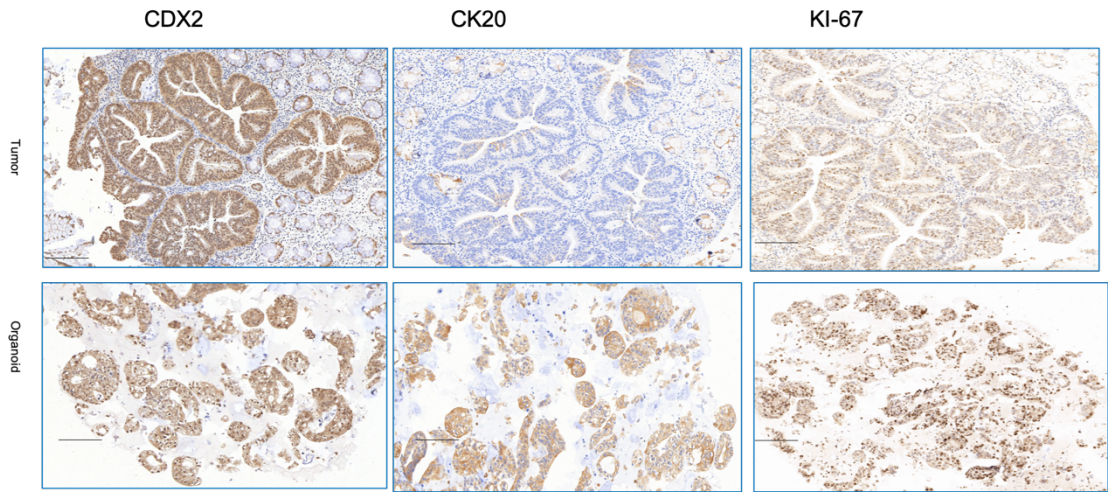

Figure 11: IHC of CRC organoids and primary tumor tissues

IHC staining for CDX2, CK20, Ki-67 reveals consistency between successfully established organoids and the primary tumor tissues. (Scale bar, 50μm)

4.4.1.2 Immunofluorescence

To further investigate the histological and morphological characteristics of the established CRC organoids, immunofluorescence staining and analysis was conducted targeting Epithelial Cell Adhesion Molecule (EpCAM) and tumor stem cell marker (CD-133). The results showed that almost all cells in the established CRC organoids expressed EpCAM, and a small subset of organoid cells expressed CD-133, which may be related to the organoids' self-renewal capacity and differentiation (Figure 12). Combined with the analysis of HE and IHC staining results, the in vitro established CRC organoids were able to recapitulate the histological and morphological characteristics of the primary tumor tissues, and a small portion of CD-133-expressing stem cells in the CRC organoids maintained self-renewal and differentiation.

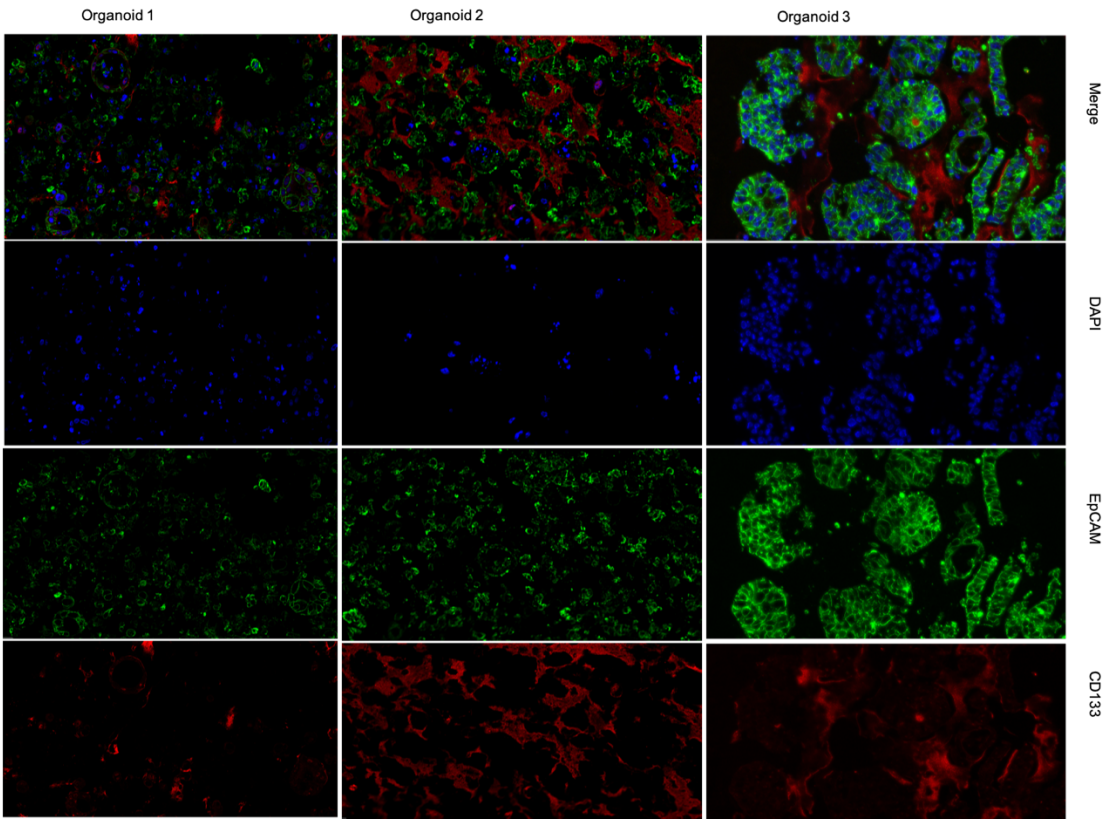

Figure 12: The localization of EpCAM, DAPI and CD-133 in CRC organoids by IF staining

In IF staining, the markers of EpCAM (Green), DAPI (Blue), and CD-133 (Red) were all expressed in the established CRC organoids, which revealed that the organoids possessed the characteristics of both epithelial cells and stem cells. (Scale bar, 50μm).

4.5 Targeted gene sequencing between primary CRC tumors and paired organoids and their molecular characterization

Organoid culture selects cancer cells with stem cell properties. To be useful in precision medicine, organoids should faithfully represent the genetic background of the tumors derived from. Four CRC organoids and paired tumor tissues were randomly selected for targeted sequencing. As expected, organoids exhibited similar overall mutation profiles as their corresponding primary tumors (Figure 13). Essentially, all the driver gene mutations, such as *TP53*, *APC*, or *KRAS*, from primary tumors were retained in the organoids, but many passenger gene mutations with low frequency were lost (Figure 13),

suggesting that organoids cannot completely recapitulate the genetic heterogeneity of primary tumors.

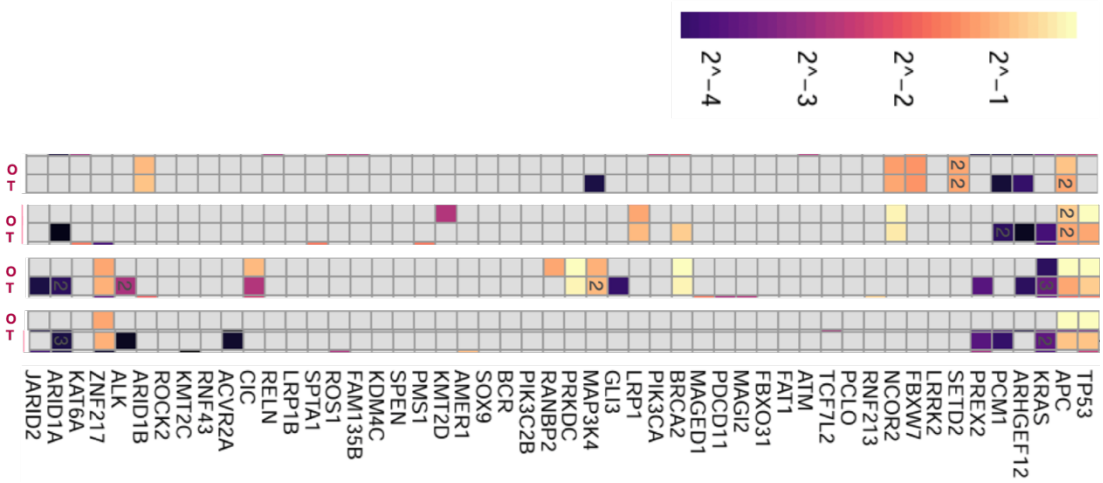

Figure 13: The genetic characteristics were maintained between the primary cancer samples and the established CRC organoids

The top 50 mutated genes were identified through sequence of targeted genes and single nucleotide variant analysis of paired primary tumor tissues and established CRC organoids. The graphic representation on the top of the figure is the distribution of the targeted genes percentage mutation for 4 paired tumor and organoid samples.

T: Tumor tissues; O: Organoids.

4.6 CRC organoid models in drug sensitivity assay and targeted therapy

Established organoids of two CRC patients were chosen to perform drug sensitivity assays.

In the first case, four chemotherapy drugs were selected based on National Comprehensive Cancer Network (NCCN) guidelines to perform *in vitro* drug sensitivity screening in a PDO culture. Drug sensitivity data clearly demonstrated that the first selected patient is more sensitive to the second-line drug, docetaxel, than the three first-line drugs recommended by NCCN guidelines, Irinotecan, Oxaliplatin and 5-FU (Figure 14).

An important molecular feature of the second CRC patient was the presence of a *HER2*-amplification. Thus, four targeted therapeutics, commonly used in CRC treatment, Trastuzumab, Trastuzumab-Deruxtecan, and Cetuximab were used to test targeted cell viability (Figure 14).

Trastuzumab demonstrated the strongest cytotoxic effects, exhibiting typical S-shaped dose-response curve characteristics. At low concentrations (0.01-0.1μM), cell viability remained at 95-100%, but at 1μM concentration, cell viability dropped sharply to 75%, and at the highest concentration of 10μM, cell viability was reduced to only 10% (Figure 14). This steep dose-response curve indicates that trastuzumab has a clear therapeutic window and potent anti-tumor effects.

Trastuzumab-Deruxtecan, as a next-generation antibody-drug conjugate (ADC), exhibited moderate but sustained cytotoxic effects. This novel drug showed some inhibitory effect at all tested concentrations, with cell viability reaching 50% at 1μM concentration, approaching its IC50 value. The dose-response relationship of Trastuzumab-Deruxtecan was relatively linear, suggesting it has progressive and cumulative killing effects,

Cetuximab displayed the mildest cytotoxic effects, with a relatively gentle dose-response curve. Even at the highest concentration of 10μM, cell viability remained around 60%, indicating relatively low cytotoxicity. This characteristic suggests that Cetuximab may be more suitable as an adjuvant therapeutic drug or for preventive treatment.

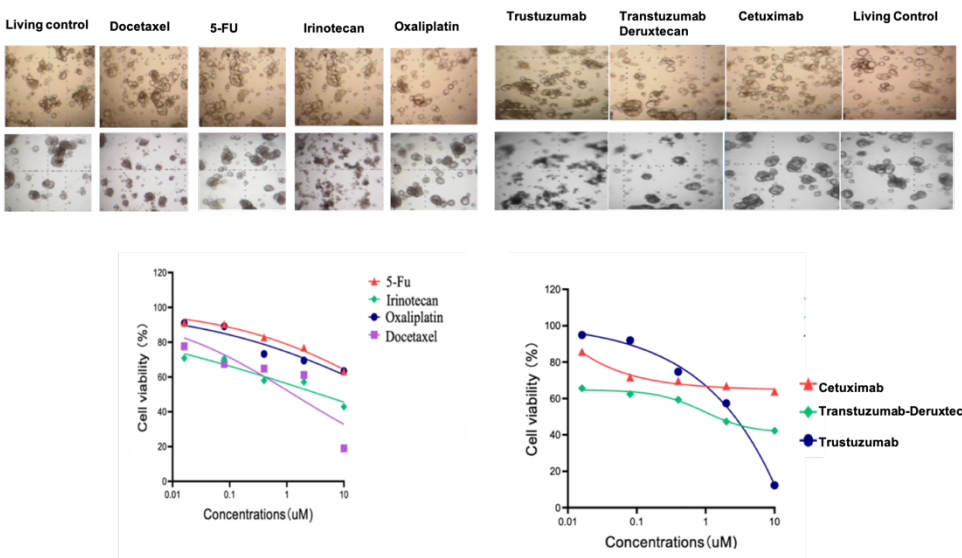

IC50 \ Drugs	5-FU	Irinotecan	Oxaliplatin	Docetaxel
IC50(μM)	64.5	3.837	56.39	1.308

IC50 \ Drugs	Cetuximab	Trastuzumab Deruxtecan	Trastuzumab
IC50(μM)	>100	1.638	1.916

Figure 14: Drug sensitivity assay

The left panel demonstrate that the selected patient was more sensitive to the second-line drug, docetaxel, than the three first-line drugs recommended by NCCN guidelines, Irinotecan, Oxaliplatin and 5-FU. The right panel show that the tumor cells of the patient were more sensitive to Trastuzumab than Cetuximab and Trastuzumab-Deruxtecan.

4.7. Establishment and Analysis of TILs

With the resected CRC tumor, 40 CRC samples corresponding to the CRC organoids establishment were performed to establish CRC TILs were established. Finally, 35 CRC TILs were successfully established with a successful establishment rate of 87.5%.

All the CRC TILs were established with the standard procedures described above. Also, 3 MSI CRC TILs could be successfully established. The clinical and pathological information of all organoids established are listed in the Figure 2 of appendix. However, 5 CRC TILs from corresponding tumors were not successfully established. The reason why they could not be successfully established probably was that there was a lack of the infiltration of lymphocytes in the tumor tissues. Therefore, it was required to perform IHC with CD-45 to validate whether lymphocytes existed in tumor tissues.

After the establishment of CRC TILs, multi-parameter of PD-1 BV421; CD-25 PE; CD-8 BV510; CD-4 FITC; CD-3 APC were performed to analyze the established CRC TILs with Flow Cytometry. The analysis results demonstrate in tumor 1: 87.4% CD3+ cells (proportion of total lymphocytes), 53.1% CD25+ cells (proportion of CD4+ cells), 76.2% CD4+ T cells (proportion of CD3+ cells), 7.27% CD8+ T cells (proportion of CD3+ cells), 17.8% PD-1+ cells (proportion within the corresponding T cell subset); in tumor 2: 98.4% CD3+ cells (proportion of total lymphocytes), 72.0% CD25+ cells (proportion of CD4+ cells), 71.4% CD4+ T cells (proportion of CD3+ cells), 14.6% CD8+ T cells (proportion of CD3+ cells), 17.7% PD-1+ cells (proportion within the corresponding T cell subset); in tumor 3: 90.4% CD3+ cells (proportion of total lymphocytes), 50.3% CD25+ cells (proportion of CD4+ cells), 74.4% CD4+ T cells (proportion of CD3+ cells), 13.5% CD8+ T cells (proportion of CD3+ cells), 17.7% PD-1+ cells (proportion within the corresponding T cell subsets).

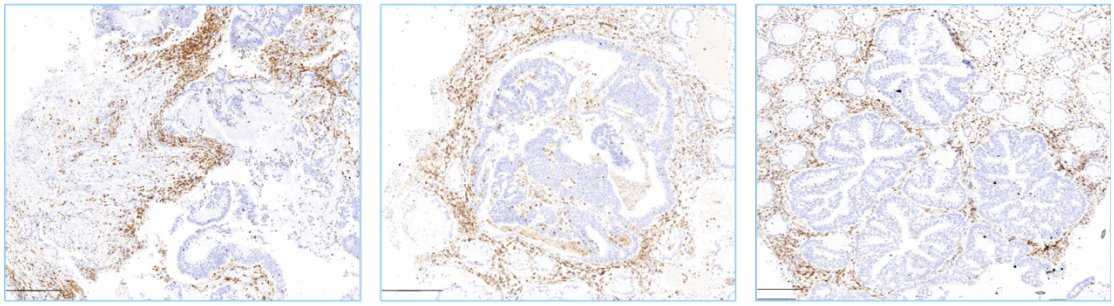

Tumor 1 Tumor 2 Tumor 3

Figure 15: CD-45 immunohistochemistry of CRC tumor tissues

The CRC tumor tissues were stained with CD45 antibodies. CD45 was used to mark and distinguish immune cells from the tumor tissues within the TME. The IHC staining with CD-45 was visualized in these tumor tissues, which demonstrates immune cells infiltrate in the tumor tissues and provide the evidence to establish TILs with these tumor tissues (Scale bar, 100μm).

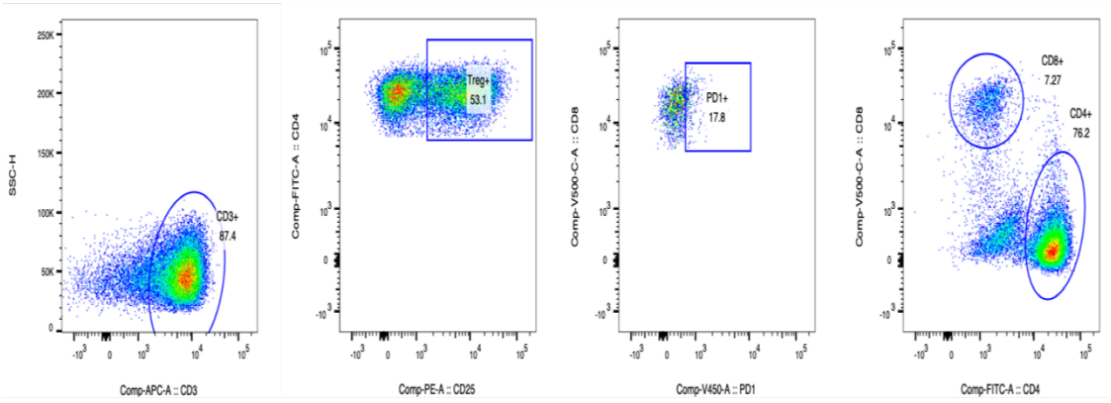

A

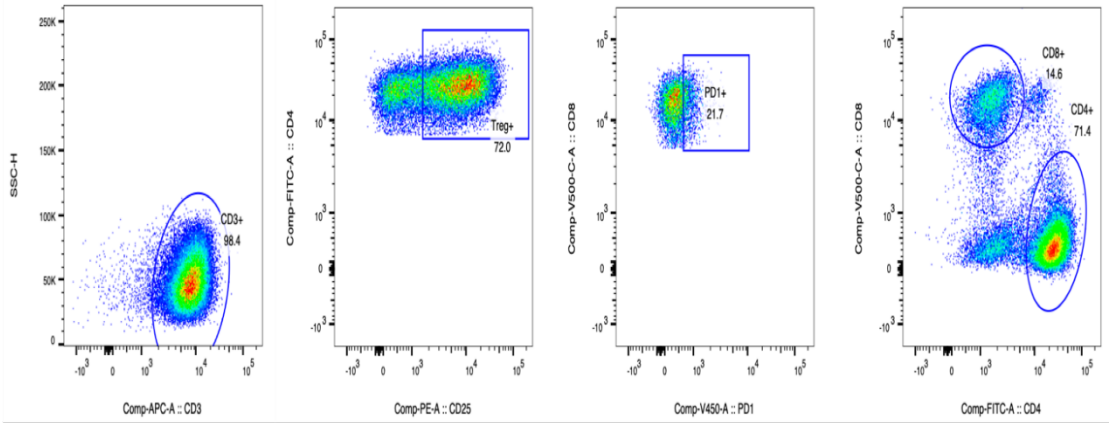

B

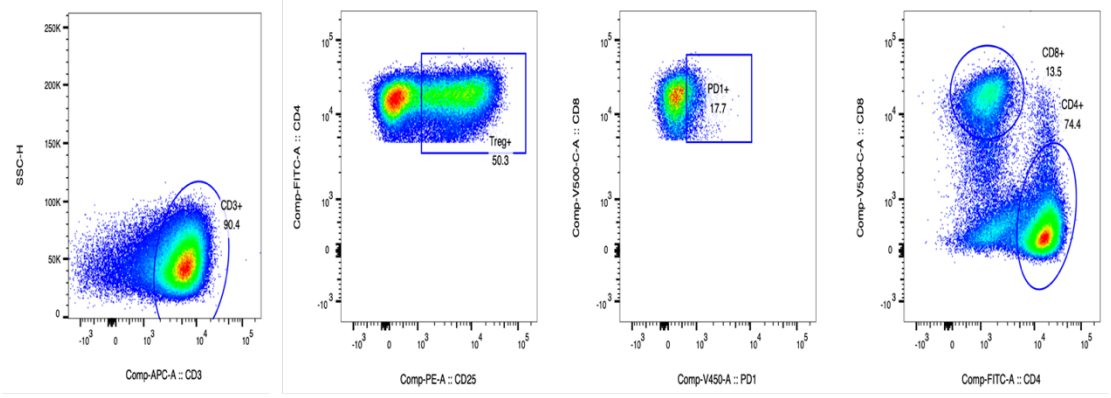

C

Figure 16: The analysis diagram of flow cytometry describes the results of multiparametric immunophenotyping of TILs from three CRC tumors

A, B and C TILs were established from tumor 1, 2 and 3 respectively above. CD3+ cells, proportion of total lymphocytes; CD4+ T cells, proportion of CD3+ CD4+cells; CD8+ T cells, proportion of CD3+ CD8+ cells; PD-1+ cells, proportion within corresponding T cell subsets; CD25+ T cells, proportion of regulatory T cells were present in the diagrams.

4.8 CRC organoid models in adoptive cell therapy

In one CRC case (demographic and genetic information) organoid and TILs coculture was performed.

Time-lapse analysis unveiled TIL-mediated cytotoxicity against CRC PDOs of CRC with microscopy over 72-hour observation. The co-culture system demonstrated temporal dynamics of TIL-mediated tumor disintegration, with organoids maintaining their characteristic 3D architecture and intact cellular boundaries at the 6-hour timepoint (Figure 17). TILs were observed in close proximity to organoid structures, establishing initial contact with the tumor targets consistent with immune synapse formation. At 24 hours post-co-culture initiation, subtle morphological changes became apparent in the organoid architecture, with slight irregularities in structural integrity and evidence of early cytotoxic effects (Figure 17). This intermediate phase corresponded with enhanced TIL infiltration and activation.

By 48 hours, substantial organoid destruction was evident, characterized by significant loss of 3D structure, cellular fragmentation, and apparent compromise of organoid integrity (Figure 17). The cytotoxic effects intensified markedly at this timepoint, reflecting the time-dependent nature of TIL-mediated tumor cell killing mechanisms including perforin-granzyme pathways and cytokine-mediated cytotoxicity. The most pronounced killing effect was observed at 72 hours, where organoid structures exhibited extensive cellular debris, near-complete loss of morphological integrity, and widespread evidence of successful TIL-mediated tumor destruction. This temporal progression aligns with established protocols for co-culture system of organoids and TILs that

demonstrates maximal cytotoxic activity within 72 hours of co-culture initiation (Figure 17).

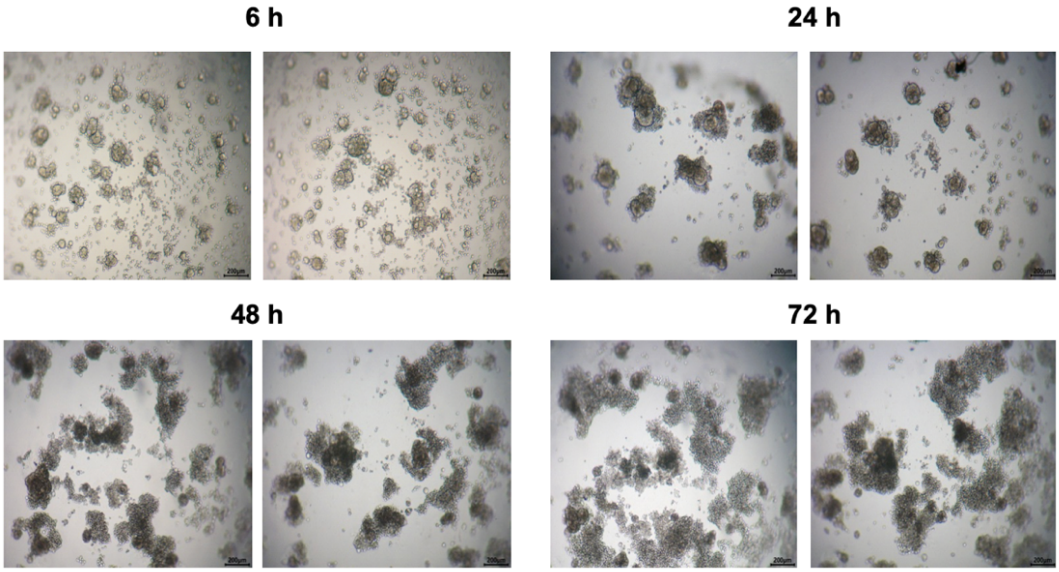

Figure 17: Co-culture system of CRC organoids and paired TILs

Until 6 hours, TILs approach to intact tumor organoids and start to attack CRC organoids. Until 72 h TIL-mediated tumor disintegration had occurred completely.

5. Discussion

5.1. Discussion of results

This study integrated CRC targeted sequencing technology, patient-derived organoid models, and tumor-infiltrating lymphocyte co-culture systems, providing an innovative research platform for CRC precision medicine. This multi-dimensional research approach not only revealed the molecular mechanisms of CRC development, but also established a solid theoretical foundation for the development of individualized treatment strategies[167-169].

5.1.1. Clinical and pathological characteristics of the CRC cohort

This study analyzed the clinical and pathological characteristics of 102 CRC patients, with a focus on the frequency of MSI. The MSI frequency in our study was 13.7% (14/102, 14 patients with known MSI status) consistent with the reported frequency[171,170]. A French multicenter study has shown an MSI frequency of 12% in CRC patients[171].

5.1.2 Molecular characterization of the CRC cohort

The genomic characteristics of CRC exhibit high heterogeneity, and the application of targeted sequencing technology enables us to systematically identify mutation patterns of key driver genes[172,173]. Through analysis of large-scale cohorts, studies have found that the mutation frequencies of genes, such as *TP53*, *APC*, and *KRAS* are significantly higher than other genes[174,175]. MSI-H tumors, along with tumors with *POLE* and *POLD1* mutations exhibit significantly increased tumor mutational burdens due to defects in mismatch repair genes, potentially generating a large number of neoantigens that

subsequently activate the immune response[176], resulting in favorable responses to immune checkpoint inhibitor therapy[177,178].

MSI-H tumors typically have a mutation burden of 10-100 mutations/Mb, but in some cases can exceed 100 mutations/Mb. This high mutation density originates from dMMR, primarily involving the functional loss of proteins such as MLH1, MSH2, MSH6, and PMS2. When these repair proteins cannot recognize and repair spontaneous mutations, significant mutation accumulation occurs within cells, leading to a substantial increase in tumor mutational burden (TMB) and alteration of microsatellite sequences[179].

Although MSI-H, *POLE*-mutated, and *POLD*1-mutated tumors all exhibit high mutation burden, there are significant differences in their mutational characteristics and immune microenvironment. MSI-H tumors are primarily characterized by MSI and dMMR, while *POLE*/*POLD1*-mutated tumors result from DNA polymerase proofreading defects[180,181]. Accurate identification of MSI-H and *POLE/POLD1* mutation status is vital for personalized immunotherapy[182,183].

The targeted sequencing approach utilized in this study represents a focused genomic profiling strategy that concentrates on the most clinically relevant genes in CRC[133,184,185]. This methodology allows for deep coverage analysis of critical driver genes while maintaining cost-effectiveness[186]. The clustering analysis enables identification of molecular subtypes within the cohort, which is essential for understanding tumor heterogeneity and potential therapeutic vulnerabilities[185,186].

Overall, our findings are largely consistent with published large-scale genomic studies[187]. The most frequently mutated genes are *TP53*, *APC*, and *KRAS*, genes well known for their roles in CRC development. *TP53* 63.7% (65/102) mutations is the most frequent alteration, consistent with reports of *TP53* mutations in 50-77% of CRC[188-191]. *APC* mutations, fundamental to the adenoma-carcinoma progression, are mutated in 55% (56/102) of tumors, also

consistent with 27-70% of mutation frequencies according to multiple studies[192-196]. Interestingly, no mutations were identified in *TP53*, *APC*, and *KRAS* in 15 tumor samples sequenced in this cohort, suggesting that these tumors may originate with different mechanisms, which warrants further studies.

The mutation patterns identified with targeted sequencing have direct implications for precision medicine in CRC[197]. *KRAS* mutations, particularly *KRAS G12* variants, have been associated with resistance to anti-EGFR therapies such as cetuximab and panitumumab, but may predict response to specific targeted therapies[198-201]. *BRAF* mutations, while conferring poor prognosis, may respond to targeted combination therapies including *BRAF* and *MEK* inhibitors[202-204]. *PIK3CA* mutations may predict sensitivity to *PI3K* pathway inhibitors, while *TP53* mutations could influence response to various therapeutic modalities including immunotherapy and DNA-damaging agents[205-209]. The targeted sequencing identifies patients who may benefit from combination therapies targeting multiple pathways simultaneously[210]. Recent studies have expanded the understanding of CRC genomics beyond traditional driver genes, identifying alterations in chromatin remodeling genes like *ARID1A*, transcription factors like SOX9, and novel targets such as *FAM123B*[211-214].

The *POLD1* gene encodes the large p125 subunit which provides the essential catalytic activities of polymerase δ (Pol δ) with a 5′–3′ DNA polymerase and a 3′–5′ exonuclease function[215]. Pol δ is essential for replication, with a primary role as the replicase for the lagging strand. Pol δ also has an important proofreading ability conferred by its exonuclease activity, which is critical for ensuring replicative fidelity, but also serves to repair DNA lesions arising as a result of exposure to mutagens. Pol δ has been shown to be important for multiple forms of DNA repair, including nucleotide excision repair, double strand break repair, base excision repair, and mismatch repair. On the other hand, the *POLE* gene encodes the catalytic subunit of DNA polymerase epsilon (Pol ε), an enzyme responsible for synthesizing the leading strand during DNA

replication[216]. Because the leading strand is synthesized continuously, requiring high fidelity to prevent mutations, it relies heavily on *POLE*'s exonuclease activity to correct errors in real time. Mutations in *POLE* can disrupt this proofreading ability, leading to an increased rate of replication errors and resulting in an ultra-mutated phenotype with a high mutation burden[217].

In the cohort study, 6.8% and 2.9% of cases harbored a *POLE* or *POLD1* mutation, respectively. Interestingly, four MSI cases overlap with cases with *POLE* and *POLD1* mutations, but the order of these events during CRC development remains unclear. Animal models that can faithfully replicate these genetic events are critical to elucidate the mechanism of tumorigenesis in these cases. Because MSI-H is one of the best biomarkers for predicting the efficacy of immunotherapy[218,219], along with more recently identified roles of *POLE* and *POLD1* mutations in cancer immunotherapy[220-222], targeted sequencing in this study clearly demonstrated its value in precision medicine.

5.1.3 Establishment of CRC organoids

The establishment of CRC organoids has equipped tumor studies with an innovative in vitro model platform[140]. Established organoids can reliably reflect primary tumor characteristics, providing revolutionary preclinical models for oncologic research, drug screening and individual precision medicine[223,224]. This 3D culture system effectively replicates key characteristics of in vivo tumor cells by tumor cells embedded in the dome of matrix gel. Results from multiple independent studies have shown that the success rate of CRC organoid establishment ranges from 71% to 81%[225-228]. In this study, the successful establishment rate of CRC organoid reaches 75% comparable with results stated in the literatures mensioned above.

5.1.4 Comparison of histomorphology, immunohistochemistry and targeted gene sequencing between primary CRC and paired organoids

Comparison of morphology and immunohistochemical marker expression between the organoid and the parental tumor showed that in all 30 pairs morphology and expression of CK-20, CDX-2 and Ki-67 was preserved which is in line with data in the literature. It has been reported that tumor organoids can represent the structure and biology of the tumors they are derived from[229,230]. Histological examination unveiled that tumor organoids were composed specially of tumor cells, and HE staining verified organoids were consistent with paired primary tumor samples such as nuclear atypia, cellular structure and differentiation[231]. IHC analysis demonstrated CRC organoids could recapitulate the protein expression of major diagnostic markers[232]. Comparable to this study, Thng et al. demonstrated that CDX-2, CK-20 and Ki-67 sustained positive expression in the majority of cancer cells, with expression patterns and proportions of positive cells consistent with primary tumors[233].

On the genetic level, the major driver gene mutations, such as *TP53*, *APC*, or *KRAS*, from primary tumors were retained in the organoids, but many passenger gene mutations were lost, suggesting that organoids cannot completely recapitulate the genetic heterogeneity of primary tumors. Also, in the literature it was shown that CRC organoids replicated the molecular characteristics of primary tumors at the genomic level. Major CRC driver gene mutations, including *TP53*, *APC*, and *KRAS*, were maintained in paired tumors and organoids[226].

5.1.5 Establishment of TILs and coculture

In the present study, TILs of 35 CRC cases could be isolated successfully, including TILs of three MSI cases. In five cases, attempts to culture TILs failed, probably due to very low content of TILs in the parental tumor. Due to limited resources, co-culture of organoid with TILs could only performed in one CRC case, demonstrating maximal cytotoxic activity of TILs within 72 hours of co-culture initiation.

Currently, the isolation of TILs with high concentration (6000IU/ml) of IL-2 and functional research of TILs have become a research hotspot in the field of CRC immunotherapy[234]. The establishment of TILs typically relies on isolating them from fresh tumor tissues, expending *in vitro* to obtain effective cell populations. These cells can serve as potential effective tools for immunotherapy[235,236]. Co-culture systems composed of TILs and organoids reflect significance in the study of tumor immunology. The established system enables the co-culture of expanded TILs *in vitro* with autologous CRC organoids to predict cellular interactions and immune responses within the TME[237,238]. Studies have confirmed that co-culture of TILs with tumor organoids can significantly activate TIL cells, as evidenced by increased CD-107a expression and enhanced cytotoxicity, while simultaneously causing destruction of organoid structures[239,240]. This phenomenon has been corroborated by both flow cytometry and histological analyses, demonstrating that this model can effectively evaluate the tumor-killing efficacy of TILs and immune tolerance mechanisms[241].

5.1.6 CRC organoid models in drug sensitivity assay and targeted therapy

Chemotherapy is an essential component for CRC patient treatment. However, current treatment planning by oncologists largely relies on clinical guidelines or past experience, essentially treating a highly heterogeneous patient population with the same regiments. Tumor organoids became an attractive solution for this clinical challenge.

To demonstrate that PDOs are helpful in clinical decision-making for personalized treatment, organoids of two CRC patients were chosen for drug sensitivity assays. In the first case, four chemotherapy drugs were selected based on National comprehensive cancer network (NCCN) guidelines to perform *in vitro* drug sensitivity screening in a PDO culture in a patient with MSS CRC. Drug sensitivity data clearly demonstrated that the selected patient is more sensitive to the second-line drug, docetaxel, than the three first-line drugs recommended by NCCN guidelines, Irinotecan, Oxaliplatin and 5-FU.

In the second case harboring a *HER2* amplification, three targeted therapeutics were tested, which are commonly used in CRC treatment such as Trastuzumab, Trastuzumab-Deruxtecan, and Cetuximab. Trastuzumab demonstrated the strongest cytotoxic effects. This characteristic suggests that cetuximab may be more suitable as an adjuvant therapeutic drug or for preventive treatment which is consistent with two reports[224,242].

These results demostrate it is necessary to combine the patient's molecular marker status, such as *RAS/BRAF* mutations, microsatellite stability, etc., and their physical condition to create the most appropriate personalized treatment plan.

In the time of precision medicine, NGS provides personalized genetic information about the tumor to identify potential targets for therapy, but

laboratory evidence is still lacking to determine whether the intended drugs are effective, especially given the high genetic heterogeneity of tumors demonstrated in this study and numerous reports in the literature[243]. In our study, tumor organoids offer solutions to this challenge.

5.2. Discussion of methods

5.2.1 Prospective cohort study

This study is a prospective study, which is related to the information of patients. Thus, for this kind of study, the privacy protection and the informed consent from these patients should be paid more attention to be anonymous. However, the limitation for this study is that the time for collecting tumor tissues was short. Therefore, prognosis data were not completely traced.

5.2.2 Target sequencing of the 818-gene mutation panel

With the advancement of genomics technologies, next-generation sequencing (NGS) has become an important method for biomedical study and clinical applications. Currently, whole-genome sequencing (WGS), whole-exome sequencing (WES), and targeted sequencing are widely applied in scientific and clinical researches. Each of the methods possesses different characteristics and plays vital roles in various application fields.

In this study, all the collected CRC tumor tissues from 102 patients were performed with targeted sequencing with 818-gene panel. The names of the 818 genes were listed in the appendix Table 1. Targeted sequencing is a technology that performs deep sequencing on specific genes or genomic regions. This technique uses pre-designed gene panels to conduct high-depth

detection of known genes to be related to specific diseases. The greatest advantage of targeted sequencing lies in its high sequencing depth (usually >500X), enabling the detection of low-frequency variants. It's cost and time effective which makes it an ideal choice for routine clinical detection.

However, the limitation of targeted sequencing lies in its inability to discover novel disease-causing genes, which requires the selection of genes based on existing knowledge.

5.2.3 The method of establishing CRC organoids

Significant progress has been made in the methods for establishing CRC organoids. Traditional CRC organoid establishment commonly employs extracellular matrices hydrogels, such as Matrigel or basement membrane extract (BME), to embed tumor cells, directly implanting tissue or single-cell suspensions into three-dimensional culture environments, effectively simulating tumor structure and microenvironment[244]. Recent developments have further optimized culture conditions, such as the discovery that Wnt-3a is not a necessary condition for maintaining long-term CRC organoid culture, and that regulation of SB202190 and oxygen concentration can significantly improve organoid generation efficiency[245-247].

CRC organoids can be derived not only from surgically resected tissues and endoscopic biopsies, but also established through isolation of CTCs, providing personalized disease models for patients whose tumor cannot be surgically resected or have multiple metastases[248]. Organoids from different sources exhibit heterogeneity in both morphological and genetic characteristics, which helps to reveal the biological properties of tumors and drug resistance mechanisms.

In the process of establishing CRC organoids, three CRC tumor tissues with MSI status were performed to establish organoids. However, it was difficult to establish CRC organoids from tumor tissues with MSI status. The reasons why the organoids of these three MSI cases could not be successfully established like tumors with MSS status are unclear. One important reason for this could be that the culture conditions or culture medium were not ideal for this tumor group. Thus, the complete culture medium for the establishment of MSI CRC organoids needs exploring. Another reason probably is that organoids from MSI CRC harboring more mutations could not survive under traditional conditions. Therefore, these reasons need exploring.

As for the genetic mutations, those mutations with higher frequency could be trans-passaged to the organoids but those mutation with lower frequency could not be trans-passaged to the organoids, which demonstrated mutations with higher frequency played more crucial role in the tumorigenesis, but is another limitation which should be taken into account.

Patient-derived organoids (PDOs) of CRC, as 3D culture models, can better preserve the histological characteristics, cellular diversity, and genetic heterogeneity of primary tumors. Compared to traditional 2D cell cultures, 3D organoid models demonstrate significant advantages in terms of cell viability, proliferation capacity, and drug response[249,250].

Despite the advantages of organoids, the use of them in clinical settings faces several challenges. Issues such as standardization of culture techniques, scalability for high-throughput drug screening, and integration into clinical workflows must be addressed[251-255].

5.2.4 The methods of establishing TILs from CRC tissues

TILs preparation methods mainly include direct culture from tumor tissue sections, enrichment of mononuclear cells after enzymatic digestion of tumor tissue to obtain single-cell suspensions, and pre-selection of CD3+T cells with magnetic beads[256,257]. Different methods exhibit variations in cell yield and functionality. For example, the expansion success rate of TILs with magnetic bead enrichment is significantly higher than that of traditional culture methods[258]. Furthermore, high-concentration of IL-2 for culturing in vitro is a classical method for achieving large-scale TILs expansion, which can yield polyclonal T cell populations with potent anti-tumor activity and is suitable for subsequent adoptive cell therapy[259].

Furthermore, while organoids provide insights into tumor biology, they may not fully replicate all aspects of the TME, systemic factors influencing cancer progression or tumor heterogeneity, as evidenced by the targeted sequencing of paired primary tumors and organoid establishment in this study[260,261] . Future research should focus on enhancing organoid models by incorporating additional cell types found within the TME, such as TILs, fibroblasts and endothelial cells[262], to create more comprehensive models for studying CRC. This study explored this area of research by establishing a TILs-organoids co-culture system, clearly demonstrating the potential of organoid technology in both mechanistic study and clinical application in precision cancer immunotherapy.

CD-45, a transmembrane glycoprotein with a molecular weight of 180-250 kDa, is highly expressed on the surface of all nucleated hematopoietic cells, making it an ideal marker for identifying immune cells. During the establishment of TILs, CD-45 plays the following key roles: Broad-spectrum immune cell recognition: CD-45 can recognize all immune cell types in tumor tissue, including T cells, B cells, NK cells, and macrophages, providing a reliable foundation for

comprehensive enrichment of TILs; Specific exclusion of non-immune cells: CD-45 is not expressed in non-hematopoietic tissues, effectively eliminating non-target cells such as tumor cells, fibroblasts, and endothelial cells, ensuring the purity of TILs.

Therefore, CD-45 plays an important role in the immunohistochemical assessment of tumor-infiltrating lymphocytes. Its broad spectrum, specificity, and stability make it an ideal marker for the establishment of TILs. In CRC tissues, the density of TILs with CD-45+ is not only correlated with patient prognosis but also has the potential to predict treatment response, providing important information for precision medicine.

However, in this study, the subtypes of immune cells were not sorted with flow cytometry to further explore the specific cellular function of TILs which is consisted of T lymphocytes (CD4+T lymphocyte, CD8+T lymphocytes, regulatory T lymphocytes), dendritic cells, B lymphocytes, natural killing cells, macrophages and so on. And during the process of co-culturing of CRC organoids and TILs, major histocompatibility complex (MHC)-I, MHC-II and PD-1 were not blocked with corresponding antibodies to test the efficacy of TILs to kill tumor cells.

5.3. Conclusion

The study presented shows that organoids and TILs from CRC patients can be established in high yield and relatively short time and can be characterized molecular genetically. The organoids established retained the major driver mutations seen in the original tumor and can be used for drug screening. It could thus be shown that this model represents an ideal approach for personalized therapy decision-making.

In the future, greater efforts must be made in the development of co-culture, as the re-infusion of TILs is a promising approach in cancer therapy.

6. Summary

In this study, a cohort consisting of 102 CRC patients was established with tumor tissues. The MSI status was determined using a novel digital PCR-based approach and 11% (11/102) MSI-H patients were identified, consistent with what has been reported in the literature. Targeted sequencing was performed to characterize the mutational landscapes of the tumor samples, with *TP53* (63.7%, 65/102), *APC* (55%, 56/102), *KRAS* (36.3%, 37/102) as the top mutated genes in this cohort.

30 tumor organoid cultures were established and characterized, including samples from 27 MSS and 3 MSI CRC patients. These organoids morphologically and histologically recapitulated their original tumor samples. These organoids exhibited similar nuclear-to-cytoplasmic ratios, cellular morphology, and nuclear atypia to primary CRC tumors. CRC Tumor-related markers such as CK-20, CDX-2 and Ki-67 could also be expressed congruently between the paired tumor samples and the established organoids. Our data demonstrated that tumor organoids can faithfully recapitulate the characteristics of the original tumors. Targeted sequencing of these organoids and matched tumor tissues found that all major genetic alterations in the primary tumors, such as driver gene mutations, were well retained in the organoids, but minor passenger mutations were frequently lost, consistent with the idea that organoid culture selects tumor cells with stem cell properties. Our data also raised important issues on how tumor organoid models should be used for precision medicine and in tumor biology. *In vitro* drug sensitivity assays for drugs commonly used in CRC chemo-therapy and targeted therapy were performed and the data further supports the importance of personalized treatment planning on the basis of laboratory evidences.

Lastly, the co-culture of CRC tumor organoids and TILs clearly demonstrated the advantage of organoid models in cancer immunotherapy. Traditional cancer

models, such as cell lines and animals, are not appropriate for modeling responses from immunotherapy. Humanized models of animals are of high time-consumption and finance-consumption, and cannot well be suited for personalized medicine. Cancer organoids have provided an ideal solution, with a timely turnaround time and truly personalized detection of therapeutic targets.

Bibliography

1. Dekker, E., Tanis, P.J., Vleugels, J.L.A., Kasi, P.M., and Wallace, M.B. (2019). Colorectal cancer. Lancet *394*, 1467-1480. 10.1016/S0140-6736(19)32319-0.

2. Siegel, R.L., Wagle, N.S., Cercek, A., Smith, R.A., and Jemal, A. (2023). Colorectal cancer statistics, 2023. CA Cancer J Clin *73*, 233-254. 10.3322/caac.21772.

3. Keum, N., and Giovannucci, E. (2019). Global burden of colorectal cancer: emerging trends, risk factors and prevention strategies. Nat Rev Gastroenterol Hepatol *16*, 713-732. 10.1038/s41575-019-0189-8.

4. Nunes, L., Li, F., Wu, M., Luo, T., Hammarstrom, K., Torell, E., Ljuslinder, I., Mezheyeuski, A., Edqvist, P.H., Lofgren-Burstrom, A., et al. (2024). Prognostic genome and transcriptome signatures in colorectal cancers. Nature *633*, 137-146. 10.1038/s41586-024-07769-3.

5. Benson, A.B., Venook, A.P., Adam, M., Chang, G., Chen, Y.J., Ciombor, K.K., Cohen, S.A., Cooper, H.S., Deming, D., Garrido-Laguna, I., et al. (2024). Colon Cancer, Version 3.2024, NCCN Clinical Practice Guidelines in Oncology. J Natl Compr Canc Netw *22*. 10.6004/jnccn.2024.0029.

6. Benson, A.B., Venook, A.P., Adam, M., Chang, G., Chen, Y.J., Ciombor, K.K., Cohen, S.A., Cooper, H.S., Deming, D., Garrido-Laguna, I., et al. (2024). NCCN Guidelines® Insights: Rectal Cancer, Version 3.2024. J Natl Compr Canc Netw *22*, 366-375. 10.6004/jnccn.2024.0041.

7. Absolute numbers, Incidence, Both sexes, in 2022,in the World. (2025). https://gco.iarc.who.int/today/en/dataviz/pie?mode=cancer&prev_time=3&populations=900.

8. Absolute numbers, Mortality, Both sexes, in 2022 in theWorld. (2025). https://gco.iarc.who.int/today/en/dataviz/pie?mode=cancer&prev_time=3&group_populations=1&populations=900&types=1.

9. Schaber, K., Leitzmann, M., Pukrop, T., Quentin, W., Stein, M.J., and Jochem, C. (2025). Burden of cancer attributable to sedentary behaviour in Germany: an epidemiological analysis of survey data. BMJ Open *15*, e094304. 10.1136/bmjopen-2024-094304.

10. Institute, R.K. (2024.12.30). Colorecral cancer. https://www.krebsdaten.de/Krebs/EN/Content/Cancer_sites/Colorectal_cancer/colorectal_cancer_node.html.

11. Zhang, T., Guo, Y., Qiu, B., Dai, X., Wang, Y., and Cao, X. (2024). Global, regional, and national trends in colorectal cancer burden from 1990 to 2021 and projections to 2040. Front Oncol *14*, 1466159. 10.3389/fonc.2024.1466159.

12. Sung, H., Ferlay, J., Siegel, R.L., Laversanne, M., Soerjomataram, I., Jemal, A., and Bray, F. (2021). Global Cancer Statistics 2020: GLOBOCAN Estimates of Incidence and Mortality Worldwide for 36 Cancers in 185 Countries. CA Cancer J Clin *71*, 209-249. 10.3322/caac.21660.

13. Calanzani, N., Chang, A., Van Melle, M., Pannebakker, M.M., Funston, G., and Walter, F.M. (2021). Recognising Colorectal Cancer in Primary Care. Adv Ther *38*, 2732-2746. 10.1007/s12325-021-01726-6.

14. Fretwell, A., Dobson, C., Orange, S.T., and Corfe, B.M. (2024). Diet and physical activity advice for colorectal cancer survivors: critical synthesis of public-facing guidance. Supportive Care in Cancer *32*. 10.1007/s00520-024-08797-5.

15. Patel, S.G., Karlitz, J.J., Yen, T., Lieu, C.H., and Boland, C.R. (2022). The rising tide of early-onset colorectal cancer: a comprehensive review of epidemiology, clinical features, biology, risk factors, prevention, and early detection. Lancet Gastroenterol Hepatol *7*, 262-274. 10.1016/S2468-1253(21)00426-X.

16. Morgan, E., Arnold, M., Gini, A., Lorenzoni, V., Cabasag, C.J., Laversanne, M., Vignat, J., Ferlay, J., Murphy, N., and Bray, F. (2023). Global burden of colorectal cancer in 2020 and 2040: incidence and mortality estimates from GLOBOCAN. Gut *72*, 338-344. 10.1136/gutjnl-2022-327736.

17. Papier, K., Bradbury, K.E., Balkwill, A., Barnes, I., Smith-Byrne, K., Gunter, M.J., Berndt, S.I., Le Marchand, L., Wu, A.H., Peters, U., et al. (2025). Diet-wide analyses for risk of colorectal cancer: prospective study of 12,251 incident cases among 542,778 women in the UK. Nat Commun *16*, 375. 10.1038/s41467-024-55219-5.

18. Sawicki, T., Ruszkowska, M., Danielewicz, A., Niedzwiedzka, E., Arlukowicz, T., and Przybylowicz, K.E. (2021). A Review of Colorectal Cancer in Terms of Epidemiology, Risk Factors, Development, Symptoms and Diagnosis. Cancers (Basel) *13*. 10.3390/cancers13092025.

19. Ionescu, V.A., Gheorghe, G., Bacalbasa, N., Chiotoroiu, A.L., and Diaconu, C. (2023). Colorectal Cancer: From Risk Factors to Oncogenesis. Medicina (Kaunas) *59*. 10.3390/medicina59091646.

20. Zhang, S., Wang, J.B., Yang, H., Fan, J.H., Qiao, Y.L., and Taylor, P.R. (2020). Body mass index and risk of upper gastrointestinal cancer: A 30-year follow-up of the Linxian dysplasia nutrition intervention trial cohort. Cancer Epidemiol *65*, 101683. 10.1016/j.canep.2020.101683.

21. Song, M., Garrett, W.S., and Chan, A.T. (2015). Nutrients, foods, and colorectal cancer prevention. Gastroenterology *148*, 1244-1260 e1216. 10.1053/j.gastro.2014.12.035.

22. Veettil, S.K., Wong, T.Y., Loo, Y.S., Playdon, M.C., Lai, N.M., Giovannucci, E.L., and Chaiyakunapruk, N. (2021). Role of Diet in Colorectal Cancer Incidence: Umbrella Review of Meta-analyses of Prospective Observational Studies. JAMA Netw Open *4*, e2037341. 10.1001/jamanetworkopen.2020.37341.

23. Vieira, A.R., Abar, L., Chan, D.S.M., Vingeliene, S., Polemiti, E., Stevens, C., Greenwood, D., and Norat, T. (2017). Foods and beverages and colorectal cancer risk: a systematic review and meta-analysis of cohort studies, an update of the evidence of the WCRF-AICR Continuous Update Project. Ann Oncol *28*, 1788-1802. 10.1093/annonc/mdx171.

24. Hickey, M., Basu, P., Sassarini, J., Stegmann, M.E., Weiderpass, E., Nakawala Chilowa, K., Yip, C.H., Partridge, A.H., and Brennan, D.J. (2024). Managing menopause after cancer. Lancet *403*, 984-996. 10.1016/S0140-6736(23)02802-7.

25. Nakhostin, L., Stadler, A., and Stute, P. (2021). Impact of menopausal hormone therapy on colorectal cancer risk-A systematic review. Clin Endocrinol (Oxf) *95*, 390-397. 10.1111/cen.14469.

26. Guo, C.-G., Ma, W., Drew, D.A., Cao, Y., Nguyen, L.H., Joshi, A.D., Ng, K., Ogino, S., Meyerhardt, J.A., Song, M., et al. (2021). Aspirin Use and Risk of Colorectal Cancer Among Older Adults. JAMA Oncology *7*, 428-435. 10.1001/jamaoncol.2020.7338.

27. Guirguis-Blake, J.M., Evans, C.V., Perdue, L.A., Bean, S.I., and Senger, C.A. (2022). Aspirin Use to Prevent Cardiovascular Disease and Colorectal Cancer: Updated Evidence Report and Systematic Review for the US Preventive Services Task Force. JAMA *327*, 1585-1597. 10.1001/jama.2022.3337.

28. Johnson, C.M., Wei, C., Ensor, J.E., Smolenski, D.J., Amos, C.I., Levin, B., and Berry, D.A. (2013). Meta-analyses of colorectal cancer risk factors. Cancer Causes Control *24*, 1207-1222. 10.1007/s10552-013-0201-5.

29. Fuchs, C.S., Giovannucci, E.L., Colditz, G.A., Hunter, D.J., Speizer, F.E., and Willett, W.C. (1994). A prospective study of family history and the risk of colorectal cancer. N Engl J Med *331*, 1669-1674. 10.1056/nejm199412223312501.

30. Stidham, R.W., and Higgins, P.D.R. (2018). Colorectal Cancer in Inflammatory Bowel Disease. Clin Colon Rectal Surg *31*, 168-178. 10.1055/s-0037-1602237.

31. Derikx, L.A., Smits, L.J., van Vliet, S., Dekker, E., Aalfs, C.M., van Kouwen, M.C., Nagengast, F.M., Nagtegaal, I.D., Hoogerbrugge, N., and Hoentjen, F. (2017). Colorectal Cancer Risk in Patients With Lynch Syndrome and Inflammatory Bowel Disease. Clin Gastroenterol Hepatol *15*, 454-458 e451. 10.1016/j.cgh.2016.08.005.

32. Zaffaroni, G., Mannucci, A., Koskenvuo, L., de Lacy, B., Maffioli, A., Bisseling, T., Half, E., Cavestro, G.M., Valle, L., Ryan, N., et al. (2024). Updated European guidelines for clinical management of familial adenomatous polyposis (FAP), MUTYH-associated polyposis (MAP), gastric adenocarcinoma, proximal polyposis of the stomach (GAPPS) and other rare adenomatous polyposis syndromes: a joint EHTG-ESCP revision. Br J Surg *111*. 10.1093/bjs/znae070.

33. Quaglio, A.E.V., Grillo, T.G., De Oliveira, E.C.S., Di Stasi, L.C., and Sassaki, L.Y. (2022). Gut microbiota, inflammatory bowel disease and colorectal cancer. World J Gastroenterol *28*, 4053-4060. 10.3748/wjg.v28.i30.4053.

34. Murthy, S.K., Feuerstein, J.D., Nguyen, G.C., and Velayos, F.S. (2021). AGA Clinical Practice Update on Endoscopic Surveillance and Management of Colorectal Dysplasia in Inflammatory Bowel Diseases: Expert Review. Gastroenterology *161*, 1043-1051 e1044. 10.1053/j.gastro.2021.05.063.

35. Stern, B., McGarrity, T., and Baker, M. (2019). Incorporating Colorectal Cancer Genetic Risk Assessment into Gastroenterology Practice. Curr Treat Options Gastroenterol *17*, 702-715. 10.1007/s11938-019-00267-w.

36. Rebuzzi, F., Ulivi, P., and Tedaldi, G. (2023). Genetic Predisposition to Colorectal Cancer: How Many and Which Genes to Test? Int J Mol Sci *24*. 10.3390/ijms24032137.

37. Joo, J.E., Viana-Errasti, J., Buchanan, D.D., and Valle, L. (2025). Genetics, genomics and clinical features of adenomatous polyposis. Fam Cancer *24*, 38. 10.1007/s10689-025-00460-0.

38. Hryhorowicz, S., Kaczmarek-Rys, M., Lis-Tanas, E., Porowski, J., Szuman, M., Grot, N., Kryszczynska, A., Paszkowski, J., Banasiewicz, T., and Plawski, A. (2022). Strong Hereditary Predispositions to Colorectal Cancer. Genes (Basel) *13*. 10.3390/genes13122326.

39. Zbuk, K.M., and Eng, C. (2007). Hamartomatous polyposis syndromes. Nat Clin Pract Gastroenterol Hepatol *4*, 492-502. 10.1038/ncpgasthep0902.

40. Jelsig, A.M., Qvist, N., Brusgaard, K., Nielsen, C.B., Hansen, T.P., and Ousager, L.B. (2014). Hamartomatous polyposis syndromes: a review. Orphanet J Rare Dis *9*, 101. 10.1186/1750-1172-9-101.

41. Dehghani, A., Sharma, A.E., Siegmund, S.E., Carreon, C.K., Stewart, C.J.R., Medeiros, F., Mirkovic, J., Nucci, M.R., Crum, C.P., Hornick, J.L., et al. (2024). STK11 (LKB1) immunohistochemistry is a sensitive and specific marker for STK11 adnexal tumours. Histopathology *85*, 769-782. 10.1111/his.15303.

42. Sayed, M.G., Ahmed, A.F., Ringold, J.R., Anderson, M.E., Bair, J.L., Mitros, F.A., Lynch, H.T., Tinley, S.T., Petersen, G.M., Giardiello, F.M., et al. (2002). GermlineSMAD4 orBMPRIA mutations and phenotype of juvenile polyposis. Annals of Surgical Oncology *9*, 901-906. 10.1007/BF02557528.

43. Rosner, G., Petel-Galil, Y., Laish, I., Levi, Z., Kariv, R., Strul, H., Gilad, O., and Gluck, N. (2022). Adenomatous Polyposis Phenotype in BMPR1A and SMAD4 Variant Carriers. Clin Transl Gastroenterol *13*, e00527. 10.14309/ctg.0000000000000527.

44. Tischkowitz, M., Colas, C., Pouwels, S., Hoogerbrugge, N., Group, P.G.D., and European Reference Network, G. (2020). Cancer Surveillance Guideline for individuals with PTEN hamartoma tumour syndrome. Eur J Hum Genet *28*, 1387-1393. 10.1038/s41431-020-0651-7.

45. Gustafson, S., Zbuk, K.M., Scacheri, C., and Eng, C. (2007). Cowden syndrome. Semin Oncol *34*, 428-434. 10.1053/j.seminoncol.2007.07.009.

46. Jaeger, E., Leedham, S., Lewis, A., Segditsas, S., Becker, M., Cuadrado, P.R., Davis, H., Kaur, K., Heinimann, K., Howarth, K., et al. (2012). Hereditary mixed polyposis syndrome is caused by a 40-kb upstream duplication that leads to increased and ectopic expression of the BMP antagonist GREM1. Nat Genet *44*, 699-703. 10.1038/ng.2263.

47. Lieberman, S., Walsh, T., Schechter, M., Adar, T., Goldin, E., Beeri, R., Sharon, N., Baris, H., Ben Avi, L., Half, E., et al. (2017). Features of Patients With Hereditary Mixed Polyposis Syndrome Caused by Duplication of GREM1 and Implications for Screening and Surveillance. Gastroenterology *152*, 1876-1880 e1871. 10.1053/j.gastro.2017.02.014.

48. Song, H., Tetangco, E., Martin, E., Willhite, D., and Yap, J.E.L. (2020). Serrated Polyposis Syndrome: Increasing Awareness and Importance. Cureus *12*, e9198. 10.7759/cureus.9198.

49. Young, J.P., Price, T.J., and Parry, S. (2017). Serrated polyposis: the problem of definition and its relationship to the population at risk for syndrome-related colorectal cancer. Translational Cancer Research, S1480-S1483.

50. Tadros, M., and Anderson, J.C. (2013). Serrated polyps: clinical implications and future directions. Curr Gastroenterol Rep *15*, 342. 10.1007/s11894-013-0342-4.

51. Fernando, W.C., Miranda, M.S., Worthley, D.L., Togashi, K., Watters, D.J., Leggett, B.A., and Spring, K.J. (2014). The CIMP Phenotype in BRAF Mutant Serrated Polyps from a Prospective Colonoscopy Patient Cohort. Gastroenterol Res Pract *2014*, 374926. 10.1155/2014/374926.

52. Wang, J.D., Xu, G.S., Hu, X.L., Li, W.Q., Yao, N., Han, F.Z., Zhang, Y., and Qu, J. (2024). The histologic features, molecular features, detection and management of serrated polyps: a review. Front Oncol *14*, 1356250. 10.3389/fonc.2024.1356250.

53. Nolano, A., Medugno, A., Trombetti, S., Liccardo, R., De Rosa, M., Izzo, P., and Duraturo, F. (2022). Hereditary Colorectal Cancer: State of the Art in Lynch Syndrome. Cancers (Basel) *15*. 10.3390/cancers15010075.

54. Moreira, L., Balaguer, F., Lindor, N., de la Chapelle, A., Hampel, H., Aaltonen, L.A., Hopper, J.L., Le Marchand, L., Gallinger, S., Newcomb, P.A., et al. (2012). Identification of Lynch syndrome among patients with colorectal cancer. JAMA *308*, 1555-1565. 10.1001/jama.2012.13088.

55. Castillo-Iturra, J., Sanchez, A., and Balaguer, F. (2024). Colonoscopic surveillance in Lynch syndrome: guidelines in perspective. Fam Cancer *23*, 459-468. 10.1007/s10689-024-00414-y.

56. Peltomaki, P., Nystrom, M., Mecklin, J.P., and Seppala, T.T. (2023). Lynch Syndrome Genetics and Clinical Implications. Gastroenterology *164*, 783-799. 10.1053/j.gastro.2022.08.058.

57. Sinicrope, F.A. (2018). Lynch Syndrome-Associated Colorectal Cancer. N Engl J Med *379*, 764-773. 10.1056/NEJMcp1714533.

58. Bolivar, A.M., Duzagac, F., Deng, N., Reyes-Uribe, L., Chang, K., Wu, W., Bowen, C.M., Taggart, M.W., Thirumurthi, S., Lynch, P.M., et al. (2024). Genomic Landscape of Lynch Syndrome Colorectal Neoplasia Identifies Shared Mutated Neoantigens for Immunoprevention. Gastroenterology *166*, 787-801 e711. 10.1053/j.gastro.2024.01.016.

59. Crisafulli, G., Sartore-Bianchi, A., Lazzari, L., Pietrantonio, F., Amatu, A., Macagno, M., Barault, L., Cassingena, A., Bartolini, A., Luraghi, P., et al. (2022). Temozolomide Treatment Alters Mismatch Repair and Boosts Mutational Burden in Tumor and Blood of Colorectal Cancer Patients. Cancer Discov *12*, 1656-1675. 10.1158/2159-8290.CD-21-1434.

60. Chung, D.C., and Rustgi, A.K. (2003). The hereditary nonpolyposis colorectal cancer syndrome: genetics and clinical implications. Ann Intern Med *138*, 560-570. 10.7326/0003-4819-138-7-200304010-00012.

61. Nomikos, I.N., Kosmas, C., and Gkretsi, V. (2025). Tumor molecular signatures: bridging the bench and the operating room. Am J Surg *246*, 116393. 10.1016/j.amjsurg.2025.116393.

62. Amiot, J., Gubeljak, L., Fontaine, A., Smith, D., Mortemousque, I., Parodi, N., Mauillon, J., Kasper, E., Baert-Desurmont, S., Tinat, J., and Houdayer, C. (2025). New RPS20 gene variant in colorectal cancer diagnosis: insight from a large series of patients. Fam Cancer *24*, 22. 10.1007/s10689-025-00446-y.

63. Borck, P.C., Boyle, I., Jankovic, K., Bick, N., Foster, K., Lau, A.C., Parker-Burns, L.I., Lubicki, D.A., Li, T., Borah, A.A., et al. (2025). SKI complex loss renders 9p21.3-deleted or MSI-H cancers dependent on PELO. Nature *638*, 1104-1111. 10.1038/s41586-024-08509-3.

64. Prindle, V., Richardson, A.E., Sher, K.R., Kongpachith, S., Kentala, K., Petiwala, S., Cheng, D., Widomski, D., Le, P., Torrent, M., et al. (2025). Synthetic lethality of mRNA quality control complexes in cancer. Nature *638*, 1095-1103. 10.1038/s41586-024-08398-6.

65. Ambrosini, M., Rousseau, B., Manca, P., Artz, O., Marabelle, A., Andre, T., Maddalena, G., Mazzoli, G., Intini, R., Cohen, R., et al. (2024). Immune checkpoint inhibitors for POLE or POLD1 proofreading-deficient metastatic colorectal cancer. Ann Oncol *35*, 643-655. 10.1016/j.annonc.2024.03.009.

66. Cecchini, M., and Sundar, R. (2024). Proofreading the way: immune checkpoint inhibitors in polymerase epsilon/polymerase delta (POLE/POLD1)-altered colorectal cancer. Ann Oncol *35*, 582-584. 10.1016/j.annonc.2024.04.006.

67. Mosalem, O., Coston, T.W., Imperial, R., Mauer, E., Thompson, C., Yilma, B., Bekaii-Saab, T.S., Stoppler, M.C., and Starr, J.S. (2024). A comprehensive analysis of POLE/POLD1 genomic alterations in colorectal cancer. Oncologist *29*, e1224-e1227. 10.1093/oncolo/oyae098.

68. Aglago, E.K., Kim, A., Lin, Y., Qu, C., Evangelou, M., Ren, Y., Morrison, J., Albanes, D., Arndt, V., Barry, E.L., et al. (2023). A Genetic Locus within the FMN1/GREM1 Gene Region Interacts with Body Mass Index in Colorectal Cancer Risk. Cancer Res *83*, 2572-2583. 10.1158/0008-5472.CAN-22-3713.

69. Sun, J., Zhao, J., Jiang, F., Wang, L., Xiao, Q., Han, F., Chen, J., Yuan, S., Wei, J., Larsson, S.C., et al. (2023). Identification of novel protein biomarkers and drug targets

for colorectal cancer by integrating human plasma proteome with genome. Genome Med *15*, 75. 10.1186/s13073-023-01229-9.

70. Mizutani, T., Boretto, M., Lim, S., Drost, J., Gonzalez, D.M., Oka, R., Geurts, M.H., Begthel, H., Korving, J., van Es, J.H., et al. (2024). Recapitulating the adenoma-carcinoma sequence by selection of four spontaneous oncogenic mutations in mismatch-repair-deficient human colon organoids. Nat Cancer *5*, 1852-1867. 10.1038/s43018-024-00841-x.

71. Dunican, D.S., McWilliam, P., Tighe, O., Parle-McDermott, A., and Croke, D.T. (2002). Gene expression differences between the microsatellite instability (MIN) and chromosomal instability (CIN) phenotypes in colorectal cancer revealed by high-density cDNA array hybridization. Oncogene *21*, 3253-3257. 10.1038/sj.onc.1205431.

72. Kasi, A., Handa, S., Bhatti, S., Umar, S., Bansal, A., and Sun, W. (2020). Molecular Pathogenesis and Classification of Colorectal Carcinoma. Curr Colorectal Cancer Rep *16*, 97-106. 10.1007/s11888-020-00458-z.

73. Muradi Muhar, A., Velaro, A.J., Prananda, A.T., Nugraha, S.E., Halim, P., and Syahputra, R.A. (2025). Precision medicine in colorectal cancer: genomics profiling and targeted treatment. Front Pharmacol *16*, 1532971. 10.3389/fphar.2025.1532971.

74. Kim, L.A., Han, J., Kim, T.I., Park, J.J., Lee, J.M., Kim, J.K., Park, S., and Lee, H. (2025). Circulating RNA Markers Associated with Adenoma-Carcinoma Sequence in Colorectal Cancer. Int J Mol Sci *26*. 10.3390/ijms26041518.

75. Tsai, P.C., Lee, T.H., Kuo, K.C., Su, F.Y., Lee, T.M., Marostica, E., Ugai, T., Zhao, M., Lau, M.C., Vayrynen, J.P., et al. (2023). Histopathology images predict multi-omics aberrations and prognoses in colorectal cancer patients. Nat Commun *14*, 2102. 10.1038/s41467-023-37179-4.

76. Luo, C., Cen, S., Ding, G., and Wu, W. (2019). Mucinous colorectal adenocarcinoma: clinical pathology and treatment options. Cancer Commun (Lond) *39*, 13. 10.1186/s40880-019-0361-0.

77. Bilal, M., Raza, S.E.A., Azam, A., Graham, S., Ilyas, M., Cree, I.A., Snead, D., Minhas, F., and Rajpoot, N.M. (2021). Development and validation of a weakly supervised deep learning framework to predict the status of molecular pathways and key mutations in colorectal cancer from routine histology images: a retrospective study. Lancet Digit Health *3*, e763-e772. 10.1016/S2589-7500(21)00180-1.

78. Ferlitsch, M., Hassan, C., Bisschops, R., Bhandari, P., Dinis-Ribeiro, M., Risio, M., Paspatis, G.A., Moss, A., Libanio, D., Lorenzo-Zuniga, V., et al. (2024). Colorectal polypectomy and endoscopic mucosal resection: European Society of Gastrointestinal Endoscopy (ESGE) Guideline - Update 2024. Endoscopy *56*, 516-545. 10.1055/a-2304-3219.

79. Sullivan, B.A., and Lieberman, D.A. (2024). Colon Polyp Surveillance: Separating the Wheat From the Chaff. Gastroenterology *166*, 743-757. 10.1053/j.gastro.2023.11.305.

80. Martin-Cullell, B., Virgili, A.C., Riera, P., Fumagalli, C., Mirallas, O., Pelegrin, F.J., Sanchez-Cabus, S., Molina, V., Szafranska, J., and Paez, D. (2024). Histopathological, Clinical, And Molecular (HICAM) score for patients with colorectal liver metastases. Br J Surg *111*. 10.1093/bjs/znae016.

81. Drewes, J.L., Rifkin, S.B., McMann, M., Glass, S., Spence, E., Wensel, C.R., Geis, A.L., Stevens, C., Gills, J.J., Wang, H., et al. (2025). Epidemiology of bacterial biofilms on polyps and normal tissues in a screening colonoscopy cohort. Gut Microbes *17*, 2452233. 10.1080/19490976.2025.2452233.

82. Tang, J., Peng, W., Tian, C., Zhang, Y., Ji, D., Wang, L., Jin, K., Wang, F., Shao, Y., Wang, X., and Sun, Y. (2024). Molecular characteristics of early-onset compared with late-onset colorectal cancer: a case controlled study. Int J Surg *110*, 4559-4570. 10.1097/JS9.0000000000001584.

83. Iris D. Nagtegaal, M.J.A., Manuel Salto-Tellez (2025). Colorectal adenocarcinoma. https://tumourclassification.iarc.who.int/chaptercontent/31/62.

84. Yaghoobi, M., Mehraban Far, P., Mbuagbaw, L., Yuan, Y., Armstrong, D., Thabane, L., and Moayyedi, P. (2023). Head-to-Head Diagnostic Test Accuracy Meta-analysis of Colonoscopy and Fecal Immunochemical Test in Detecting Advanced Colon Neoplasia. Middle East J Dig Dis *15*, 5-11. 10.34172/mejdd.2023.313.

85. Zhao, S., Wang, S., Pan, P., Xia, T., Chang, X., Yang, X., Guo, L., Meng, Q., Yang, F., Qian, W., et al. (2019). Magnitude, Risk Factors, and Factors Associated With Adenoma Miss Rate of Tandem Colonoscopy: A Systematic Review and Meta-analysis. Gastroenterology *156*, 1661-1674 e1611. 10.1053/j.gastro.2019.01.260.

86. Ahn, S.B., Han, D.S., Bae, J.H., Byun, T.J., Kim, J.P., and Eun, C.S. (2012). The Miss Rate for Colorectal Adenoma Determined by Quality-Adjusted, Back-to-Back Colonoscopies. Gut Liver *6*, 64-70. 10.5009/gnl.2012.6.1.64.

87. de Haan, M.C., van Gelder, R.E., Graser, A., Bipat, S., and Stoker, J. (2011). Diagnostic value of CT-colonography as compared to colonoscopy in an asymptomatic screening population: a meta-analysis. Eur Radiol *21*, 1747-1763. 10.1007/s00330-011-2104-8.

88. Plumb, A.A., Halligan, S., Pendse, D.A., Taylor, S.A., and Mallett, S. (2014). Sensitivity and specificity of CT colonography for the detection of colonic neoplasia after positive faecal occult blood testing: systematic review and meta-analysis. Eur Radiol *24*, 1049-1058. 10.1007/s00330-014-3106-0.

89. Duffy, M.J. (2001). Carcinoembryonic antigen as a marker for colorectal cancer: is it clinically useful? Clin Chem *47*, 624-630.

90. Zhao, S., Ju, Y., Gao, B., Chu, F., Lu, B., Bao, G., Ding, S., and Liu, Y. (2024). The value of FPR, FAR, CAR, CPR in the auxiliary diagnosis of colon cancer. Medicine (Baltimore) *103*, e39133. 10.1097/MD.0000000000039133.

91. Luo, S., Ou, Y., Zheng, T., Jiang, H., Wu, Y., Zhao, J., and Zhang, Z. (2021). Optimal Strategy for Colorectal Cancer Patients' Diagnosis Based on Circulating Tumor Cells

and Circulating Tumor Endothelial Cells by Subtraction Enrichment and Immunostaining-Fluorescence In Situ Hybridization Combining with CEA and CA19-9. J Oncol *2021*, 1517488. 10.1155/2021/1517488.

92. Nakamura, Y., Watanabe, J., Akazawa, N., Hirata, K., Kataoka, K., Yokota, M., Kato, K., Kotaka, M., Kagawa, Y., Yeh, K.H., et al. (2024). ctDNA-based molecular residual disease and survival in resectable colorectal cancer. Nat Med *30*, 3272-3283. 10.1038/s41591-024-03254-6.

93. Amin, M.B., Greene, F.L., Edge, S.B., Compton, C.C., Gershenwald, J.E., Brookland, R.K., Meyer, L., Gress, D.M., Byrd, D.R., and Winchester, D.P. (2017). The Eighth Edition AJCC Cancer Staging Manual: Continuing to build a bridge from a population-based to a more "personalized" approach to cancer staging. CA Cancer J Clin *67*, 93-99. 10.3322/caac.21388.

94. Cancer Stat Facts: Colorectal Cancer. (2025). https://seer.cancer.gov/statfacts/html/colorect.html.

95. Survival statistics for colorectal cancer. (2025). https://cancer.ca/en/cancer-information/cancer-types/colorectal/prognosis-and-survival/survival-statistics.

96. Chemotherapy for Colorectal Cancer. (2025). https://www.cancer.org/cancer/types/colon-rectal-cancer/treating/chemotherapy.html.

97. Chemotherapy for colon cancer. (2025). https://www.cancerresearchuk.org/about-cancer/bowel-cancer/treatment/treatment-colon/colon-chemotherapy.

98. Neugut, A.I., Lin, A., Raab, G.T., Hillyer, G.C., Keller, D., O'Neil, D.S., Accordino, M.K., Kiran, R.P., Wright, J., and Hershman, D.L. (2019). FOLFOX and FOLFIRI Use in Stage IV Colon Cancer: Analysis of SEER-Medicare Data. Clin Colorectal Cancer *18*, 133-140. 10.1016/j.clcc.2019.01.005.

99. Muro, K., Boku, N., Shimada, Y., Tsuji, A., Sameshima, S., Baba, H., Satoh, T., Denda, T., Ina, K., Nishina, T., et al. (2010). Irinotecan plus S-1 (IRIS) versus fluorouracil and folinic acid plus irinotecan (FOLFIRI) as second-line chemotherapy for metastatic colorectal cancer: a randomised phase 2/3 non-inferiority study (FIRIS study). Lancet Oncol *11*, 853-860. 10.1016/S1470-2045(10)70181-9.

100. Singh, M., Morris, V.K., Bandey, I.N., Hong, D.S., and Kopetz, S. (2024). Advancements in combining targeted therapy and immunotherapy for colorectal cancer. Trends Cancer *10*, 598-609. 10.1016/j.trecan.2024.05.001.

101. Ganesh, K., Stadler, Z.K., Cercek, A., Mendelsohn, R.B., Shia, J., Segal, N.H., and Diaz, L.A., Jr. (2019). Immunotherapy in colorectal cancer: rationale, challenges and potential. Nat Rev Gastroenterol Hepatol *16*, 361-375. 10.1038/s41575-019-0126-x.

102. Winder, T., and Lenz, H.J. (2010). Vascular endothelial growth factor and epidermal growth factor signaling pathways as therapeutic targets for colorectal cancer. Gastroenterology *138*, 2163-2176. 10.1053/j.gastro.2010.02.005.

103. Janani, B., Vijayakumar, M., Priya, K., Kim, J.H., Prabakaran, D.S., Shahid, M., Al-Ghamdi, S., Alsaidan, M., Othman Bahakim, N., Hassan Abdelzaher, M., and Ramesh,

T. (2022). EGFR-Based Targeted Therapy for Colorectal Cancer-Promises and Challenges. Vaccines (Basel) *10*. 10.3390/vaccines10040499.

104. Holderfield, M., Lee, B.J., Jiang, J., Tomlinson, A., Seamon, K.J., Mira, A., Patrucco, E., Goodhart, G., Dilly, J., Gindin, Y., et al. (2024). Concurrent inhibition of oncogenic and wild-type RAS-GTP for cancer therapy. Nature *629*, 919-926. 10.1038/s41586-024-07205-6.

105. Zhao, Y., Murciano-Goroff, Y.R., Xue, J.Y., Ang, A., Lucas, J., Mai, T.T., Da Cruz Paula, A.F., Saiki, A.Y., Mohn, D., Achanta, P., et al. (2021). Diverse alterations associated with resistance to KRAS(G12C) inhibition. Nature *599*, 679-683. 10.1038/s41586-021-04065-2.

106. Takeda, M., Yoshida, S., Inoue, T., Sekido, Y., Hata, T., Hamabe, A., Ogino, T., Miyoshi, N., Uemura, M., Yamamoto, H., et al. (2025). The Role of KRAS Mutations in Colorectal Cancer: Biological Insights, Clinical Implications, and Future Therapeutic Perspectives. Cancers (Basel) *17*. 10.3390/cancers17030428.

107. Miao, R., Yu, J., and Kim, R.D. (2025). Targeting the KRAS Oncogene for Patients with Metastatic Colorectal Cancer. Cancers (Basel) *17*. 10.3390/cancers17091512.

108. Singh, R.R., and O'Reilly, E.M. (2020). New Treatment Strategies for Metastatic Pancreatic Ductal Adenocarcinoma. Drugs *80*, 647-669. 10.1007/s40265-020-01304-0.

109. Chen, Y., Yin, Z., Westover, K.D., Zhou, Z., and Shu, L. (2025). Advances and Challenges in RAS Signaling Targeted Therapy in Leukemia. Mol Cancer Ther *24*, 33-46. 10.1158/1535-7163.MCT-24-0504.

110. Hitchen, N., Williams, S., and Desai, J. (2025). Recent advances in therapeutic targeting of the KRAS pathway in cancer. Pharmacol Ther, 108889. 10.1016/j.pharmthera.2025.108889.

111. Fakih, M.G., Salvatore, L., Esaki, T., Modest, D.P., Lopez-Bravo, D.P., Taieb, J., Karamouzis, M.V., Ruiz-Garcia, E., Kim, T.W., Kuboki, Y., et al. (2023). Sotorasib plus Panitumumab in Refractory Colorectal Cancer with Mutated KRAS G12C. N Engl J Med *389*, 2125-2139. 10.1056/NEJMoa2308795.

112. LaFargue, C.J., Amero, P., Noh, K., Mangala, L.S., Wen, Y., Bayraktar, E., Umamaheswaran, S., Stur, E., Dasari, S.K., Ivan, C., et al. (2023). Overcoming adaptive resistance to anti-VEGF therapy by targeting CD5L. Nat Commun *14*, 2407. 10.1038/s41467-023-36910-5.

113. Elez, E., Yoshino, T., Shen, L., Lonardi, S., Van Cutsem, E., Eng, C., Kim, T.W., Wasan, H.S., Desai, J., Ciardiello, F., et al. (2025). Encorafenib, Cetuximab, and mFOLFOX6 in BRAF-Mutated Colorectal Cancer. N Engl J Med. 10.1056/NEJMoa2501912.

114. Grothey, A., Fakih, M., and Tabernero, J. (2021). Management of BRAF-mutant metastatic colorectal cancer: a review of treatment options and evidence-based guidelines. Ann Oncol *32*, 959-967. 10.1016/j.annonc.2021.03.206.

115. Ntomi, V., Foukas, P., Papaconstantinou, D., Antonopoulou, I., Pikoulis, A., Panagiotides, I., Pikoulis, E., and Syrigos, K. (2021). The clinical significance of PD-L1 in colorectal cancer (Review). Oncol Rep *45*. 10.3892/or.2021.8043.

116. Casak, S.J., Marcus, L., Fashoyin-Aje, L., Mushti, S.L., Cheng, J., Shen, Y.L., Pierce, W.F., Her, L., Goldberg, K.B., Theoret, M.R., et al. (2021). FDA Approval Summary: Pembrolizumab for the First-line Treatment of Patients with MSI-H/dMMR Advanced Unresectable or Metastatic Colorectal Carcinoma. Clin Cancer Res *27*, 4680-4684. 10.1158/1078-0432.CCR-21-0557.

117. Phillips, C. (2025). FDA Approval Likely to Change Initial Treatment for Some People with Advanced Colorectal Cancer. https://www.cancer.gov/news-events/cancer-currents-blog/2025/fda-nivolumab-ipilimumab-dmmr-colorectal-cancer.

118. Fridman, W.H., Pages, F., Sautes-Fridman, C., and Galon, J. (2012). The immune contexture in human tumours: impact on clinical outcome. Nat Rev Cancer *12*, 298-306. 10.1038/nrc3245.

119. Galon, J., Costes, A., Sanchez-Cabo, F., Kirilovsky, A., Mlecnik, B., Lagorce-Pagès, C., Tosolini, M., Camus, M., Berger, A., Wind, P., et al. (2006). Type, density, and location of immune cells within human colorectal tumors predict clinical outcome. Science *313*, 1960-1964. 10.1126/science.1129139.

120. Rosenberg, S.A. (2024). Lymphocytes as a living drug for cancer. Science *385*, 25-26. doi:10.1126/science.adp1130.

121. Parums, D.V. (2024). Editorial: First Regulatory Approval for Adoptive Cell Therapy with Autologous Tumor-Infiltrating Lymphocytes (TILs) - Lifileucel (Amtagvi). Med Sci Monit *30*, e944927. 10.12659/MSM.944927.

122. Chesney, J., Lewis, K.D., Kluger, H., Hamid, O., Whitman, E., Thomas, S., Wermke, M., Cusnir, M., Domingo-Musibay, E., Phan, G.Q., et al. (2022). Efficacy and safety of lifileucel, a one-time autologous tumor-infiltrating lymphocyte (TIL) cell therapy, in patients with advanced melanoma after progression on immune checkpoint inhibitors and targeted therapies: pooled analysis of consecutive cohorts of the C-144-01 study. J Immunother Cancer *10*. 10.1136/jitc-2022-005755.

123. Amaria, R.N., McQuade, J.L., Davies, M.A., Glitza, I.C., Jose, S., Cressman, E.N.K., Clausell, A.L., Bassett, R.L., Patel, S.P., Diab, A., et al. (2024). OBX-115, an interleukin 2 (IL2)-sparing engineered tumor-infiltrating lymphocyte (TIL) cell therapy, in patients (pts) with immune checkpoint inhibitor (ICI)-resistant unresectable or metastatic melanoma. Journal of Clinical Oncology *42*, 9515-9515. 10.1200/JCO.2024.42.16_suppl.9515.

124. Lovgren, T., Wolodarski, M., Wickstrom, S., Edback, U., Wallin, M., Martell, E., Markland, K., Blomberg, P., Nystrom, M., Lundqvist, A., et al. (2020). Complete and long-lasting clinical responses in immune checkpoint inhibitor-resistant, metastasized melanoma treated with adoptive T cell transfer combined with DC vaccination. Oncoimmunology *9*, 1792058. 10.1080/2162402X.2020.1792058.

125. Borch, T.H., Andersen, R., Ellebaek, E., Met, O., Donia, M., and Svane, I.M. (2020). Future role for adoptive T-cell therapy in checkpoint inhibitor-resistant metastatic melanoma. J Immunother Cancer *8*. 10.1136/jitc-2020-000668.

126. Chen, L., Hu, H., Yuan, Y., and Weng, S. (2024). CSCO guidelines for colorectal cancer version 2024: Updates and discussions. Chin J Cancer Res *36*, 233-239. 10.21147/j.issn.1000-9604.2024.03.01.

127. Somasundaram, A., Moore, D.T., Turk, A.A., Imanirad, I., Cohen, S.A., Ciombor, K.K., Triglianos, T., McRee, A.J., Lee, M.S., and Sanoff, H.K. (2025). Phase II Study of Ipilimumab, Nivolumab, and Panitumumab in Patients With KRAS/NRAS/BRAF Wild-Type Microsatellite Stable Metastatic Colorectal Cancer. JCO Oncology Advances. 10.1200/oa-24-00086.

128. Venook, A.P. (2025). Updates in Metastatic Colorectal Cancer. Journal of the National Comprehensive Cancer Network *23*. 10.6004/jnccn.2025.5017.

129. Bando, H., Ohtsu, A., and Yoshino, T. (2023). Therapeutic landscape and future direction of metastatic colorectal cancer. Nat Rev Gastroenterol Hepatol *20*, 306-322. 10.1038/s41575-022-00736-1.

130. Westphalen, C.B., Krebs, M.G., Le Tourneau, C., Sokol, E.S., Maund, S.L., Wilson, T.R., Jin, D.X., Newberg, J.Y., Fabrizio, D., Veronese, L., et al. (2021). Genomic context of NTRK1/2/3 fusion-positive tumours from a large real-world population. NPJ Precis Oncol *5*, 69. 10.1038/s41698-021-00206-y.

131. Battaglin, F., Ou, F.S., Qu, X., Hochster, H.S., Niedzwiecki, D., Goldberg, R.M., Mayer, R.J., Ashouri, K., Zemla, T.J., Blanke, C.D., et al. (2024). HER2 Gene Expression Levels Are Predictive and Prognostic in Patients With Metastatic Colorectal Cancer Enrolled in CALGB/SWOG 80405. J Clin Oncol *42*, 1890-1902. 10.1200/JCO.23.01507.

132. Cortese, M., Torchiaro, E., D'Andrea, A., Petti, C., Invrea, F., Franco, L., Donini, C., Leuci, V., Leto, S.M., Vurchio, V., et al. (2024). Preclinical efficacy of a HER2 synNotch/CEA-CAR combinatorial immunotherapy against colorectal cancer with HER2 amplification. Mol Ther *32*, 2741-2761. 10.1016/j.ymthe.2024.06.023.

133. Guo, L., Wang, Y., Yang, W., Wang, C., Guo, T., Yang, J., Shao, Z., Cai, G., Cai, S., Zhang, L., et al. (2023). Molecular Profiling Provides Clinical Insights Into Targeted and Immunotherapies as Well as Colorectal Cancer Prognosis. Gastroenterology *165*, 414-428 e417. 10.1053/j.gastro.2023.04.029.

134. Johnson, D., Chee, C.E., Wong, W., Lam, R.C.T., Tan, I.B.H., and Ma, B.B.Y. (2024). Current advances in targeted therapy for metastatic colorectal cancer - Clinical translation and future directions. Cancer Treat Rev *125*, 102700. 10.1016/j.ctrv.2024.102700.

135. Ros, J., Vaghi, C., Baraibar, I., Saoudi Gonzalez, N., Rodriguez-Castells, M., Garcia, A., Alcaraz, A., Salva, F., Tabernero, J., and Elez, E. (2024). Targeting KRAS G12C Mutation in Colorectal Cancer, A Review: New Arrows in the Quiver. Int J Mol Sci *25*. 10.3390/ijms25063304.

136. Lee, C.S., Song, I.H., Lee, A., Kang, J., Lee, Y.S., Lee, I.K., Song, Y.S., and Lee, S.H. (2021). Enhancing the landscape of colorectal cancer using targeted deep sequencing. Sci Rep *11*, 8154. 10.1038/s41598-021-87486-3.

137. Raskin, L., Guo, Y., Du, L., Clendenning, M., Rosty, C., Lindor, N.M., Gruber, S.B., and Buchanan, D.D. (2017). Targeted sequencing of established and candidate colorectal cancer genes in the Colon Cancer Family Registry Cohort. Oncotarget *8*, 93450-93463. 10.18632/oncotarget.18596.

138. D'Haene, N., Fontanges, Q., De Nève, N., Blanchard, O., Melendez, B., Delos, M., Dehou, M.F., Maris, C., Nagy, N., Rousseau, E., et al. (2018). Clinical application of targeted next-generation sequencing for colorectal cancer patients: a multicentric Belgian experience. Oncotarget *9*, 20761-20768. 10.18632/oncotarget.25099.

139. Abbas, Z.N., Al-Saffar, A.Z., Jasim, S.M., and Sulaiman, G.M. (2023). Comparative analysis between 2D and 3D colorectal cancer culture models for insights into cellular morphological and transcriptomic variations. Sci Rep *13*, 18380. 10.1038/s41598-023-45144-w.

140. Barbachano, A., Fernandez-Barral, A., Bustamante-Madrid, P., Prieto, I., Rodriguez-Salas, N., Larriba, M.J., and Munoz, A. (2021). Organoids and Colorectal Cancer. Cancers (Basel) *13*. 10.3390/cancers13112657.

141. Luo, L., Ma, Y., Zheng, Y., Su, J., and Huang, G. (2022). Application Progress of Organoids in Colorectal Cancer. Front Cell Dev Biol *10*, 815067. 10.3389/fcell.2022.815067.

142. Cordeiro, S., Oliveira, B.B., Valente, R., Ferreira, D., Luz, A., Baptista, P.V., and Fernandes, A.R. (2024). Breaking the mold: 3D cell cultures reshaping the future of cancer research. Front Cell Dev Biol *12*, 1507388. 10.3389/fcell.2024.1507388.

143. Driehuis, E., van Hoeck, A., Moore, K., Kolders, S., Francies, H.E., Gulersonmez, M.C., Stigter, E.C.A., Burgering, B., Geurts, V., Gracanin, A., et al. (2019). Pancreatic cancer organoids recapitulate disease and allow personalized drug screening. Proc Natl Acad Sci U S A *116*, 26580-26590. 10.1073/pnas.1911273116.

144. Thorel, L., Perreard, M., Florent, R., Divoux, J., Coffy, S., Vincent, A., Gaggioli, C., Guasch, G., Gidrol, X., Weiswald, L.B., and Poulain, L. (2024). Patient-derived tumor organoids: a new avenue for preclinical research and precision medicine in oncology. Exp Mol Med *56*, 1531-1551. 10.1038/s12276-024-01272-5.

145. Kapalczynska, M., Kolenda, T., Przybyla, W., Zajaczkowska, M., Teresiak, A., Filas, V., Ibbs, M., Blizniak, R., Luczewski, L., and Lamperska, K. (2018). 2D and 3D cell cultures - a comparison of different types of cancer cell cultures. Arch Med Sci *14*, 910-919. 10.5114/aoms.2016.63743.

146. Sakshaug, B.C., Folkesson, E., Haukaas, T.H., Visnes, T., and Flobak, A. (2023). Systematic review: predictive value of organoids in colorectal cancer. Sci Rep *13*, 18124. 10.1038/s41598-023-45297-8.

147. Vlachogiannis, G., Hedayat, S., Vatsiou, A., Jamin, Y., Fernandez-Mateos, J., Khan, K., Lampis, A., Eason, K., Huntingford, I., Burke, R., et al. (2018). Patient-derived organoids model treatment response of metastatic gastrointestinal cancers. Science *359*, 920-926. 10.1126/science.aao2774.

148. Seidlitz, T., and Stange, D.E. (2021). Gastrointestinal cancer organoids-applications in basic and translational cancer research. Exp Mol Med *53*, 1459-1470. 10.1038/s12276-021-00654-3.

149. Frappart, P.O., Walter, K., Gout, J., Beutel, A.K., Morawe, M., Arnold, F., Breunig, M., Barth, T.F., Marienfeld, R., Schulte, L., et al. (2020). Pancreatic cancer-derived organoids - a disease modeling tool to predict drug response. United European Gastroenterol J *8*, 594-606. 10.1177/2050640620905183.

150. Pasch, C.A., Favreau, P.F., Yueh, A.E., Babiarz, C.P., Gillette, A.A., Sharick, J.T., Karim, M.R., Nickel, K.P., DeZeeuw, A.K., Sprackling, C.M., et al. (2019). Patient-Derived Cancer Organoid Cultures to Predict Sensitivity to Chemotherapy and Radiation. Clin Cancer Res *25*, 5376-5387. 10.1158/1078-0432.CCR-18-3590.

151. Esposito, A., Ferraresi, A., Vallino, L., Garavaglia, B., Dhanasekaran, D.N., and Isidoro, C. (2024). Three-Dimensional In Vitro Cell Cultures as a Feasible and Promising Alternative to Two-Dimensional and Animal Models in Cancer Research. Int J Biol Sci *20*, 5293-5311. 10.7150/ijbs.96469.

152. Cekanova, M., and Rathore, K. (2014). Animal models and therapeutic molecular targets of cancer: utility and limitations. Drug Des Devel Ther *8*, 1911-1921. 10.2147/DDDT.S49584.

153. Mestas, J., and Hughes, C.C. (2004). Of mice and not men: differences between mouse and human immunology. J Immunol *172*, 2731-2738. 10.4049/jimmunol.172.5.2731.

154. Sellers, R.S. (2017). Translating Mouse Models. Toxicol Pathol *45*, 134-145. 10.1177/0192623316675767.

155. Jagadesan, S., Mondal, P., Carlson, M.A., and Guda, C. (2023). Evaluation of Five Mammalian Models for Human Disease Research Using Genomic and Bioinformatic Approaches. Biomedicines *11*. 10.3390/biomedicines11082197.

156. Betge, J., Rindtorff, N., Sauer, J., Rauscher, B., Dingert, C., Gaitantzi, H., Herweck, F., Srour-Mhanna, K., Miersch, T., Valentini, E., et al. (2022). The drug-induced phenotypic landscape of colorectal cancer organoids. Nat Commun *13*, 3135. 10.1038/s41467-022-30722-9.

157. Ahmad Zawawi, S.S., Salleh, E.A., and Musa, M. (2024). Spheroids and organoids derived from colorectal cancer as tools for in vitro drug screening. Explor Target Antitumor Ther *5*, 409-431. 10.37349/etat.2024.00226.

158. Koch, M., Beckhove, P., Op den Winkel, J., Autenrieth, D., Wagner, P., Nummer, D., Specht, S., Antolovic, D., Galindo, L., Schmitz-Winnenthal, F.H., et al. (2006). Tumor infiltrating T lymphocytes in colorectal cancer: Tumor-selective activation and cytotoxic

activity in situ. Ann Surg *244*, 986-992; discussion 992-983. 10.1097/01.sla.0000247058.43243.7b.

159. Rosenberg, S.A., Yang, J.C., Sherry, R.M., Kammula, U.S., Hughes, M.S., Phan, G.Q., Citrin, D.E., Restifo, N.P., Robbins, P.F., Wunderlich, J.R., et al. (2011). Durable complete responses in heavily pretreated patients with metastatic melanoma using T-cell transfer immunotherapy. Clin Cancer Res *17*, 4550-4557. 10.1158/1078-0432.CCR-11-0116.

160. Topalian, S.L., Taube, J.M., Anders, R.A., and Pardoll, D.M. (2016). Mechanism-driven biomarkers to guide immune checkpoint blockade in cancer therapy. Nat Rev Cancer *16*, 275-287. 10.1038/nrc.2016.36.

161. Pages, F., Mlecnik, B., Marliot, F., Bindea, G., Ou, F.S., Bifulco, C., Lugli, A., Zlobec, I., Rau, T.T., Berger, M.D., et al. (2018). International validation of the consensus Immunoscore for the classification of colon cancer: a prognostic and accuracy study. Lancet *391*, 2128-2139. 10.1016/S0140-6736(18)30789-X.

162. Chen, S. (2023). Ultrafast one-pass FASTQ data preprocessing, quality control, and deduplication using fastp. Imeta *2*, e107. 10.1002/imt2.107.

163. Li, H., and Durbin, R. (2010). Fast and accurate long-read alignment with Burrows-Wheeler transform. Bioinformatics *26*, 589-595. 10.1093/bioinformatics/btp698.

164. Li, H., Handsaker, B., Wysoker, A., Fennell, T., Ruan, J., Homer, N., Marth, G., Abecasis, G., Durbin, R., and Genome Project Data Processing, S. (2009). The Sequence Alignment/Map format and SAMtools. Bioinformatics *25*, 2078-2079. 10.1093/bioinformatics/btp352.

165. Cibulskis, K., Lawrence, M.S., Carter, S.L., Sivachenko, A., Jaffe, D., Sougnez, C., Gabriel, S., Meyerson, M., Lander, E.S., and Getz, G. (2013). Sensitive detection of somatic point mutations in impure and heterogeneous cancer samples. Nat Biotechnol *31*, 213-219. 10.1038/nbt.2514.

166. Nakken, S., Fournous, G., Vodak, D., Aasheim, L.B., Myklebost, O., and Hovig, E. (2018). Personal Cancer Genome Reporter: variant interpretation report for precision oncology. Bioinformatics *34*, 1778-1780. 10.1093/bioinformatics/btx817.

167. Bayle, A., Basile, D., Garinet, S., Rance, B., Laurent-Puig, P., Blons, H., Taieb, J., and Perkins, G. (2021). Next-Generation Sequencing Targeted Panel in Routine Care for Metastatic Colon Cancers. Cancers (Basel) *13*. 10.3390/cancers13225750.

168. Jan, Y.H., Tan, K.T., Chen, S.J., Yip, T.T.C., Lu, C.T., and Lam, A.K. (2022). Comprehensive assessment of actionable genomic alterations in primary colorectal carcinoma using targeted next-generation sequencing. Br J Cancer *127*, 1304-1311. 10.1038/s41416-022-01913-4.

169. Pearlman, R., Frankel, W.L., Swanson, B., Zhao, W., Yilmaz, A., Miller, K., Bacher, J., Bigley, C., Nelsen, L., Goodfellow, P.J., et al. (2017). Prevalence and Spectrum of Germline Cancer Susceptibility Gene Mutations Among Patients With Early-Onset Colorectal Cancer. JAMA Oncol *3*, 464-471. 10.1001/jamaoncol.2016.5194.

170. Gutierrez, C., Ogino, S., Meyerhardt, J.A., and Iorgulescu, J.B. (2023). The Prevalence and Prognosis of Microsatellite Instability-High/Mismatch Repair-Deficient Colorectal Adenocarcinomas in the United States. JCO Precis Oncol *7*, e2200179. 10.1200/PO.22.00179.

171. Tougeron, D., Sickersen, G., Mouillet, G., Zaanan, A., Trouilloud, I., Coriat, R., Aparicio, T., Des Guetz, G., Lecaille, C., Artru, P., et al. (2015). Predictors of disease-free survival in colorectal cancer with microsatellite instability: An AGEO multicentre study. Eur J Cancer *51*, 925-934. 10.1016/j.ejca.2015.03.011.

172. Han, S.W., Kim, H.P., Shin, J.Y., Jeong, E.G., Lee, W.C., Lee, K.H., Won, J.K., Kim, T.Y., Oh, D.Y., Im, S.A., et al. (2013). Targeted sequencing of cancer-related genes in colorectal cancer using next-generation sequencing. PLoS One *8*, e64271. 10.1371/journal.pone.0064271.

173. Zhao, Q., Wang, F., Chen, Y.X., Chen, S., Yao, Y.C., Zeng, Z.L., Jiang, T.J., Wang, Y.N., Wu, C.Y., Jing, Y., et al. (2022). Comprehensive profiling of 1015 patients' exomes reveals genomic-clinical associations in colorectal cancer. Nat Commun *13*, 2342. 10.1038/s41467-022-30062-8.

174. Hayashi, H., Takiguchi, Y., Minami, H., Akiyoshi, K., Segawa, Y., Ueda, H., Iwamoto, Y., Kondoh, C., Matsumoto, K., Takahashi, S., et al. (2020). Site-Specific and Targeted Therapy Based on Molecular Profiling by Next-Generation Sequencing for Cancer of Unknown Primary Site: A Nonrandomized Phase 2 Clinical Trial. JAMA Oncol *6*, 1931-1938. 10.1001/jamaoncol.2020.4643.

175. Postwala, H., Shah, Y., Parekh, P.S., and Chorawala, M.R. (2023). Unveiling the genetic and epigenetic landscape of colorectal cancer: new insights into pathogenic pathways. Med Oncol *40*, 334. 10.1007/s12032-023-02201-8.

176. Bai, Z., Zhou, Y., Ye, Z., Xiong, J., Lan, H., and Wang, F. (2021). Tumor-Infiltrating Lymphocytes in Colorectal Cancer: The Fundamental Indication and Application on Immunotherapy. Front Immunol *12*, 808964. 10.3389/fimmu.2021.808964.

177. Yu, B., Kang, J., Lei, H., Li, Z., Yang, H., and Zhang, M. (2024). Immunotherapy for colorectal cancer. Front Immunol *15*, 1433315. 10.3389/fimmu.2024.1433315.

178. Vuchkovska, A., Murt, M., Zhou, B., Kalos, M., and Rodriguez, R. (2024). 400 Circulating tumor reactive lymphocytes (cTRLs) isolated from colorectal cancer (CRC) patients are reactive against autologous tumors and show less exhaustion than tumor-infiltrating lymphocytes (TILs). Regular and Young Investigator Award Abstracts.

179. Zou, D., and Xu, T. (2024). Construction and validation of a colon cancer prognostic model based on tumor mutation burden-related genes. Sci Rep *14*, 2867. 10.1038/s41598-024-53257-z.

180. Mei, W.J., Mi, M., Qian, J., Xiao, N., Yuan, Y., and Ding, P.R. (2022). Clinicopathological characteristics of high microsatellite instability/mismatch repair-deficient colorectal cancer: A narrative review. Front Immunol *13*, 1019582. 10.3389/fimmu.2022.1019582.

181. Coston, T., Mauer, E., Jones, J.C., Hubbard, J.M., Bekaii-Saab, T.S., Stoppler, M.C., and Starr, J.S. (2023). Characterizing the genomic landscape of POLE/POLD1-mutated colorectal adenocarcinoma. Journal of Clinical Oncology *41*, 199-199. 10.1200/JCO.2023.41.4_suppl.199.

182. Garmezy, B., Gheeya, J., Lin, H.Y., Huang, Y., Kim, T., Jiang, X., Thein, K.Z., Pilie, P.G., Zeineddine, F., Wang, W., et al. (2022). Clinical and Molecular Characterization of POLE Mutations as Predictive Biomarkers of Response to Immune Checkpoint Inhibitors in Advanced Cancers. JCO Precis Oncol *6*, e2100267. 10.1200/PO.21.00267.

183. Andrianova, M.A., Seplyarskiy, V.B., Terradas, M., Sanchez-Heras, A.B., Mur, P., Soto, J.L., Aiza, G., Borras, E., Kondrashov, F.A., Kondrashov, A.S., et al. (2024). Discovery of recessive effect of human polymerase delta proofreading deficiency through mutational analysis of POLD1-mutated normal and cancer cells. Eur J Hum Genet *32*, 837-845. 10.1038/s41431-024-01598-8.

184. Jamalinia, M., and Weiskirchen, R. (2025). Advances in personalized medicine: translating genomic insights into targeted therapies for cancer treatment. Ann Transl Med *13*, 18. 10.21037/atm-25-34.

185. Sun, Z., Chung, D., Neelon, B., Millar-Wilson, A., Ethier, S.P., Xiao, F., Zheng, Y., Wallace, K., and Hardiman, G. (2023). A Bayesian framework for pathway-guided identification of cancer subgroups by integrating multiple types of genomic data. Stat Med *42*, 5266-5284. 10.1002/sim.9911.

186. Shi, J., Wang, L., Yin, X., Wang, L., Bo, L., Liu, K., Feng, K., Lin, S., Xu, Y., Ning, S., and Zhao, H. (2022). Comprehensive characterization of clonality of driver genes revealing their clinical relevance in colorectal cancer. J Transl Med *20*, 362. 10.1186/s12967-022-03529-x.

187. Gavrić, I., Hodžić, E., Sarajlić, L., Salibašić, M., Bajramagić, S., Dizdarević, A., and Kulović, E. (2024). Analysis of TP53, APC, KRAS, and MMR Genetic mutations in colorectal cancer: A review article. Sanamed *19*, 333-341. 10.5937/sanamed0-52803.

188. Pan, M., Jiang, C., Tse, P., Solorzano-Pinto, A.V., Chung, E., Truong, T.-G., Arora, A., Sundaresan, T.K., Suga, J.M.M., Habel, L.A., and Thomas, S.P. (2021). Association of TP53 mutation with decreased prevalence of MSI-high, RAS and PI3KCA mutations in metastatic colorectal cancer. Journal of Clinical Oncology *39*, e15578-e15578. 10.1200/JCO.2021.39.15_suppl.e15578.

189. Khushman, M.d.M., Gandhi, N., Xiu, J., Manne, U., Lou, E., Shields, A.F., El-Deiry, W.S., Braxton, D.R., Oberley, M.J., Marshall, J., et al. (2023). The molecular signature of gain-of-function (GOF) vs. non-GOF classification TP53 mutations in colorectal cancer. Journal of Clinical Oncology *41*, e15612-e15612. 10.1200/JCO.2023.41.16_suppl.e15612.

190. Hassin, O., Nataraj, N.B., Shreberk-Shaked, M., Aylon, Y., Yaeger, R., Fontemaggi, G., Mukherjee, S., Maddalena, M., Avioz, A., Iancu, O., et al. (2022). Different hotspot p53 mutants exert distinct phenotypes and predict outcome of colorectal cancer patients. Nat Commun *13*, 2800. 10.1038/s41467-022-30481-7.

191. Godai, T.I., Suda, T., Sugano, N., Tsuchida, K., Shiozawa, M., Sekiguchi, H., Sekiyama, A., Yoshihara, M., Matsukuma, S., Sakuma, Y., et al. (2009). Identification of colorectal cancer patients with tumors carrying the TP53 mutation on the codon 72 proline allele that benefited most from 5-fluorouracil (5-FU) based postoperative chemotherapy. BMC Cancer *9*, 420. 10.1186/1471-2407-9-420.

192. Jauhri, M., Bhatnagar, A., Gupta, S., Bp, M., Minhas, S., Shokeen, Y., and Aggarwal, S. (2017). Prevalence and coexistence of KRAS, BRAF, PIK3CA, NRAS, TP53, and APC mutations in Indian colorectal cancer patients: Next-generation sequencing-based cohort study. Tumour Biol *39*, 1010428317692265. 10.1177/1010428317692265.

193. Peng, H., Ying, J., Zang, J., Lu, H., Zhao, X., Yang, P., Wang, X., Li, J., Gong, Z., Zhang, D., and Wang, Z. (2023). Specific Mutations in APC, with Prognostic Implications in Metastatic Colorectal Cancer. Cancer Res Treat *55*, 1270-1280. 10.4143/crt.2023.415.

194. Aitchison, A., Hakkaart, C., Day, R.C., Morrin, H.R., Frizelle, F.A., and Keenan, J.I. (2020). APC Mutations Are Not Confined to Hotspot Regions in Early-Onset Colorectal Cancer. Cancers (Basel) *12*. 10.3390/cancers12123829.

195. Xicola, R.M., Manojlovic, Z., Augustus, G.J., Kupfer, S.S., Emmadi, R., Alagiozian-Angelova, V., Triche, T., Jr., Salhia, B., Carpten, J., Llor, X., and Ellis, N.A. (2018). Lack of APC somatic mutation is associated with early-onset colorectal cancer in African Americans. Carcinogenesis *39*, 1331-1341. 10.1093/carcin/bgy122.

196. Shida, D., Kuchiba, A., Shibata, T., Hamaguchi, T., Yamasaki, S., Ito, M., Kobatake, T., Tonooka, T., Masaki, T., Shiozawa, M., et al. (2023). Genomic landscape and its prognostic significance in stage III colorectal cancer: JCOG1506A1, an ancillary of JCOG0910. Cancer Sci *114*, 3352-3363. 10.1111/cas.15834.

197. van de Haar, J., Ma, X., Ooft, S.N., van der Helm, P.W., Hoes, L.R., Mainardi, S., Pinato, D.J., Sun, K., Salvatore, L., Tortora, G., et al. (2023). Codon-specific KRAS mutations predict survival benefit of trifluridine/tipiracil in metastatic colorectal cancer. Nat Med *29*, 605-614. 10.1038/s41591-023-02240-8.

198. Yang, M., Wang, H., Davis, T.B., Pflieger, L., Thota, R., Pledger, W.J., and Yeatman, T.J. (2022). Abstract 5366: Hotspot mutations of TP53 sensitize APC-mutated colorectal cancer cells to cetuximab in vitro. Cancer Research *82*, 5366-5366. 10.1158/1538-7445.Am2022-5366.

199. Merz, V., Gaule, M., Zecchetto, C., Cavaliere, A., Casalino, S., Pesoni, C., Contarelli, S., Sabbadini, F., Bertolini, M., Mangiameli, D., et al. (2021). Targeting KRAS: The Elephant in the Room of Epithelial Cancers. Front Oncol *11*, 638360. 10.3389/fonc.2021.638360.

200. Misale, S., Yaeger, R., Hobor, S., Scala, E., Janakiraman, M., Liska, D., Valtorta, E., Schiavo, R., Buscarino, M., Siravegna, G., et al. (2012). Emergence of KRAS mutations and acquired resistance to anti-EGFR therapy in colorectal cancer. Nature *486*, 532-536. 10.1038/nature11156.

201. Favazza, L.A., Parseghian, C.M., Kaya, C., Nikiforova, M.N., Roy, S., Wald, A.I., Landau, M.S., Proksell, S.S., Dueker, J.M., Johnston, E.R., et al. (2020). KRAS amplification in metastatic colon cancer is associated with a history of inflammatory bowel disease and may confer resistance to anti-EGFR therapy. Mod Pathol *33*, 1832-1843. 10.1038/s41379-020-0560-x.

202. Astaras, C., De Vito, C., Chaskar, P., Bornand, A., Khanfir, K., Sciarra, A., Letovanec, I., Corro, C., Dietrich, P.Y., Tsantoulis, P., and Koessler, T. (2023). The first comprehensive genomic characterization of rectal squamous cell carcinoma. J Gastroenterol *58*, 125-134. 10.1007/s00535-022-01937-w.

203. Greger, J.G., Eastman, S.D., Zhang, V., Bleam, M.R., Hughes, A.M., Smitheman, K.N., Dickerson, S.H., Laquerre, S.G., Liu, L., and Gilmer, T.M. (2012). Combinations of BRAF, MEK, and PI3K/mTOR inhibitors overcome acquired resistance to the BRAF inhibitor GSK2118436 dabrafenib, mediated by NRAS or MEK mutations. Mol Cancer Ther *11*, 909-920. 10.1158/1535-7163.MCT-11-0989.

204. Misale, S., Arena, S., Lamba, S., Siravegna, G., Lallo, A., Hobor, S., Russo, M., Buscarino, M., Lazzari, L., Sartore-Bianchi, A., et al. (2014). Blockade of EGFR and MEK Intercepts Heterogeneous Mechanisms of Acquired Resistance to Anti-EGFR Therapies in Colorectal Cancer. Science Translational Medicine *6*, 224ra226-224ra226. doi:10.1126/scitranslmed.3007947.

205. Yasin, F., Sokol, E., Vasan, N., Pavlick, D.C., Huang, R.S.P., Pelletier, M., Levy, M.A., Pusztai, L., Lacy, J., Zhang, J.Y., et al. (2024). Molecular characteristics of advanced colorectal cancer and multi-hit PIK3CA mutations. Oncologist *29*, 1059-1067. 10.1093/oncolo/oyae259.

206. Li, W., Li, L., Yang, H., Shi, C., Lei, Z., Guo, L., and Wang, Y. (2024). Unraveling the Role of TP53 in Colorectal Cancer Therapy: From Wild-Type Regulation to Mutant. Front Biosci (Landmark Ed) *29*, 272. 10.31083/j.fbl2907272.

207. Aslam, R., Richards, C.E., Fay, J., Hudson, L., Workman, J., Lee, C.L., Murphy, A., O'Neill, B., Toomey, S., and Hennessy, B.T. (2024). Synergistic Effects of the Combination of Alpelisib (PI3K Inhibitor) and Ribociclib (CDK4/6 Inhibitor) in Preclinical Colorectal Cancer Models. Int J Mol Sci *25*. 10.3390/ijms252413264.

208. Shin, A.E., Sugiura, K., Kariuki, S.W., Cohen, D.A., Flashner, S.P., Klein-Szanto, A.J., Nishiwaki, N., De, D., Vasan, N., Gabre, J.T., et al. (2025). LIN28B-mediated PI3K/AKT pathway activation promotes metastasis in colorectal cancer models. J Clin Invest *135*. 10.1172/JCI186035.

209. Yang, H., Xiao, X., Zeng, L., Zeng, H., Zheng, Y., Wang, J., Li, G., Dai, W., He, Y., Wang, S., et al. (2024). Integrating cfDNA liquid biopsy and organoid-based drug screening reveals PI3K signaling as a promising therapeutic target in colorectal cancer. J Transl Med *22*, 132. 10.1186/s12967-023-04675-6.

210. Tang, Y., and Fan, Y. (2024). Combined KRAS and TP53 mutation in patients with colorectal cancer enhance chemoresistance to promote postoperative recurrence and metastasis. BMC Cancer *24*, 1155. 10.1186/s12885-024-12776-8.

211. Zhang, J., Yan, B., Spath, S.S., Qun, H., Cornelius, S., Guan, D., Shao, J., Hagiwara, K., Van Waes, C., Chen, Z., et al. (2015). Integrated transcriptional profiling and genomic analyses reveal RPN2 and HMGB1 as promising biomarkers in colorectal cancer. Cell Biosci *5*, 53. 10.1186/s13578-015-0043-9.

212. Cui, L., Liu, R., Han, S., Zhang, C., Wang, B., Ruan, Y., Yu, X., Li, Y., Yao, Y., Guan, X., et al. (2025). Targeting Arachidonic Acid Metabolism Enhances Immunotherapy Efficacy in ARID1A-Deficient Colorectal Cancer. Cancer Res *85*, 925-941. 10.1158/0008-5472.CAN-24-1611.

213. Wanna-Udom, S., Aluksanasuwan, S., Somsuan, K., Mongkolwat, W., and Sakulsak, N. (2024). ARID1A overexpression inhibits colorectal cancer cell migration through the regulation of epithelial-mesenchymal transition. Mol Med Rep *30*. 10.3892/mmr.2024.13325.

214. Lieu, C.H., Golemis, E.A., Serebriiskii, I.G., Newberg, J., Hemmerich, A., Connelly, C., Messersmith, W.A., Eng, C., Eckhardt, S.G., Frampton, G., et al. (2019). Comprehensive Genomic Landscapes in Early and Later Onset Colorectal Cancer. Clin Cancer Res *25*, 5852-5858. 10.1158/1078-0432.CCR-19-0899.

215. Nicolas, E., Golemis, E.A., and Arora, S. (2016). POLD1: Central mediator of DNA replication and repair, and implication in cancer and other pathologies. Gene *590*, 128-141. 10.1016/j.gene.2016.06.031.

216. Pursell, Z.F., and Kunkel, T.A. (2008). DNA polymerase epsilon: a polymerase of unusual size (and complexity). Prog Nucleic Acid Res Mol Biol *82*, 101-145. 10.1016/S0079-6603(08)00004-4.

217. Park, V.S., and Pursell, Z.F. (2019). POLE proofreading defects: Contributions to mutagenesis and cancer. DNA Repair (Amst) *76*, 50-59. 10.1016/j.dnarep.2019.02.007.

218. Landre, T., and Des Guetz, G. (2025). Microsatellite instability-high status as a pan-cancer biomarker for immunotherapy efficacy. Cancer Immunol Immunother *74*, 122. 10.1007/s00262-025-03980-x.

219. Le, D.T., Durham, J.N., Smith, K.N., Wang, H., Bartlett, B.R., Aulakh, L.K., Lu, S., Kemberling, H., Wilt, C., Luber, B.S., et al. (2017). Mismatch repair deficiency predicts response of solid tumors to PD-1 blockade. Science *357*, 409-413. 10.1126/science.aan6733.

220. Ma, X., Dong, L., Liu, X., Ou, K., and Yang, L. (2022). POLE/POLD1 mutation and tumor immunotherapy. J Exp Clin Cancer Res *41*, 216. 10.1186/s13046-022-02422-1.

221. Knoll, M.A., Griffith, K.A., Jones, R.D., and Jagsi, R. (2019). Association of Gender and Parenthood With Conference Attendance Among Early Career Oncologists. JAMA Oncol *5*, 1503-1504. 10.1001/jamaoncol.2019.1864.

222. Niu, Y., Ma, T., Niu, Y., and Li, T. (2021). Investigating the various predictive values of POLE/POLD1 mutations for response to immune checkpoint inhibitors (ICIs) in different solid tumors. Journal of Clinical Oncology *39*, 2606-2606. 10.1200/JCO.2021.39.15_suppl.2606.

223. Wu, Y., Sha, Y., Guo, X., Gao, L., Huang, J., and Liu, S.B. (2025). Organoid models: applications and research advances in colorectal cancer. Front Oncol *15*, 1432506. 10.3389/fonc.2025.1432506.

224. Luo, Z., Wang, B., Luo, F., Guo, Y., Jiang, N., Wei, J., Wang, X., Tseng, Y., Chen, J., Zhao, B., and Liu, J. (2023). Establishment of a large-scale patient-derived high-risk colorectal adenoma organoid biobank for high-throughput and high-content drug screening. BMC Med *21*, 336. 10.1186/s12916-023-03034-y.

225. Weeber, F., van de Wetering, M., Hoogstraat, M., Dijkstra, K.K., Krijgsman, O., Kuilman, T., Gadellaa-van Hooijdonk, C.G., van der Velden, D.L., Peeper, D.S., Cuppen, E.P., et al. (2015). Preserved genetic diversity in organoids cultured from biopsies of human colorectal cancer metastases. Proc Natl Acad Sci U S A *112*, 13308-13311. 10.1073/pnas.1516689112.

226. van de Wetering, M., Francies, H.E., Francis, J.M., Bounova, G., Iorio, F., Pronk, A., van Houdt, W., van Gorp, J., Taylor-Weiner, A., Kester, L., et al. (2015). Prospective derivation of a living organoid biobank of colorectal cancer patients. Cell *161*, 933-945. 10.1016/j.cell.2015.03.053.

227. He, X., Jiang, Y., Zhang, L., Li, Y., Hu, X., Hua, G., Cai, S., Mo, S., and Peng, J. (2023). Patient-derived organoids as a platform for drug screening in metastatic colorectal cancer. Front Bioeng Biotechnol *11*, 1190637. 10.3389/fbioe.2023.1190637.

228. Yao, L., Zao, X.L., Pan, X.F., Zhang, H.G., Wang, F.J., and Qiao, P.F. (2023). Application of tumoroids derived from advanced colorectal cancer patients to predict individual response to chemotherapy. J Chemother *35*, 104-116. 10.1080/1120009x.2022.2045827.

229. Han, J., Jeong, H.J., Choi, J., Kim, H., Kwon, T., Myung, K., Park, K., Park, J.I., Sanchez, S., Jung, D.B., et al. (2025). Bioprinted Patient-Derived Organoid Arrays Capture Intrinsic and Extrinsic Tumor Features for Advanced Personalized Medicine. Adv Sci (Weinh) *12*, e2407871. 10.1002/advs.202407871.

230. Lo, Y.H., Karlsson, K., and Kuo, C.J. (2020). Applications of Organoids for Cancer Biology and Precision Medicine. Nat Cancer *1*, 761-773. 10.1038/s43018-020-0102-y.

231. Fujii, M., Shimokawa, M., Date, S., Takano, A., Matano, M., Nanki, K., Ohta, Y., Toshimitsu, K., Nakazato, Y., Kawasaki, K., et al. (2016). A Colorectal Tumor Organoid Library Demonstrates Progressive Loss of Niche Factor Requirements during Tumorigenesis. Cell Stem Cell *18*, 827-838. 10.1016/j.stem.2016.04.003.

232. Esposito, A., Agostini, A., Quero, G., Piro, G., Priori, L., Caggiano, A., Scaglione, G., Battaglia, A., Calegari, M.A., Salvatore, L., et al. (2024). Colorectal cancer patients-derived immunity-organoid platform unveils cancer-specific tissue markers associated with immunotherapy resistance. Cell Death Dis *15*, 878. 10.1038/s41419-024-07266-5.

233. Thng, D.K.H., Hooi, L., Siew, B.E., Lee, K.Y., Tan, I.J., Lieske, B., Lin, N.S., Kow, A.W.C., Wang, S., Rashid, M., et al. (2024). A functional personalised oncology

approach against metastatic colorectal cancer in matched patient derived organoids. NPJ Precis Oncol *8*, 52. 10.1038/s41698-024-00543-8.

234. Feng, Z., Li, Y., Wu, J., Yin, J., Wang, R., and Liang, S. (2025). Establishment of a Co-culture System of Patient-Derived Colorectal Tumor Organoids and Tumor-Infiltrating Lymphocytes (TILs). J Vis Exp. 10.3791/68346.

235. Dijkstra, K.K., Vendramin, R., Karagianni, D., Witsen, M., Galvez-Cancino, F., Hill, M.S., Foster, K.A., Barbe, V., Angelova, M., Hynds, R.E., et al. (2025). Subclonal immune evasion in non-small cell lung cancer. Cancer Cell. 10.1016/j.ccell.2025.06.012.

236. Kraja, F.P., Jurisic, V.B., Hromic-Jahjefendic, A., Rossopoulou, N., Katsila, T., Mirjacic Martinovic, K., De Las Rivas, J., Diaconu, C.C., and Szoor, A. (2025). Tumor-infiltrating lymphocytes in cancer immunotherapy: from chemotactic recruitment to translational modeling. Front Immunol *16*, 1601773. 10.3389/fimmu.2025.1601773.

237. Wang, Q., Yuan, F., Zuo, X., and Li, M. (2025). Breakthroughs and challenges of organoid models for assessing cancer immunotherapy: a cutting-edge tool for advancing personalised treatments. Cell Death Discov *11*, 222. 10.1038/s41420-025-02505-w.

238. Yao, N., Jing, N., Lin, J., Niu, W., Yan, W., Yuan, H., Xiong, Z., Hou, Q., Qiao, X., Liu, Q., et al. (2025). Patient-derived tumor organoids for cancer immunotherapy: culture techniques and clinical application. Invest New Drugs *43*, 394-404. 10.1007/s10637-025-01523-w.

239. Dijkstra, K.K., Cattaneo, C.M., Weeber, F., Chalabi, M., van de Haar, J., Fanchi, L.F., Slagter, M., van der Velden, D.L., Kaing, S., Kelderman, S., et al. (2018). Generation of Tumor-Reactive T Cells by Co-culture of Peripheral Blood Lymphocytes and Tumor Organoids. Cell *174*, 1586-1598 e1512. 10.1016/j.cell.2018.07.009.

240. Cattaneo, C.M., Dijkstra, K.K., Fanchi, L.F., Kelderman, S., Kaing, S., van Rooij, N., van den Brink, S., Schumacher, T.N., and Voest, E.E. (2020). Tumor organoid-T-cell coculture systems. Nat Protoc *15*, 15-39. 10.1038/s41596-019-0232-9.

241. Olivo Pimentel, V., Yaromina, A., Marcus, D., Dubois, L.J., and Lambin, P. (2020). A novel co-culture assay to assess anti-tumor CD8(+) T cell cytotoxicity via luminescence and multicolor flow cytometry. J Immunol Methods *487*, 112899. 10.1016/j.jim.2020.112899.

242. Taieb, J., Balogoun, R., Le Malicot, K., Tabernero, J., Mini, E., Folprecht, G., Van Laethem, J.L., Emile, J.F., Mulot, C., Fratte, S., et al. (2017). Adjuvant FOLFOX +/- cetuximab in full RAS and BRAF wildtype stage III colon cancer patients. Ann Oncol *28*, 824-830. 10.1093/annonc/mdw687.

243. Fisher, R., Pusztai, L., and Swanton, C. (2013). Cancer heterogeneity: implications for targeted therapeutics. Br J Cancer *108*, 479-485. 10.1038/bjc.2012.581.

244. Yang, C., Xiao, W., Wang, R., Hu, Y., Yi, K., Sun, X., Wang, G., and Xu, X. (2023). Tumor organoid model of colorectal cancer (Review). Oncol Lett *26*, 328. 10.3892/ol.2023.13914.

245. Shin, W., Wu, A., Min, S., Shin, Y.C., Fleming, R.Y.D., Eckhardt, S.G., and Kim, H.J. (2020). Spatiotemporal Gradient and Instability of Wnt Induce Heterogeneous Growth and Differentiation of Human Intestinal Organoids. iScience *23*, 101372. 10.1016/j.isci.2020.101372.

246. Costa, D., Vene, R., Coco, S., Longo, L., Tosetti, F., Scabini, S., Mastracci, L., Grillo, F., Poggi, A., and Benelli, R. (2023). SB202190 Predicts BRAF-Activating Mutations in Primary Colorectal Cancer Organoids via Erk1-2 Modulation. Cells *12*. 10.3390/cells12040664.

247. Walaas, G.A., Gopalakrishnan, S., Bakke, I., Skovdahl, H.K., Flatberg, A., Ostvik, A.E., Sandvik, A.K., and Bruland, T. (2023). Physiological hypoxia improves growth and functional differentiation of human intestinal epithelial organoids. Front Immunol *14*, 1095812. 10.3389/fimmu.2023.1095812.

248. Zhang, L., Mo, S., Hu, X., Ma, X., Jin, W., Peng, D.H., Zhou, Y., Liang, X., Rao, X., Xu, X., et al. (2020). Establishment and identification of organoids from human circulating colorectal cancer cells. Clin Transl Med *10*, e247. 10.1002/ctm2.247.

249. Wang, J., Tao, X., Zhu, J., Dai, Z., Du, Y., Xie, Y., Chu, X., Fu, G., and Lei, Z. (2025). Tumor organoid-immune co-culture models: exploring a new perspective of tumor immunity. Cell Death Discov *11*, 195. 10.1038/s41420-025-02407-x.

250. Magre, L., Verstegen, M.M.A., Buschow, S., van der Laan, L.J.W., Peppelenbosch, M., and Desai, J. (2023). Emerging organoid-immune co-culture models for cancer research: from oncoimmunology to personalized immunotherapies. J Immunother Cancer *11*. 10.1136/jitc-2022-006290.

251. Xu, H., Jiao, D., Liu, A., and Wu, K. (2022). Tumor organoids: applications in cancer modeling and potentials in precision medicine. J Hematol Oncol *15*, 58. 10.1186/s13045-022-01278-4.

252. Xiang, D., He, A., Zhou, R., Wang, Y., Xiao, X., Gong, T., Kang, W., Lin, X., Wang, X., Consortium, P.D.-b.D., et al. (2024). Building consensus on the application of organoid-based drug sensitivity testing in cancer precision medicine and drug development. Theranostics *14*, 3300-3316. 10.7150/thno.96027.

253. Yan, Y., Cheong, I.H., Chen, P., Li, X., Wang, X., and Wang, H. (2022). Patient-derived rectal cancer organoids-applications in basic and translational cancer research. Front Oncol *12*, 922430. 10.3389/fonc.2022.922430.

254. Brennen, W.N., Le Magnen, C., Karkampouna, S., Anselmino, N., Bock, N., Choo, N., Clark, A.K., Coleman, I.M., Dolgos, R., Ferguson, A.M., et al. (2024). Defining the challenges and opportunities for using patient-derived models in prostate cancer research. Prostate *84*, 623-635. 10.1002/pros.24682.

255. Yang, J., Huang, S., Cheng, S., Jin, Y., Zhang, N., and Wang, Y. (2021). Application of Ovarian Cancer Organoids in Precision Medicine: Key Challenges and Current Opportunities. Front Cell Dev Biol *9*, 701429. 10.3389/fcell.2021.701429.

256. Gezgin, G., Visser, M., Ruano, D., Santegoets, S.J., de Miranda, N., van der Velden, P.A., Luyten, G.P.M., van der Burg, S.H., Verdegaal, E.M., and Jager, M.J. (2022). Tumor-Infiltrating T Cells Can Be Expanded Successfully from Primary Uveal Melanoma after Separation from Their Tumor Environment. Ophthalmol Sci *2*, 100132. 10.1016/j.xops.2022.100132.

257. Dudley, M.E., Wunderlich, J.R., Shelton, T.E., Even, J., and Rosenberg, S.A. (2003). Generation of tumor-infiltrating lymphocyte cultures for use in adoptive transfer therapy for melanoma patients. J Immunother *26*, 332-342. 10.1097/00002371-200307000-00005.

258. Baldan, V., Griffiths, R., Hawkins, R.E., and Gilham, D.E. (2015). Efficient and reproducible generation of tumour-infiltrating lymphocytes for renal cell carcinoma. Br J Cancer *112*, 1510-1518. 10.1038/bjc.2015.96.

259. Yu, Z., Shi, J., Fang, Y., Zhao, Y., Xu, A., and Li, N. (2024). Developing innovative strategies of tumor-infiltrating lymphocyte therapy for tumor treatment. Oncol Rep *51*. 10.3892/or.2024.8744.

260. Chen, Y., Wang, D., Li, Y., Qi, L., Si, W., Bo, Y., Chen, X., Ye, Z., Fan, H., Liu, B., et al. (2024). Spatiotemporal single-cell analysis decodes cellular dynamics underlying different responses to immunotherapy in colorectal cancer. Cancer Cell *42*, 1268-1285 e1267. 10.1016/j.ccell.2024.06.009.

261. Zhang, W., Wu, C., Huang, H., Bleu, P., Zambare, W., Alvarez, J., Wang, L., Paty, P.B., Romesser, P.B., Smith, J.J., and Chen, X.S. (2025). Enhancing chemotherapy response prediction via matched colorectal tumor-organoid gene expression analysis and network-based biomarker selection. Transl Oncol *52*, 102238. 10.1016/j.tranon.2024.102238.

262. Zhang, H., Li, S., Wang, D., Liu, S., Xiao, T., Gu, W., Yang, H., Wang, H., Yang, M., and Chen, P. (2024). Metabolic reprogramming and immune evasion: the interplay in the tumor microenvironment. Biomark Res *12*, 96. 10.1186/s40364-024-00646-1.

IV. Appendix

Table 1. The 818 genes included in the targeted sequencing panel.

ABI1	ABL1	ABL2	ABRAXAS 1	ACSL6	ACTB	ACVR1B	ACVR2A	ADAM29	ADGRA2
AFDN	AFF1	AFF4	AGTR2	AKT1	AKT2	AKT3	ALK	AMER1	APC
APH1A	AR	ARAF	ARFRP1	ARHGAP26	ARHGEF12	ARID1A	ARID1B	ARID2	ARNT
ASMTL	ASXL1	ATF1	ATG5	ATIC	ATM	ATR	ATRX	AURKA	AURKB
AXIN1	AXIN2	AXL	B2M	BACH1	BAP1	BARD1	BCL10	BCL11A	BCL11B
BGL2	BGL2L1	BCL2L1	BCL2L2	BCL3	BCL6	BCL7A	BCL9	BCOR	BCORL1
BCR	BIRC3	BIRC5	BLK	BLM	BMPR1A	BMX	BRAF	BRCA1	BRCA2
BRD1	BRD4	BRIP1	BRSK1	BTG1	BTG2	BTK	BTLA	CAD	CAMTAI
CARD 11	CARS	CBFA2T3	CBFB	CBL	CCNB1	CCND1	CCND2	CCND3	CCNE1
CCT6B	CD22	CD274	CD36	CD58	CD70	CD79A	CD79B	CDC73	CDH1
CDK2	CDK7	CDK12	CDK4	CDK6	CDK8	CDK9	CDKN1A	CDKN1B	CDKN2A
CDKN2B	CDKN2C	CDX2	CEBPA	CHD2	CHD4	CHEK1	CHEK2	CHIC2	CHN1
CIC	CIITA	CKS1B	CLP1	CLTC	CLTCL1	CNTRL	COL1A1	CPS1	CRBN
CREB3L1	CREB3L2	CREBBP	CRKL	CRLF2	CSF1	CSF1R	CSF3R	CSK	CSNK1A1
CTCF	CTNNA1	CTNNB1	CUL3	CUL4A	CUX1	CXCR4	CYLD	DAXX	DDIT3
DDR1	DDR2	DDX10	DDX3X	DDX6	DEK	DICER1	DNM2	DNMT3A	DOT IL
DTX1	DUSP2	DUSP22	DUSP9	EBF1	ECT2L	EED	EGF	EGFR	EIF4A2
ELF4	ELL	ELN	ELP2	EML4	EMSY	ENO1	EP300	EPCAM	EPHA2
EPHA3	EPHA5	EPHA7	EPHB1	EPOR	EPS 15	ERAS	ERBB2	ERBB3	ERBB4
ERCC1	ERCC2	ERG	ERRFI1	ESRI	ETS1	ETV1	ETV4	ETV5	ETV6
EWSR1	EXOSC6	EZH1	EZH2	FAAP24	FAF1	FAM135B	FAM46C	FANCA	FANCB
FANCC	FANCD2	FANCE	FANCF	FANCG	FANCI	FANCL	FANCM	FAS	FAT1
FBXO11	FBXO31	FBXW7	FCGR2B	FCRL4	FEV	FGF1	FGF2	FGF3	FGF4
FGF5	FGF6	FGF7	FGF8	FGF9	FGF10	FGF16	FGF17	FGF18	FGF19
FGF20	FGF21	FGF22	FGF23	FGFR1	FGFR1OP	FGFR2	FGFR3	FGFR4	FGR
FH	FHIT	FLCN	FLU	FLT1	FLT3	FLT4	FLYWCH1	FNBP1	FOXL2
FOXO1	FOXO3	FOXO4	FOXP1	FRS2	FSTL3	FUBP1	FUS	FYN	GABRA6
GADD45B	GAS7	GATA1	GATA2	GATA3	GATA4	GATA6	GID4	GLI1	GLI2
GLI3	GMPS	GNA11	GNA12	GNA13	GNAQ	GNAS	GPHN	GREM1	GRIN2A
GRM3	GSK3B	GTSE1	H3F3A	HCK	HDAC1	HDAC4	HDAC7	HERPUD1	HEY1
HGF	HIP1	HIST1H1C	HIST1H1D	HIST1H1E	HIST1H2AC	HIST1H2AG	HIST1H2AL	HIST1H2AM	HIST1H2BC
HIST1H2BJ	HIST1H2BK	HIST1H2BO	HIST1H3B	HLF	HMGA1	HMGA2	HNF1A	HOXA11	HOXA13
HOXA3	HOXA9	HOXB13	HOXC11	HOXC13	HOXD11	HOXD13	HRAS	HSD3B1	HSP90AA1
HSP90AB1	ICK	ID3	IDH1	IDH2	IGF1R	IGF2	IKBKE	IKZF1	IKZF2
IKZF3	IL21R	IL3	IL6	IL7R	INHBA	INPP4B	INPP5D	IRAK4	IRF1
IRF2	IRF4	IRF8	IRS2	ITK	JAK1	JAK2	JAK3	JARID2	JAZF1
JUN	KAT6A	KDM2B	KDM4C	KDM5A	KDM5C	KDM6A	KDR	KDSR	KEAP1
KEL	KIT	KLHL6	KMT2A	KMT2C	KMT2D	KRAS	LASPI	LCK	LCP1
LEF1	LIMK1	LMO1	LMO2	LOC102724428	LPP	LRP1	LRP1B	LRRK2	LYL1
LYN	LZTR1	MAF	MAFB	MAGED1	MAGI2	MALT1	MAP2K1	MAP2K2	MAP2K4
MAP3K1	MAP3K13	MAP3K14	MAP3K4	MAP3K6	MAP3K7	MAP3K8	MAP4K5	MAPK1	MAPK3
MAX	MCL1	MCPH1	MDM2	MDM4	MDS2	MEGOM	MED 12	MEF2B	MEF2C
MEN1	MET	MIB1	MITF	MKI67	MKL1	MLF1	MLH1	MLLT1	MLLT10
MLLT3	MLLT6	MN1	MNX1	MPL	MRAS	MRE11	MS4A1	MSH2	MSH3
MSH6	MSI2	MSN	MST1R	MTOR	MUC1	MUTYH	MYB	MYC	MYCL
MYCN	MYD88	MYH11	MYH9	MYO18A	MYT1	NACA	NBEAP1	NBN	NCOA2
NCOR2	NCSTN	NDRG1	NEK 11	NF1	NF2	NFE2L2	NFE2L3	NFKB2	NFKBIA
NIN	NKX2-1	NODI	NOTCH 1	NOTCH2	NOTCH3	NPM1	NR4A3	NRAS	NRG1
NRG3	NSD1	NSD2	NSD3	NT5C2	NTRK1	NTRK2	NTRK3	NUMA1	NUP214
NUP93	NUP98	NUTM2A	OMD	P2RY8	PAFAH1B2	PAG1	PAK1	PAK3	PALB2
PALLD	PARP1	PARP2	PASK	PAX3	PAX5	PAX7	PBRM1	PBX1	PC
PCBP1	PCLO	PCM1	PCSK7	PDCD1	PDCD11	PDCD1LG2	PDE4DIP	PDGFB	PDGFRA
PDGFRB	PDK1	PERI	PHF1	PHF6	PICALM	PIK3C2B	PIK3C2G	PIK3C3	PIK3CA
PIK3CB	PIK3CD	PIK3CG	PIK3R1	PIK3R2	PIM1	PKD2	PLA2G1B	PLAG1	PLCG2
PML	PMS1	PMS2	POLD1	POLE	POTI	POU2AF1	PPP1CB	PPP2R1A	PPP2R2A
PRDM1	PRDM16	PREX2	PRKAR1A	PRKCI	PRKDC	PRKN	PRRX1	PRSS8	PSIP1
PTCHI	PTEN	PTENP1	PTK2	PTK6	PTK7	PTPN11	PTPN2	PTPN6	PTPRO
QKI	RABEP1	RAC1	RAC2	RAD21	RAD50	RAD51	RAD51B	RAD51C	RAD51D
RAD52	RAD54L	RAFI	RALGDS	RANBP2	RAP1GDS1	RARA	RASA1	RASGEF1A	RBI
RBM10	RBM15	RELN	RET	RHEB	RHOA	RHOH	RICTOR	RIT1	RNF213
RNF43	ROCK1	ROCK2	ROS1	RPA1	RPL22	RPN1	RPS4Y1	RPTOR	RUNX1
RUNX1T1	RUNX2	RXRA	S1PR2	SDC4	SDHA	SDHAF2	SDHB	SDHC	SDHD
SEG31A	SERP2	SET	SETBP1	SETD2	SF3B1	SGK1	SH3GL1	SLC1A2	SLIT2
SMAD2	SMAD3	SMAD4	SMARCA1	SMARCA4	SMARCB1	SMC1A	SMC3	SMO	SNCAIP
SNX29	SOCS1	SOCS2	SOCS3	SOS1	SOXIO	SOX2	SOX9	SPEN	SPOP
SPTA1	SRC	SRMS	SRSF2	SRSF3	SRY	SS18	SSX1	SSX2	SSX4
STAG2	STAT3	STAT4	STAT5A	STAT5B	STAT6	STK11	STK24	SUFU	SUZ12
SYK	TACC3	TAF1	TAF15	TALI	TAL2	TBL1XR1	TBL1Y	TBX3	TCF3
TCF7L2	TCL1A	TEC	TEK	TERT	TET1	TET2	TFE3	TFG	TFPT
TFRC	TGFBR1	TGFBR2	TIE1	TIPARP	TLL2	TLX1	TLX3	TMEM127	TMEM30A
TMPRSS2	TNFAIP3	TNFRSF11A	TNFRSF14	TNFRSF17	TNFSF11	TNK2	TOPI	TOP2A	TP53
TP53BP1	TP63	TRAF2	TRAF3	TRAF5	TRIM24	TRIP 11	TSC1	TSC2	TSHR
TTL	TUSC3	TYK2	U2AF1	U2AF2	USP6	VEGFA	VHL	WDR90	WEE1
WEE2	WISP3	WRN	WT1	XBP1	XIAP	XPO1	XRCC1	XRCC2	XRCC3
YES1	YPEL5	YY1AP1	ZBTB16	ZBTB2	ZMYM2	ZMYM3	ZNF217	ZNF24	ZNF384
ZNF521	ZNF703	ZNF750	ZRSR2	UGT1A1	UGT1A6	UGT1A9	UMPS	WNT5B	XRCC4
BCL2	CCDC6	CIT	EPB41	ESRP1	EZR	FN1	GOPC	KIAA1549	KIF5B
KLC1	MAGI3	SEC16A	SLC45A3	TPM4	TERT	PTENP1	TERC	NQO1	SLCO1B1
KDM1A	MERTK	TGFB1	TGFBR2	TOP1	TP53	TYMP	TYMS	UBE2I	UGT1A
SLC22A7	ABCC2	ABCC5	ABCG1	ABCG2	AREG	CASP7	CDA	CYP19A1	CYP1B1
DCBLD1	DPYD	ENOSF1	ERCC1	GALNT14	GSTP1	HLA-G	LGR5	MTHFR	NOS3
PARD3B	PON1	PTGS2	RGS5	RRM1	SEMA3C	SHMT1	SLC19A1		

Supplement Figure 1: Established CRC organoids

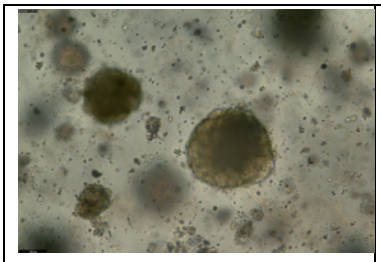 CRC-OR-01; Male; T4N1M0; UICC II; MSS	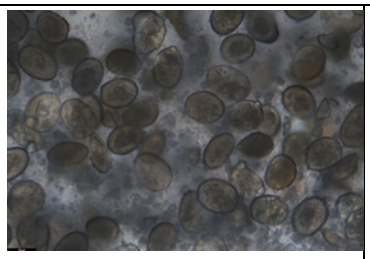 CRC-OR-02; Male; T4N2M0; UICC III; MSS	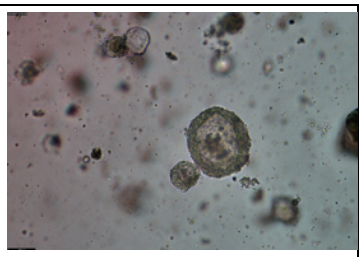 CRC-OR-03; Male; T3N1M0; UICC III; MSS
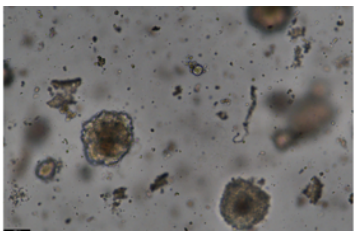 CRC-OR-04; Male; T3N1M0; UICC III; MSS	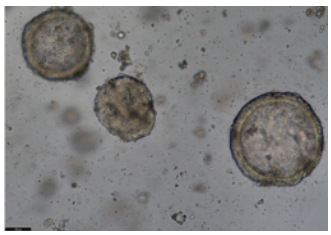 CRC-OR-05; Male; T3N0M0; UICC II; MSS	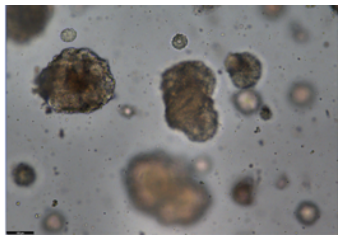 CRC-OR-06; Male; T3N0M0; UICC II; MSS
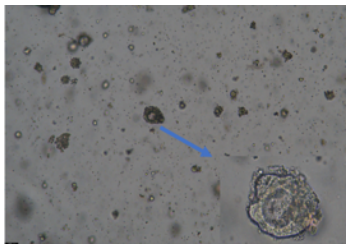 CRC-OR-07; Female; T4N1M0; UICC III; MSI-H	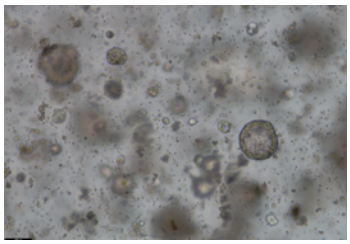 CRC-OR-08; Male; T3N0M0; UICC II; MSS-H	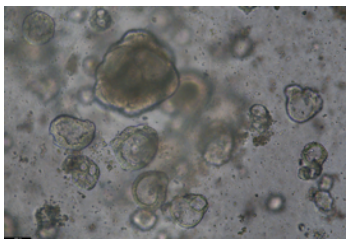 CRC-OR-09; Male; T2N1M0; UICC III; MSS
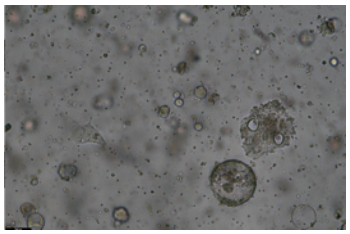 CRC-OR-10; Male; T2N2M0; UICC III; MSS	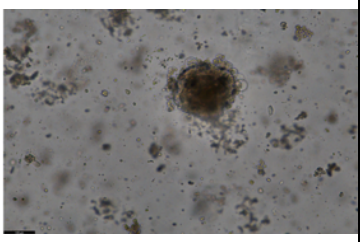 CRC-OR-11; Male; T3N0M0; UICC II; MSS	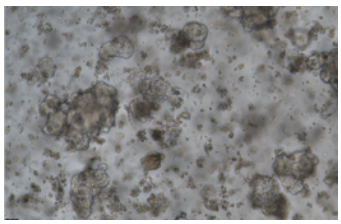 CRC-OR-12; Male; T3N0M0; UICC II; MSS

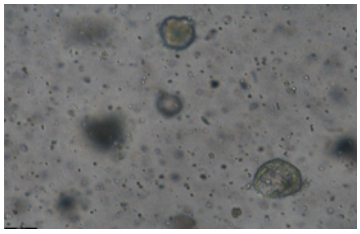 CRC-OR-13; Male; T2N2M0; UICC III; MSS	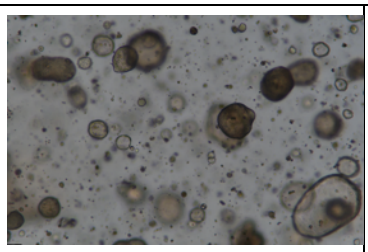 CRC-OR-14; Male; T3N2M1; UICC IV; MSS	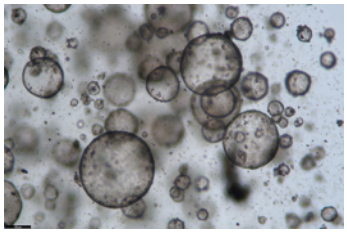 CRC-OR-15; Male; T3N0M0; UICC II; MSS
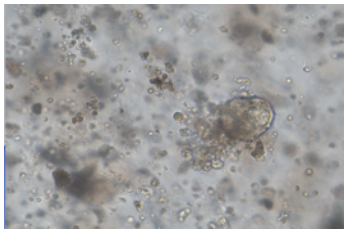 CRC-OR-16; Male; T3N0M0; UICC II; MSI-H	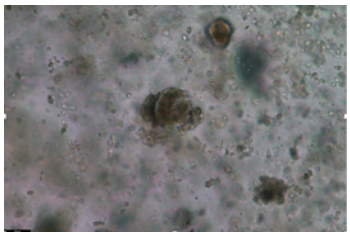 CRC-OR-17; Male; T3N0M1; UICC IV; MSS	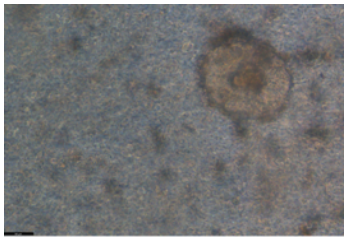 CRC-OR-18; Female; T3N1M0; UICC III; MSS
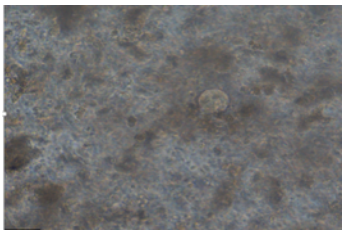 CRC-OR-19; Male; T4N1M1; UICC IV; MSS	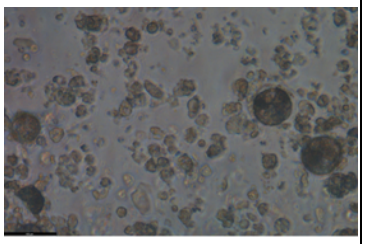 CRC-OR-20; Female; T2N0M0; UICC I; MSS	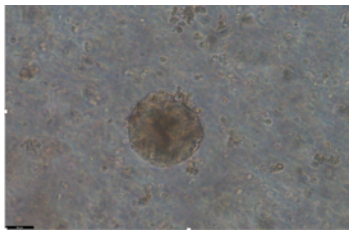 CRC-OR-21; Female; T2N0M0; UICC I; MSS
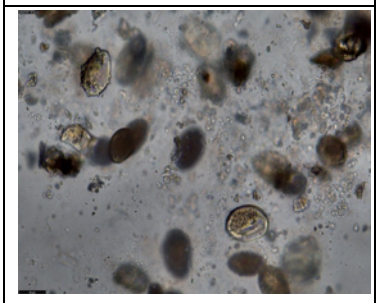 CRC-OR-22; Female; T2N0M0; UICC I; MSS	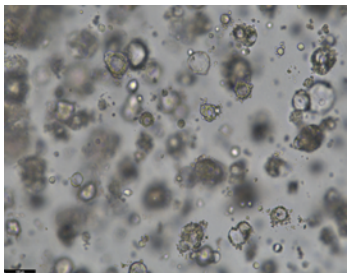 CRC-OR-23; Male; T3N2M0; UICC III; MSS	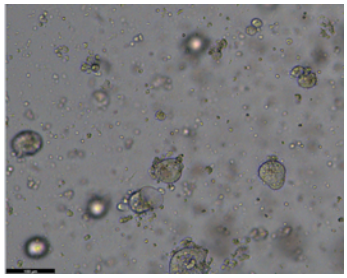 CRC-OR-24; Male; T1N0M0; UICC I; MSS
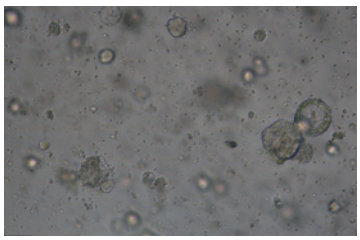 CRC-OR-25; Male; T2N0M0; UICC I; MSS	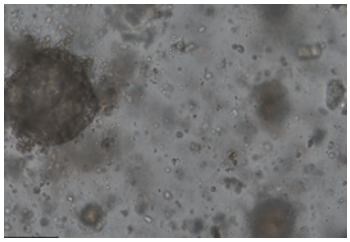 CRC-OR-26; Male; T3N0M0; UICC II; MSS	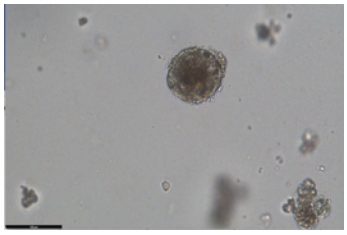 CRC-OR-27; Male; T3N0M0; UICC II; MSS

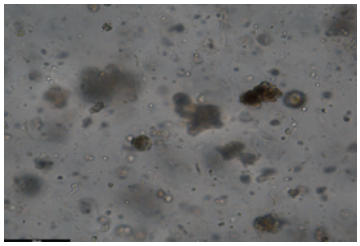 CRC-OR-28; Female; T2N0M0; UICC I; MSS	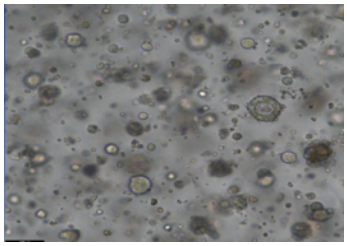 CRC-OR-29; Female; T3N0M0; UICC II; MSS	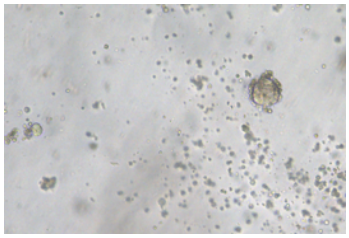 CRC-OR-30; Female; T3N0M0; UICC II; MSS

Supplement Figure 2: Established CRC TILs

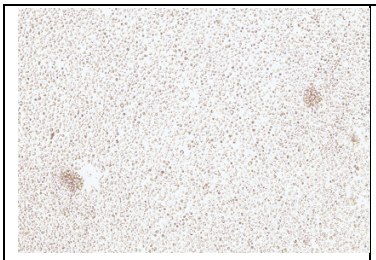 CRC-TIL-01; Male; T4N1M0; UICC II; MSS	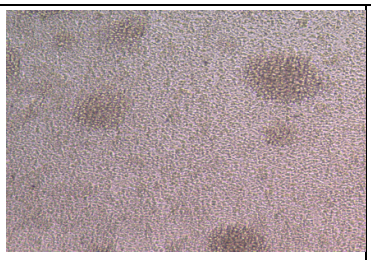 CRC-TIL-02; Male; T4N2M0; UICC III; MSS	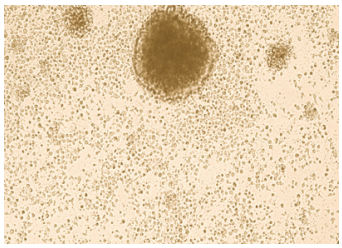 CRC-TIL-03; Male; T3N1M0; UICC III; MSS
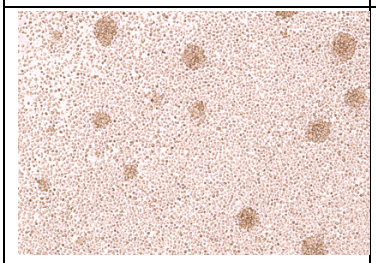 CRC-TIL-04; Male; T3N1M0; UICC III; MSS	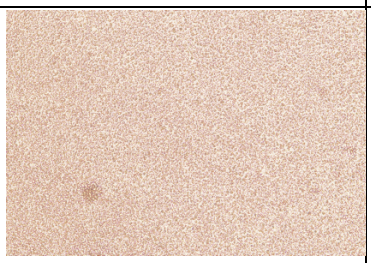 CRC-TIL-05; Male; T3N0M0; UICC II; MSS	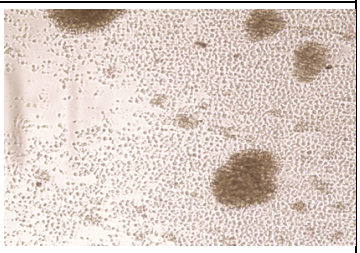 CRC-TIL-06; Male; T3N0M0; UICC II; MSS
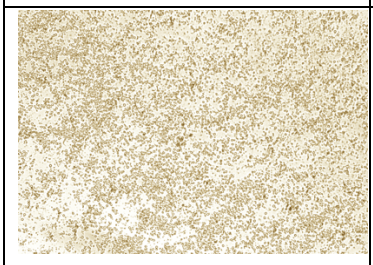 CRC-TIL-07; Female; T4N1M0; UICC III; MSI-H	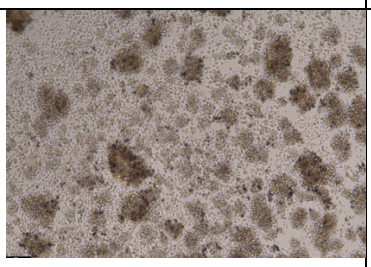 CRC-TIL-08; Male; T3N0M0; UICC II; MSS-H	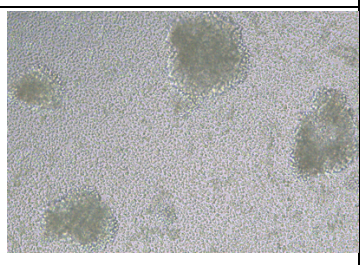 CRC-TIL-09; Male; T2N1M0; UICC III; MSS

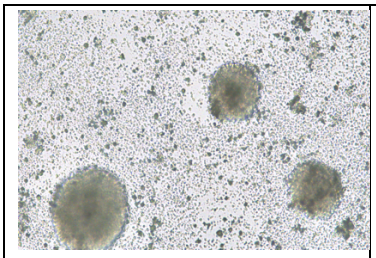 CRC-TIL-10; Male; T2N2M0; UICC III; MSS	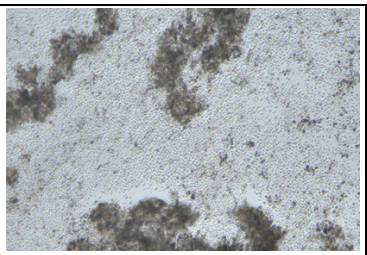 CRC-TIL-11; Male; T3N0M0; UICC II; MSS	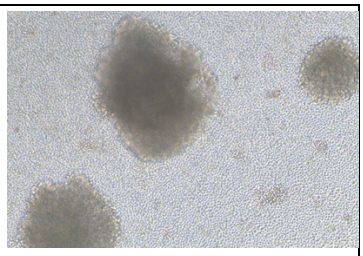 CRC-TIL-12; Male; T3N0M0; UICC II; MSS
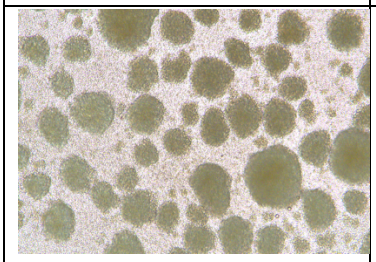 CRC-TIL-13; Male; T2N2M0; UICC III; MSS	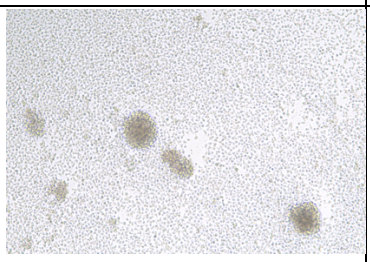 CRC-TIL-14; Male; T3N2M1; UICC IV; MSS	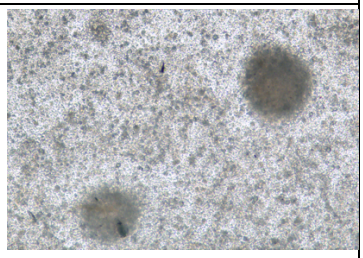 CRC-TIL-15; Male; T3N0M0; UICC II; MSS
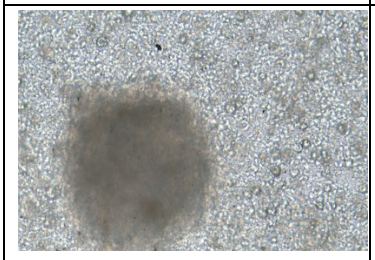 CRC-TIL-16; Male; T3N0M0; UICC II; MSI-H	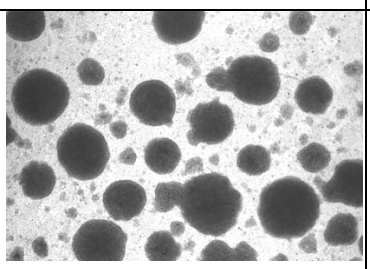 CRC-TIL-17; Male; T3N0M1; UICC IV; MSS	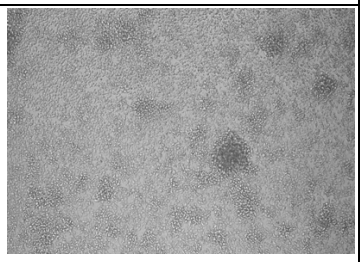 CRC-TIL-18; Female; T3N1M0; UICC III; MSS
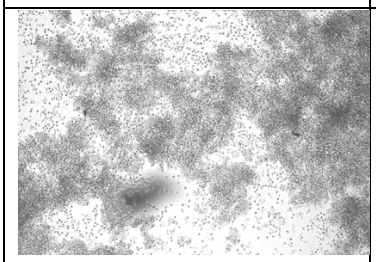 CRC-TIL-19; Male; T4N1M1; UICC IV; MSS	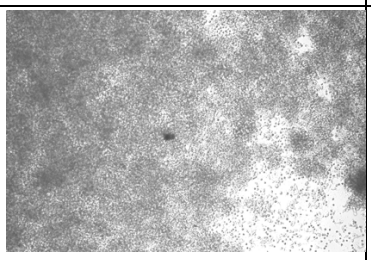 CRC-TIL-20; Female; T2N0M0; UICC I; MSS	 CRC-TIL-21; Female; T2N0M0; UICC I; MSS
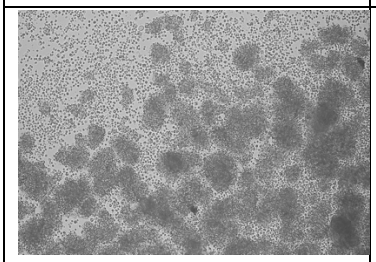 CRC-TIL-22; Female; T2N0M0; UICC I; MSS	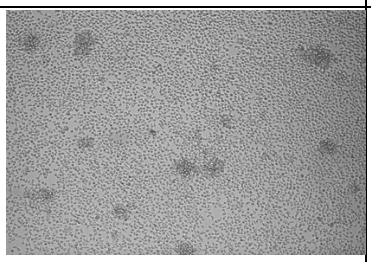 CRC-TIL-23; Male; T3N2M0; UICC III; MSS	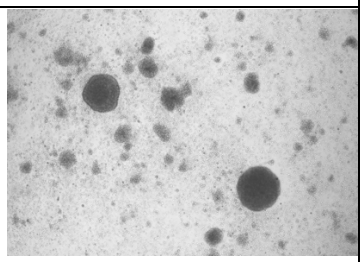 CRC-OR-24; Male; T1N0M0; UICC I; MSS

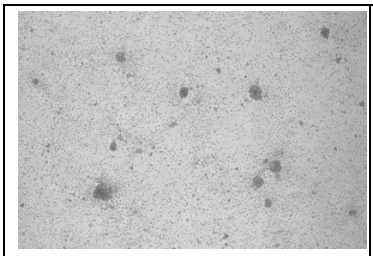 CRC-TIL-25; Male; T2N0M0; UICC I; MSS	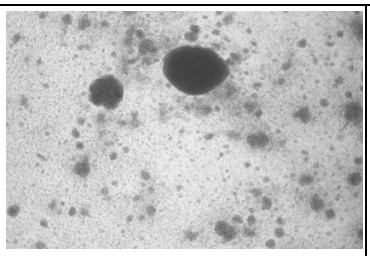 CRC-TIL-26; Male; T3N0M0; UICC II; MSS	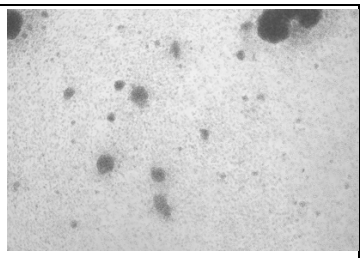 CRC-TIL-27; Male; T3N0M0; UICC II; MSS
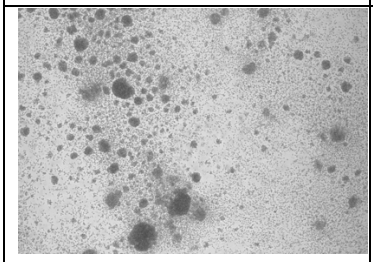 CRC-TIL-28; Female; T2N0M0; UICC I; MSS	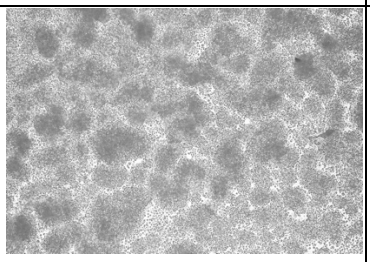 CRC-TIL-29; Female; T3N0M0; UICC II; MSS	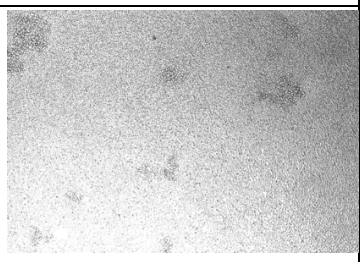 CRC-TIL-30; Female; T3N0M0; UICC II; MSS
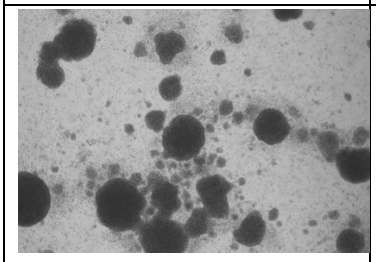 CRC-TIL-31; Male; T3N1M0; UICC III; MSS	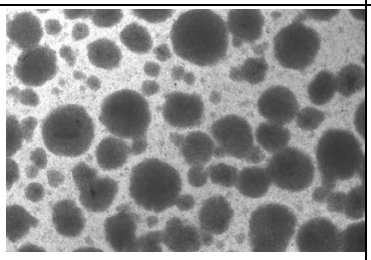 CRC-TIL-32; Female; T1N1M0; UICC I; MSS	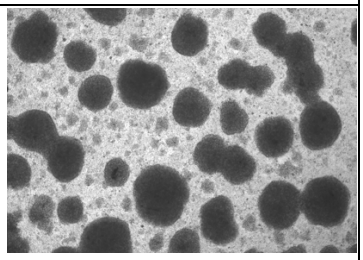 CRC-TIL-33; Male; T3N0M0; UICC II; MSS
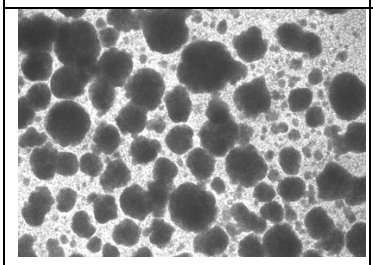 CRC-TIL-34; Female; T2N0M0; UICC I; MSS	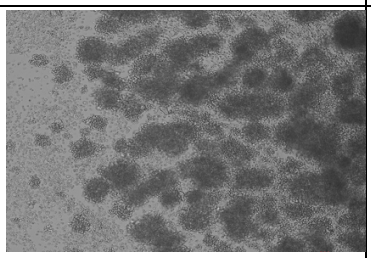 CRC-TIL-35; Male; T4N0M1; UICC IV; MSS	

V. Dissertation statements

- Colorectal cancer (CRC) ranks as the third most prevalent and the second deadliest cancer in the world, constituting about 10% of all cancer diagnoses. The therapy of CRC has evolved into a personalized, multimodal approaches that combines surgical resection, radiotherapy, chemotherapy, targeted therapies and immunotherapy with specific molecular characteristics.
- Organoids are miniature, simplified versions of organs produced *in vitro* from tissues and/or biopsies. They replicate the architecture and functionality of their corresponding tissues, making them invaluable for studying disease mechanisms, drug responses, and therapeutic strategies. In the context of CRC, patient-derived organoids (PDOs) as organoids have emerged as powerful tools for modeling tumor biology and assessing treatment efficacy, allowing researchers to investigate the molecular underpinnings of CRC initiation and progression.
- Integrating studies of tumor-infiltrating lymphocytes (TILs) with organoid technology present a novel approach to understanding immune-tumor interactions in CRC. By co-culturing organoids with TILs derived from patient samples, researchers can observe how these immune cells interact with tumor cells in a controlled environment that closely resembles the original tumor context. This approach not only enhances our understanding of immune evasion mechanisms but also aids in identifying potential therapeutic targets for immunotherapy.
- Targeted sequencing possesses high sequencing sensitivity and depth, which can help for those detection of genetic variants with low-frequency. For the well-known driver mutations and pathogenic genes, targeted sequencing can be able to achieve treatment guidance or personalized screening.
- This study is a prospective CRC cohort study focusing on establishment of

CRC organoid and TILs as preclinical models for therapy prediction, aimed to perform drug screening, targeted therapy and explore tumor microenvironment etc..

- The primary tumors were extensively characterized molecular genetically by large-scale parallel sequencing using NGS and droplet digital PCR for MSI detection.
- The targeted gene penal sequencing proved that the most frequent genetic mutations are *TP53*, *APC*, *KRAS* in Chinese CRC patients. *POLE* or *POLD1* mutations were detected in a low fraction of CRC. MSI was found in 13.7% of patients.
- In 75% and 87.5% of cases organoid and TILs could be established, respectively. CRC tumor organoids can faithfully recapitulate the characteristics of the original tumors which can be used for pre-clinical models.
- Based on the sequencing results, genetic mutations in primary tumors can be retained in the organoids, but mutations with low frequency will be lost which demonstrates that during the culturing period, tumor cells with stem-cell properties will be selected and maintained in the successfully established organoids.
- TILs from the tumor tissues play a vital role in the tumor microenvironment by recognizing and killing tumor cells which can regulate the immune response and make them a crucial cell population for tumor immunotherapy.
- Co-culture of CRC organoids and TILs can be used to explore tumor microenvironment.

VI. Acknowledgement

I had a wonderful time in Germany in the past years. I would like to give my sincere appreciation to my colleges and friends who have helped me in the period of my study.

I sincerely appreciate PD Dr. med Annette Zimpfer for providing the crucial and precious help and suggestions to complete my dissertation.

I want to thank to China Scholarship Council of my homeland. The finance covered the cost of my study and life in Germany and to finish my dissertation.

I would like to thank Dr. Xin Huang and Mr. Ying Jiang in Mission Medical to supply the experimental platform for me to carry out the project.

And I am extremely grateful for Dr. Kun Liu from the Department of General Surgery in Ruijin Hospital to provide colorectal cancer tissues and the patients who made their tumor tissues available for the project.

I especially would like to thank my family members. The love from all of them supported me to insist my study and complete my dissertation.

VII. Personal Curriculum Vitae

Personal Details

Name: Dai, Meng

Gender: Male

Data of birth: 10th January 1989

Nationality: China

Telephone: +49 015254668579

Email: 15211280028@fudan.edu.cn; meng.dai@uni-rostock.de

Private Address: Virchowstr.60, 66424 Homburg(Saar), Germany

Education and Professional Experience

2021 - now	University of Rostock, Germany
2018 - 2021	Shanghai Eastern Hepatobillary Surgery Hospital (Resident and attending surgeon), Shanghai, China
2015 - 2018	Master of Surgery, Fudan University, Shanghai, China
2010 - 2015	Bachelor of Clinical Medicine, Wannan Medical College, Anhui, China
2006 - 2010	No.3 High School of Fuyang, Anhui Province, China

Publications

First Author Publications

1. **Dai, M.**, Mullins, C. S., Lu, L., Alsfasser, G. & Linnebacher, M. Recent advances in diagnosis and treatment of gastroenteropancreatic neuroendocrine neoplasms. World J Gastrointest Surg 14, 383-396, doi:10.4240/wjgs.v14.i5.383 (2022).
2. **Dai, M.**, Su, Y. & Wu, Z. Downregulated expression of plakophilin-2 gene in patients with colon adenocarcinoma predicts an unfavorable prognosis and immune infiltrate. J Gene Med, e3592, doi:10.1002/jgm.3592 (2023).

Co-author Publications

3. Lu, L., **Dai, M.**, Mullins, C. S., Schafmayer, C. & Linnebacher, M. Global Association of Cause-specific Mortality between the Major Gastrointestinal Cancers and Parkinson's Disease for the First Two Decades of the New Millennium. Aging Dis 13, 534-539, doi:10.14336/AD.2021.1016 (2022).
4. Lu, L., **Dai, M** et al. Microsatellite Status and IkappaBalpha Expression Levels Predict Sensitivity to Pharmaceutical Curcumin in Colorectal Cancer Cells. Cancers (Basel) 14, doi:10.3390/cancers14041032 (2022).

Honors and Awards

2021 China Scholarship Council (grant number: 202108080085)

2014 National Scholarship for Encouragement of China

2013 Excellent Scholarship

2012 Excellent Scholarship

2011 Excellent Scholarship

Signature

Rostock, …… ……

VIII. Eidestattliche Erlärungen/Declarations

I hereby declare that I have independently written this thesis on the topic: “Establishment of Preclinical Tumor Models for Colorectal Cancer Precision Medicine.”

I declare under oath that I have written this dissertation independently and only using the sources and resources indicated. Any content taken from other literature is identified as such. I confirm that I have not used the paid services of any agencies or consultants (doctoral advisors or other persons) in the preparation of this thesis.

I further declare that I have produced my scientific work in accordance with the principles of good scientific practice as set out in the valid “Statutes of the University of Rostock for Ensuring Good Scientific Practice.”

Signature

Rostock, …… ……